2020

Producing chiral amines: a bi-enzymatic cascade involving Old Yellow Enzymes and amine dehydrogenases

DELFT UNIVERSITY OF TECHNOLOGY
FACULTY OF APPLIED SCIENCES
DEPARTMENT OF BIOTECHNOLOGY
BIOCATALYSIS

E.P.J. JONGKIND: 4438418
MASTER THESIS PROJECT: LM3901
START DATE: 02-09-2019
END DATE: 24-04-2020

SUPERVISOR: DR. C.E. PAUL
2ND EXAMINER: PROF. U. HANEFELD
3RD EXAMINER: DR. A.J.J. STRAATHOF

1. Abstract

Chiral amines are valuable compounds for their use as building blocks for pharmaceutical and fine chemical industries. Previously, chiral amines were made with metals as catalysts, but these are unsustainable and difficult to remove from the product. Organocatalysis is a sustainable alternative, but requires chiral ligands, which are costly. Over the last decade, biocatalytic methods have been developed as well. Our goal was to produce chiral amines with our designed bi-enzymatic cascades, containing an ene reductase and amine dehydrogenase. We produced and purified ene reductases and assayed the asymmetric reduction of our proposed substrate scope, consisting of unsaturated ketones and aldehydes. We also investigated the impact of multiple reaction conditions on these performances that are optimal for amine dehydrogenases. Starting with 10 mM of substrate, we obtained concentrations up to 9.7 mM amine. Also, we obtained 3-methylcyclohexylamine with an enantiomeric and diastereomeric excess up to 99%. Therefore, we conclude that this bi-enzymatic cascade is capable of producing chiral amines with both high enantiomeric and diastereomeric excess. Further research to perform cascades on a larger scale is recommended.

Table of Contents

2. Introduction

Chiral amines are molecules that are valuable in a wide range of industries. For instance, chiral amines are applied for the synthesis of pharmaceutical building blocks and agrochemicals, in addition to being used as resolving agents for diastereomeric salt crystallization.[1] It is important that these products have a high purity and enantioselectivity, as the wrong enantiomer could cause different and undesired effects, such as inactivity or even toxicity.[2-3] An example of a catalyst that is used for their synthesis contain (precious) transition metals, such as rhodium.[4] Drawbacks of using metal catalysts are the unsustainability and difficulty to remove the catalyst from the product.[5-6] Alternatively, organocatalysts can be used, contain no metals and therefore are more sustainable. However, to produce chiral compounds, chiral ligands are required, which are expensive.[7] Over the last decade, biocatalytic methods with enzymes were applied as well, such as for the production of sitagliptin.[8] Enzymes are able to produce enantiopure compounds with high efficiency, also, enzymes require milder conditions than regular catalysts, which are easier to establish and decrease formation of side products.[2]

2.1. Biocatalytic methods for chiral amine production

Enzymes are categorized in different classes: oxidoreductases, transferases, hydrolases, lyases, isomerases and ligases.[2] Different approaches to produce chiral amines with enzymes from several classes of enzymes are briefly described here.[9] Lipases, from the class of hydrolases, catalyse the cleavage of an amide or an ester, resulting into an alcohol and an amine or acid.[3] Lipases are useful to apply for racemic mixtures of amines. Because lipases are enantioselective, one enantiomer undergoes esterification while the other enantiomer is catalysed in a much lower rate: this process is called kinetic resolution. In this way, the enantiomeric excess of the amine is increased. The drawback of kinetic resolution is that the maximum theoretical yield is 50%.[10] By adding another catalyst responsible for racemizing the mixture, which is called dynamic kinetic resolution, it is possible to exceed 50% yield.[10-11] Other applicable enzymes are transaminases (TAs), from the class of transferases. TAs catalyse the reversible reaction of amination of ketones into chiral amines with the aid of an amine donor.[12] These enzymes require the cofactor pyridoxal phosphate (PLP).

Another suitable enzyme is the imine reductase (IRED), which requires the nicotinamide adenine dinucleotide cofactor (NAD(P)H) to reduce an imine into an amine. The imine intermediate could also be formed from a mixture of a carbonyl substrate and an amine donor, so the IRED can form the amine.[13-14] Reductive aminases (RedAms) are even able to catalyse both the imine formation and the reduction of the imine.[15] Amine oxidases (AOs) are an option for both producing an imine intermediate as well as forming chiral amines through kinetic resolution.[3] These enzymes fall in the class of oxidoreductases, which are enzymes that catalyse reactions involving the transfer of electrons. Oxidoreductases are interesting enzymes because there are efficient and usually form no side-products, especially with the use of NADH or NADPH as a cofactor. Because these cofactors are expensive, a recycling system is required. In this thesis, we focused on this type of oxidoreductases.

2.2. Cascade reaction method

We envisioned a bi-enzymatic cascade consisting of an ene reductase (ER) from the old yellow enzyme family (OYE) and an amine dehydrogenase (AmDH, Figure 1). Cascade processes are reactions that contain multiple steps towards making a product, without isolating the intermediate.[16] When enzymes are involved, it is called a biocatalytic cascade.[17]

Biocatalytic cascades are classified into *in vitro* and *in vivo* cascades.[18] *In vitro* cascades are cascades that are performed outside of the cell, whereas *in vivo* cascades, reactions are performed within the cell. What makes *in vitro* suitable is that it enables to perform reactions with all known compound concentrations. The disadvantage is the enzyme must be purified, which could be costly, and still requires the addition of cofactors. On the contrary, *in vivo* reactions require no purification, and already contain important compounds such as cofactors.[18] However, it leaves the risk of other enzymes catalysing side-reactions, and the removal of the product out of the cell could be difficult.[18]

Using cascades prevents any loss of yield by the work-up of intermediates. Also, less compounds are used in the system, which increases the efficiency and thus decreases the required costs to perform such a reaction.[17] Cofactors such as NADPH are costly, so efficient usage of the cofactor is of high interest. Self-sufficient process where the cofactor is recycled inherently with the different steps of the cascade are attractive solutions, like the "hydrogen borrowing system" used by Mutti *et al.*, which limits the amount of the nicotinamide cofactor required in this *in vitro* cascade.[18-20] The main challenge of cascades in general is that the applied enzymes have different conditions in which these perform optimally.[17]

Cascade processes are classified into linear, orthogonal, cyclic, parallel, convergent and divergent cascades.[17] Our proposed process is a linear cascade, where the unsaturated substrate is reduced first, and reductive amination occurs in a consecutive step. $NAD(P)^+$ is reduced by glucose dehydrogenase (GDH) oxidizing glucose to gluconolactone. Both the Old Yellow Enzyme (OYE, discussed below) and amine dehydrogenase (AmDH) require NAD(P)H, so this so-called recycling system increases the efficiency of this cascade, and thus could lead to more amine formation, at reduced costs.[21]

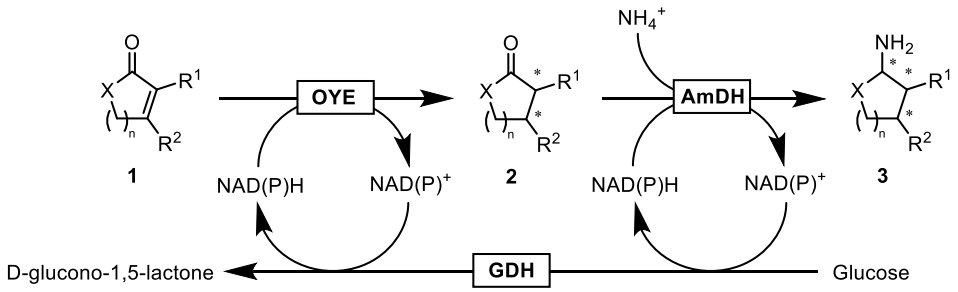

Figure 1. Proposed bi-enzymatic cascade to produce chiral amines. By adding glucose dehydrogenase (GDH) and glucose to the cascade, a NAD(P)H cofactor recycling system is used by both the OYE and AmDH.

2.3. Old Yellow Enzymes

The Old Yellow Enzymes (OYEs) are an enzyme family that are flavin-containing ene reductases (ERs).[22] OYEs are found in several microorganisms, including plants, bacteria and fungi.[6] These enzymes catalyse the asymmetric hydrogenation with the aid of a cofactor NAD(P)H, which reduces the flavin mononucleotide (FMN) in the enzyme. The ERs are useful for the *trans*-hydrogenation of a wide range of substrates that are activated alkenes, such as α,β-unsaturated ketones.[6] NAD(P)H donates a hydride to the flavin, which is able to then transfer it to the unsaturated molecule (Figure 2).[6] This will lead to a hydrogen bond formed with the proton from an adjacent tyrosine in the enzyme.[2]

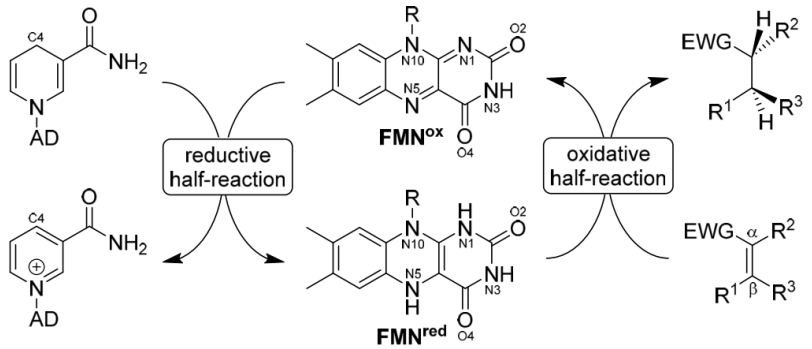

Figure 2. Reaction mechanism of OYEs with the NADPH, flavin mononucleotide (FMN) and α,β-unsaturated substrate with an electron withdrawing group (EWG).[6]

Within the OYE family, three different classes were distinguished based on the origin of the enzyme, amino acid sequence, and substrate specificity.[6] One of the OYEs in class III, the 'thermophilic-like' OYEs, was discovered in the bacterium *Thermus scotoductus*.[23] This enzyme abbreviated as *Ts*OYE (Figure 3a) is thermostable and shows its highest activity at 65 °C.[23] The isoalloxazine ring of the flavin inside the enzyme is coordinated (Figure 3b) by hydrogen bonds with nitrogen and oxygen atoms from adjacent histidine (His174, His177) and tyrosine residues (Tyr27). *Ts*OYE contains a TIM-barrel domain (Figure 3c) above which the flavin, the NAD(P)H cofactor and the substrate are coordinated during the mechanism.[24] The loops between the β-sheets and α-helices form the active site of *Ts*OYE.[25] The asymmetric reduction proceeds by the bi-bi ping-pong mechanism, meaning that NAD(P)H is coordinated at the *si*-side of the flavin first, and will leave the active site so the substrate can be reduced by the FMN.[6] When NAD(P)H is oxidized, the hydride on the C4 position will bind on the N5 position of the flavin. This causes the N1 position to be stabilized by His172 and His175 (Figure 3d). When a substrate is positioned at the *si*-side of the flavin, it will be stabilized by the same histidines through hydrogen bonding. Tyr27 binds with the carbonyl group of certain substrates.[24] The hydride on the N5 position will then be transferred to the unsaturated substrate. The double bond opens, and the α-carbon obtains the hydrogen from Tyr177 residual group.

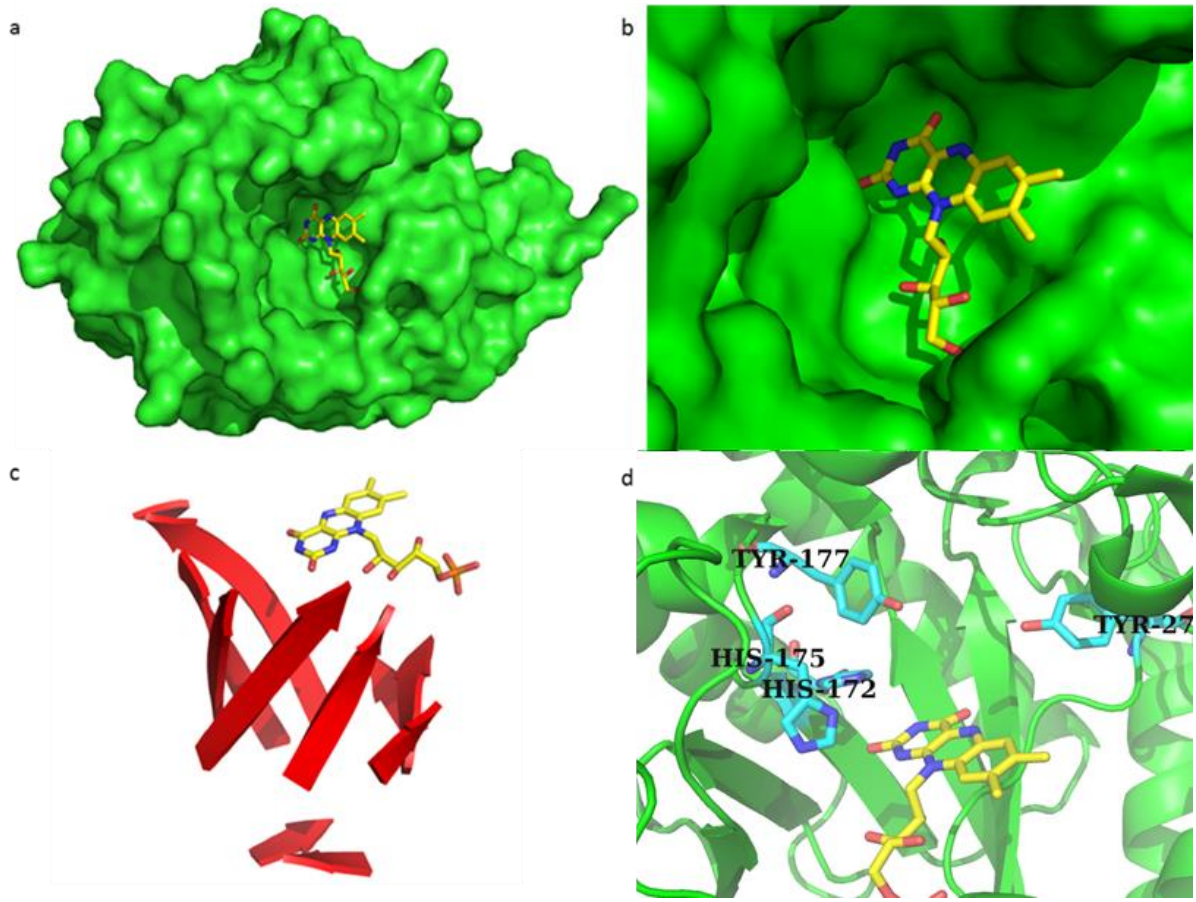

Figure 3. Protein structures obtained with PyMol. a: surface of a *Ts*OYE monomer (green), with flavin (yellow) incorporated in the structure. b: Close-up of the active site with FMN coordinated inside. c: TIM-barrel (red) structure with the flavin. (yellow) coordinated above the domain. d: Coordination of the flavin (yellow) in relation to important amino acids (cyan). Tyr177 functions as a proton donor while Tyr27, His172 and His175 stabilize the position of the substrate through hydrogen bonding interactions.

2.4. Amine dehydrogenases

The amine dehydrogenase (AmDH) catalyses the reductive amination of a ketone into an amine (Figure 4) with an external amine donor, ammonia, and the reducing agent NAD(P)H which provides the hydride for the reduction of the iminium intermediate.[26] Before the identification of native AmDHs by a group in Genoscope, there was no gene coding for such activity except the well-characterized amino-acid dehydrogenase (AADHs) catalysing the same chemical transformation, reductive amination, but only with ketone bearing a carboxylic acid in vicinal position. So, the highly abundant AADHs were designed into AmDHs by removing the interaction of the undesired carboxylic acid with residues identified for this interaction, mainly lysine and asparagine.[9, 27]

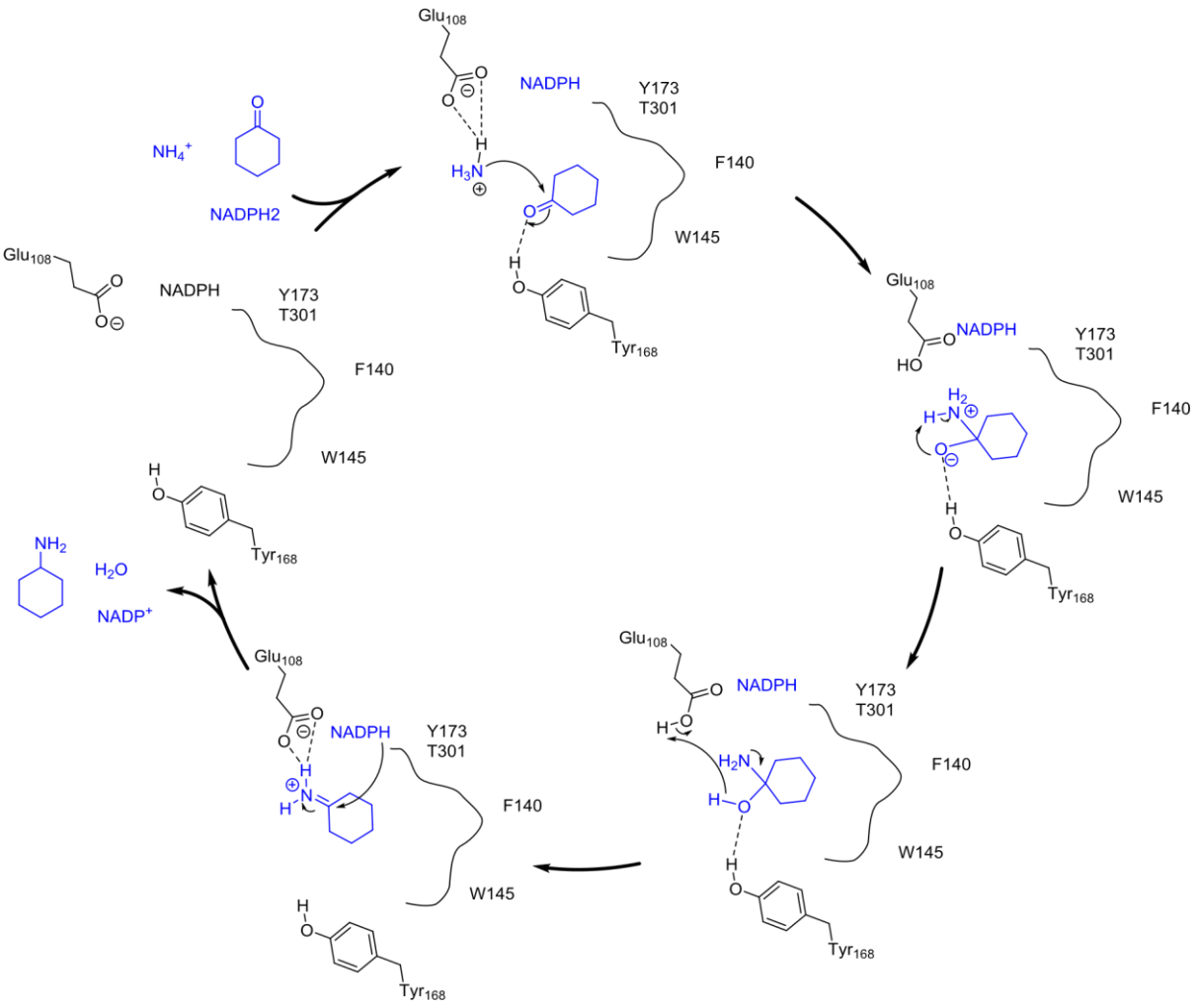

Figure 4. Proposed reaction mechanism of reductive amination of cyclohexanone by *Cfus*AmDH. From Mayol *et al.*.[5]

However, native AmDHs have recently shown to catalyse the reductive amination of a ketone different to α-ketoacids.[5, 28] These showed a proper affinity towards substrates such as aldehydes and prochiral ketones.[5] For example, one of these enzymes was found in the *Mycobacterium smegmatis* (*Msme*AmDH) and its structure solved by X-ray crystallography (Figure 5a). The NAD(P)H is present in a tight pocket (Figure 5b) formed by bulky amino acid side chains as phenylalanine (Phe169) and tyrosine (Tyr164). *Msme*AmDH contains a Rossmann-fold domain (Figure 5c), which is shown by six parallel β-sheets.[25] The mechanism of the reductive amination by *Msme*AmDH is proposed to be similar to some AADHs such as meso-diaminopimelate dehydrogenases (DAPDHs).[5] Trp167 makes hydrogen bonds with the carbonyl of the substrate, while the conserved negatively charged glutamate (Glu104) interacts with the amine donor ammonia (Figure 5d). The amine is then close enough to the substrate to attack the carbonyl group. An iminium intermediate is formed, followed by attack of the hydride of the cofactor NADPH.

Other native AmDHs recently discovered from the *Microbacterium* sp. (*Micro*AmDH) and *Aminomonas paucivorans* (*Apau*AmDH), have similarities in amino acid sequence. *Micro*AmDH has a tyrosine, Tyr169, whereas *Msme*AmDH has a phenylalanine, as residue hypothesized to close the active site. For the residue binding the ketone, *Apau*AmDH bears a tyrosine Tyr164, whereas *Msme*AmDH has a tryptophan residue Trp164. The similarities of these amino acids are that the side

chains are large, forming a restricted active site pocket. The main similarity between the enzymes is the Glu104 residue, which is crucial for activation of ammonia and charge stabilisation with the iminium ion during the catalytic cycle. More recently, exploration of metagenomic data led to the discovery of other native AmDHs including MATOU-568 (= MATOUAmDH2) which shares the conserved glutamate and bulky residues tyrosine Tyr171 and 176 equivalent to Trp164 and Phe169 of *Msme*AmDH respectively.[29]

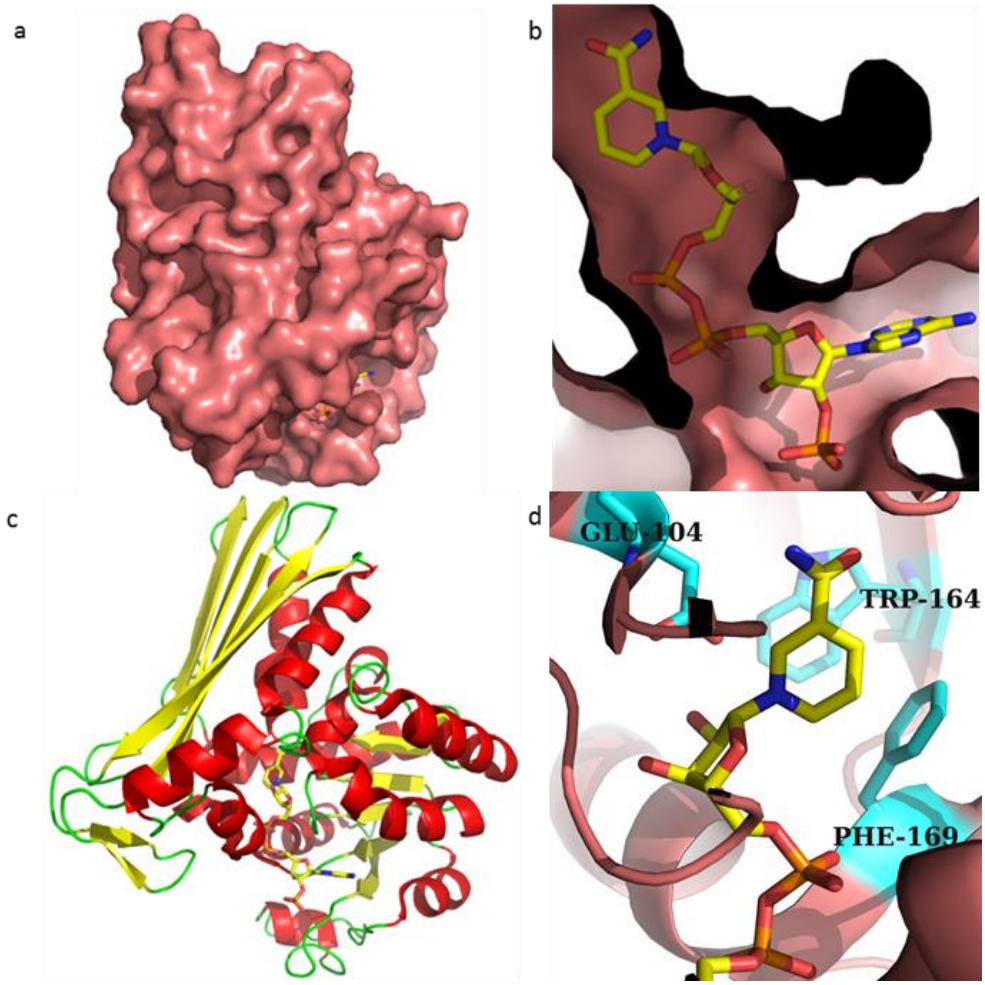

Figure 5. Protein structures obtained with PyMol. a: surface of the *Msme*AmDH, with the NADPH coordinated within the structure. b: Close up of the pocket in which the NADPH (yellow) is positioned. c: *Msme*AmDH cartoon coloured by secondary structure. At the right, six parallel β-sheets are present, which represents the Rossmann-fold domain. d: coordination of NADPH in relation to important amino acids (cyan): Glu104 is in hydrogen bonding distance with the amine group of the substrate, whereas Phe169 and Trp164 form a pocket with the nicotinamide ring.

2.5. Current challenges in chiral amine production

Each biocatalytic method has its own challenges to improve on. For lipases, dynamic kinetic resolution is highly dependent on the rate of the racemization catalyst, and the enantioselectivity of the lipase.[10] Amine production by IREDs is very versatile, but the activity of IREDs are usually low.[9] Regarding TAs, these enzymes require the cofactor PLP and high concentrations of amine donor such

as isopropyl amine.[30-31] TAs catalyse equilibrium reactions for which forcing by reaction design is necessary.[12] AmDHs and TAs are both prone to product inhibition.[26] Also, AmDHs currently have a limited substrate scope and show low diastereomeric excess on chiral ketones .[28] This enumeration shows that each method has its flaws, which should be taken into account when choosing one of these enzymes to work with.

2.6. Objectives

The objective was to establish a bi-enzymatic cascade with the *Ts*OYE and AmDH enzymes to produce various (chiral) amines. This was assayed by purifying *Ts*OYE and determining the performance of its asymmetric reductions of different substrates under different conditions. The substrates selected are based on the acceptance by the AmDHs described by Mayol *et al*.[5] Then, based on the observations by the Genoscope (Paris, France), we designed for multiple substrates the most optimal enzyme combinations and reaction conditions. These cascades were analysed based on the conversion and enantiomeric (and if applicable diastereomeric) excess of the desired chiral compounds.

3. Material and methods

All chemicals were obtained from commercial suppliers and used without further purification.

3.1. Protein purification of *Ts*OYE WT and C25D/I67T double mutant.

LB medium was prepared in 1 L and 250 mL flasks. LB medium contained 10 g/L yeast extract, 10 g/L sodium chloride and 5 g/L tryptone. 2 M NaOH was added until pH 7.0, and all solutions were autoclaved overnight.

The genes encoding for wild-type *Ts*OYE and the double mutant C25D/I67T were previously transformed and overexpressed in *Escherichia coli* (*E.coli*) and kept in 30% glycerol stock solutions at -80 °C. LB-agar plates were prepared with 100 mL of agar gel, containing 100 µL of 100 mg/mL ampicillin and 50 mg/ml kanamycin stock solution. The wild-type (WT) culture was used to create a preculture with 10 mL LB, whereas the cells with mutant *Ts*OYE were taken directly from the glycerol stock.

The 10 mL LB overnight pre-cultures were diluted 1:100 into 1 L of LB medium in two 2-L flasks. These were shaken at 37 °C at 180 rpm until the OD_{600} equalled to 0.6 (± 0.1). IPTG was added to a final concentration of 100 µM, and the culture was shaken at 25 °C at 180 rpm for 18 hours (± 1 hour). The broth was then centrifuged at 4 °C, at 10,000 rpm for 10 minutes. The supernatant was removed, and the cell pellet was resuspended in 75 mL 50 mM MOPS buffer, (pH 7, NaOH). This was again centrifuged at 4,000 rpm at 4 °C for 15 minutes. The supernatant was removed from the cell pellet, and the pellet was stored overnight at -20 °C. The pellet was defrosted naturally and resuspended in 75 mL MOPS buffer. This mixture was then injected into the RM6 LAUDA cell disrupter. This mixture was then centrifuged at 10,000 rpm and 4 °C for 30 minutes. The supernatant was collected and incubated at 70 °C for 1.5 hours. The suspension was then centrifuged at 8,000 rpm at 4 °C for 30 minutes. To freeze the OYE immediately, the supernatant from the centrifugation was added dropwise to liquid nitrogen, which could be stored overnight at -80 °C.

To ensure all OYEs contain the required FMN cofactor, 600 µL 5 mM stock of FMN was added to the thawed enzyme solution. The solution was then concentrated with the aid of an ultrafiltration centrifugal filter (30 kDa cut-off membrane, Amicon) to a final volume of around 5 mL.[32] The excess of FMN was removed by passing the solution (2 × 2.5 mL) through a PD-10 Desalting column from GE Healthcare which was equilibrated with the aforementioned MOPS buffer.[33] This led to the final volume of approximately 7.2 mL of *Ts*OYE wild-type and mutant, which were both stored in aliquots at -20 °C.

The next batch was performed with a total of 5 L of medium to produce the WT *Ts*OYE, divided over four 1.25 L flasks. The same concentrations were used for the preparation of the medium. Performing the incubation, inhibiting with IPTG and incubation at 25 °C were performed identical to the first batch. However, the purifying steps where a centrifuge is involved was slightly different. All centrifugation steps were performed with 10,000 rpm at 4 °C. Also, the centrifugation after heat purification took 10 minutes instead of 15 minutes.

With the aid of weighing the pellet, it was concluded that the cell concentration was estimated to be 7.5 g/L. After heat purification, an excess of FMN was added (total of 57 µM). During the desalting

column, every purified sample of enzyme was added into one flask, in order to keep the concentration constant for all stock solutions. With the aid of UV, it was determined that the enzyme concentration of the whole stock was equal to 60 µM.

3.2. SDS-PAGE sample preparation

Samples were prepared by mixing samples with Laemmli buffer and 5% v/v dithiothreitol (DTT). In case a cell pellet was loaded on the gel, an equivalent volume of Milli-Q was added to suspend the pellet as much as possible. Then, the mixture was repeatedly put through the syringe for 30 times to break the cells, DNA and RNA as much as possible.

3.3. UV-spectrometry and BC Assay

A spectrophotometer was used to visualize the spectrum of the enzyme between wavelengths of 300 and 600 nm. The batches were diluted in water and the wavelengths were measured. Then, 20 µL of 10% sodium dodecyl sulfate (SDS) detergent was added. The wavelength was measured repetitively until the spectrum stopped changing. From this spectrum, the concentrations were calculated (see Appendix 2). The concentration was also calculated with a bicinchoninic acid (BC) assay by making a calibration curve (see Appendix 3). Samples were prepared as described by Uptima.[34]

3.4. Asymmetric reduction reactions *Ts*OYE

Three buffers were initially prepared to perform the reactions: 50 mM Tris-HCl buffer pH 8.0, 50 mM Na_2CO_3 pH 9 and 250 mM NH_4COO^- pH 8 To increase the pH of the last two buffers, ammonium hydroxide solution was added dropwise to the buffer. Also, to analyse the impact of the ammonium formate on the reaction, a 25 mM NH_4COO^- buffer is made by diluting the 250 mM buffer 10 times (pH was measured at 7.86). The substrates were dissolved in dimethyl sulfoxide (DMSO), in order to make a 1 M stock. NADPH was dissolved in a 50 mM Tris-H_2SO_4 buffer.

The enzymatic reactions were performed in a total volume of 1 mL in plastic tubes. The reactions contained 2 µM *Ts*OYE and 10 mM of substrate (in this case 2-methylcyclohexen-2-one). Two different types of cofactors were added to the reaction. For the recycling system, 0.1 mM NADPH, 11 mM glucose (anhydrous) and 5 mg/ml GDH (Evozymes, lyophilized powder, 35 U/mg) were added to the enzyme. Without the recycling system, 11 mM synthetic cofactor BNAH was added, which is equal to 2.4 mg of powder. Another method was to dissolve BNAH powder in DMSO first, so the mixture could be added to the reaction, with a final BNAH concentration of 15 mM in the reaction.

The reaction tubes were covered in parafilm and placed in an Eppendorf thermoshaker (900 rpm, 30 °C). The reactions were stopped after 1 hour by placing the reaction plastic tubes on ice and adding 500 µL of ethyl acetate (EtOAc). This mixture was vortexed for around eight seconds and were then centrifuged for 1 minute at 13,000 rpm. The EtOAc was then extracted and dried with $MgSO_4$ for analysis by GC. In some cases, this extraction with EtOAc was performed twice. An example of a reaction mixture is shown in Table 1 to reduce substrate 2-methyl-2-cyclohexen-1-one.

Table 1. Reaction mixture to reduce 2-methyl-2-cyclohexen-1-one from TsOYE including a recycling system.

Compound	Added mass / volume
GDH (Evozymes)	5 mg
Tris buffer 50 mM pH 8.0	949 µL
***Ts*OYE WT**	18 µL
11 mM glucose monohydrate	13 µL
0.1 mM NADPH	10 µL
10 mM 2-methyl-2-cyclohexen-1-one	10 µL

3.5. Screening ERs from Johnson Matthey

The Johnson Matthey (JM) biocatalysis enzyme kit contained amine dehydrogenases, ene reductases (ERs), and glucose dehydrogenase GDH-101. The ERs that were tested were labelled as ENE-101, ENE-102, ENE-107, ENE-108 and ENE-109. Reactions were performed in a Tris-HCl buffer pH 8.0, containing 10 mM substrate, 12 mM glucose, 1 mM $NAD(P)^+$ and 1 mg/ml GDH-101.

3.6. Determining specific activity conditions

For every reaction, a 2 mL cuvette is used to determine the decrease in NADPH at a wavelength of 340 nm. In 2 mL of buffer, 10 mM of 2-cyclohexen-1-one and 40 µL of NADPH was added to observe the absorbance at a proper intensity. The amount of enzyme was determined by trial and error: if the slope was between 0.5-2.0 A/min, it was sufficient to perform calculations with.

The same counts for the specific activities of the enzymes with different substrates. However, for all substrates, 20mM of glucose and 100 U/mL glucose oxidase were added as well. In both cases, the slope of the mixture except the enzyme was checked as a blank to confirm that no NADPH is reduced by any other source.

3.7. GC sample preparation

Compound analyses were carried out on Shimadzu GC-2010 gas chromatographs (Shimadzu, Japan) with an AOC-20i Auto injector equipped with a flame ionization detector (FID), using nitrogen or helium as the carrier gas. Compounds were dissolved in EtOAc, resulting into a solution with approximately 10 mM compound. These were then dried with $MgSO_4$ by adding a scoop to the mix and centrifuge it at 13,000 rpm for 1 minute. In case of substrates with low boiling points, diethyl ether (Et_2O) was used as a solvent instead (see Appendix 5 for different GC methods).

3.8. Cascade preparations and experiments

Thanks to the group of Vergne-Vaxelaire at the Genoscope, we received different purified amine dehydrogenases that showed activity towards the reduced substrates (**2a**-**m**). These were the following enzymes:

- *Micro*AmDH, 2.78 mg/mL
- MATOU-568, 4.179 mg/mL
- *Msme*AmDH, 6.76 mg/mL
- ApauAmDH, 2.07 mg/mL

- GDH-105 (Codexis), 123 mg, 50 U/mg

For every cascade, 0.5 mg/mL was used, so these given enzymes were diluted by the cascade reaction mixture. Also, 3 U/mL GDH-105 was used, which is done by dissolving 3 mg in Milli-Q so that 20 µL of this stock corresponded with the desired number. A 1 M glucose stock was made in Milli-Q. Furthermore, 10 mM $NADP^+$ was prepared in Milli-Q as well. Reactions were performed in a 1 M ammonium formate buffer (pH 8, 2 M NaOH). To reach the desired concentration of 1 M ammonium formate, a concentrated stock of 6.67 M was prepared, which was added to every reaction mixture in order to obtain 1 M of ammonium formate (Table 2). Reactions were performed at 30 °C, in a thermoshaker (400 rpm, 30 °C).

Table 2. Example of compounds added in a cascade reaction mixture.

Compound	**volume (µL)**
Milli-Q	489
6.7 M buffer concentrate	150
1 M glucose (Milli-Q)	24
150 U/mL GDH in (Milli-Q)	20
0.5 mg/mL AmDH	120
10 mM $NADP^+$ in Milli-Q	20
60 µM *Ts*OYE	167
1 M 2-cyclohexen-1-one (DMSO)	10
Total	**1000**

3.9. AmDH performance under different conditions

Reactions with the amine dehydrogenases labelled AmDH-3 from the Johnson Matthey biocatalysis enzyme kit were performed in a 2 M ammonium chloride buffer, pH 9.6, adjusted with 6 M HCl. Reactions were performed in a total volume of 1 mL. The reaction mix contained 25 mM glucose, 1 mM NAD^+, 5 mg/mL GDH-101, 10 mM 2-pentanone (**2i**) and the amine dehydrogenase labelled AmDH-3. The substrate stock had a concentration of 1 M in isoamyl acetate.

3.10. Amine purification

To purify the amine from the reaction mixture, an equivalent volume of 10 M NaOH was added to the mixture. After vortexing, half the equivalent reaction volume of EtOAc was added and shaken thoroughly. After centrifugation, the top layer was extracted. This extraction was performed twice. The obtained top layer was then dried with $MgSO_4$ for analysis with GC.

3.11. GC calibration curve preparation

In 1 M ammonium formate buffer, different concentrations of substrate, intermediate and product (from a 1 M stock in DMSO) were added in a total volume of 500 µL. To these mixtures, 500 µL 10 M NaOH was added, which was thoroughly vortexed. Then, 250 µL EtOAc was added. These mixtures were then vortexed thoroughly and centrifuged at 13,000 rpm for 1 minute. The extraction was performed as previously described for amine purification.

3.12. Amine derivatization

The amines labelled as **3e**, **3g**, **3i** and **3k** were derivatised in order to determine the enantiomeric excess and diastereomeric ratio (see Appendix 10). A small scoop of potassium carbonate (K_2CO_3) and a few drops (4 to 5 per mL of reaction mixture) of acetic anhydride were added to the extracted amine. This was shaken at 400 rpm at 30 °C for 1 hour. Then, half the equivalent volume of Milli-Q was added. This was shaken at 400 rpm at 30 °C for 30 minutes. The top organic layer of this mixture was separated and dried with $MgSO_4$ for analysis with GC.

4. Results

4.1. Production and protein concentration of OYEs

To use the *Ts*OYE as a catalyst for the cascade process, we produced this enzyme by recombinant expression in *E. coli* and purified it as previously described.[24, 35] SDS-PAGE confirmed the enzyme was obtained in high purity (Appendix 1). We determined protein concentrations by UV spectroscopy and a BC Assay. From the purification, five different stocks were obtained with different concentrations. With the UV spectra, we determined the concentrations of the different batches (Table 3, see Appendix 2). Also, UV spectra of already purified stocks of OYE2 and YqjM were measured. These are family members of *Ts*OYE, which could be used in the cascade if certain substrates are not accepted by the *Ts*OYE. The OYE2 stock concentration equalled to 78 µM, while the YqjM stock had a concentration of 341 µM.

In order to determine the concentrations by the BC Assay, we made a calibration with known BSA concentrations (see Appendix 3). The enzyme solutions were diluted until the concentrations would fit within the prepared calibration curve. The adsorptions were measured at a wavelength of 513 nm. With these absorption values, we were able to calculate the enzyme concentration of the stocks (Table 3). In some cases, the concentrations of this method matched with the concentrations determined by UV. However, most concentrations differed significantly, because BC assays do not only show concentrations of flavin-containing enzymes, but also of other proteins. Also, because the calibration curve consisted of only a few data points, the BC Assay probably had inaccuracies. So, the data obtained from UV was considered more reliable, and thus those numbers were applied to prepare reaction mixtures.

Table 3. Concentrations of the different enzyme stocks in µM and mg/mL.

Sample type	**UV spectroscopy**	**BC Assay** [a]
	concentration (µM)	concentration (µM)
***Ts*OYE #1**	108	109
***Ts*OYE #2**	159	177
***Ts*OYE #3**	60	46
C25D/I67T #1	108	174
C25D/I67T #2	126	108

[a] Except for the data for batch C25D/I67T #1 , all BC Assay results have an error below 10%.

4.2. Substrate scope of OYEs

We selected a panel of substrates that would lead to the desired chiral amine compounds. These substrates and the expected products from reduction by *Ts*OYE (Figure 6) were based on the substrates converted by the amine dehydrogenase as is described by Mayol *et al.* (see Appendix 4).[5] To analyse the conversion of *Ts*OYE for these substrates, references were made and loaded onto multiple GC-columns (Appendix 5).

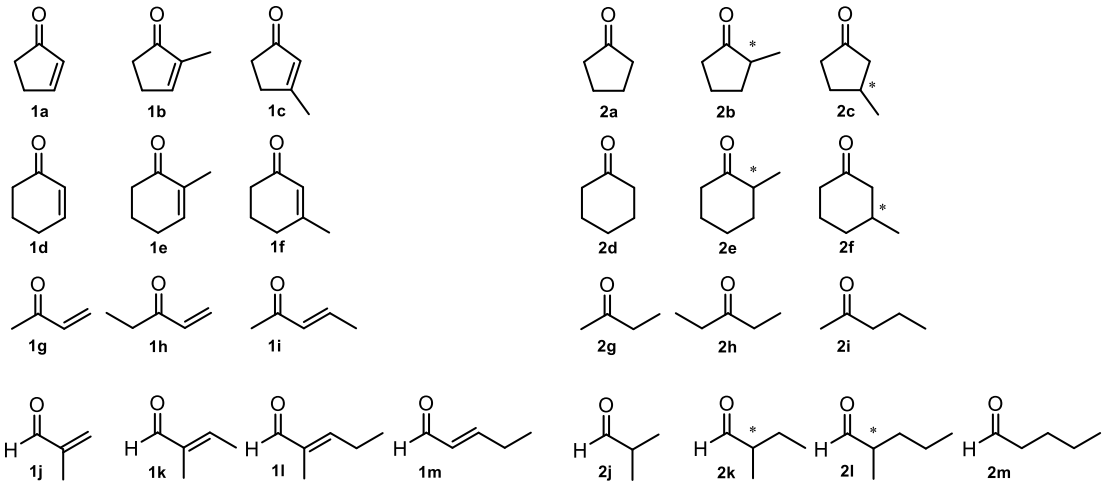

Figure 6. Overview of all alkene substrates and expected saturated carbonyl products with assigned numbers.

We determined the specific activity for 12 out of the 13 substrates in order to compare the performances of *Ts*OYE with different substrates (Figure 7). At a wavelength of 340 nm, the oxidation of NADPH was determined. This is different to the amount of substrate reduced by the enzyme, because oxygen could oxidize FMN as well, which is then able to oxidize NADPH. An excess of glucose and glucose oxidase were added to the mixture, so all oxygen in the reaction mixture was used to oxidize glucose.

By measuring the decrease of NADPH in the reaction mixture, it is possible to calculate the rate of conversion of substrate into product in µmol/min (U). This is because 1 mol of enzyme can be reduced by 1 mol NADPH, and 1 mol of enzyme can reduce 1 mol of substrate. Also, by knowing the amount of enzyme added to the reaction, it was possible to calculate the specific activity (U/mg) for different substrates (see Appendix 6).

We obtained the highest specific activities for the smallest unsaturated ketone and aldehyde (**1g** and **1j**). Larger substrates with longer chains decreased the *Ts*OYE activity. The activity was even lower for methylated cyclic enones (**1b**, **1e** and **1f**). Without any methylated group, 2-cyclohexen-1-one (**1d**) was one of the most preferred substrates out of the selection. The conversions of ß-methylated cyclic enones (**1b** and **1f**) gave the lowest activities.

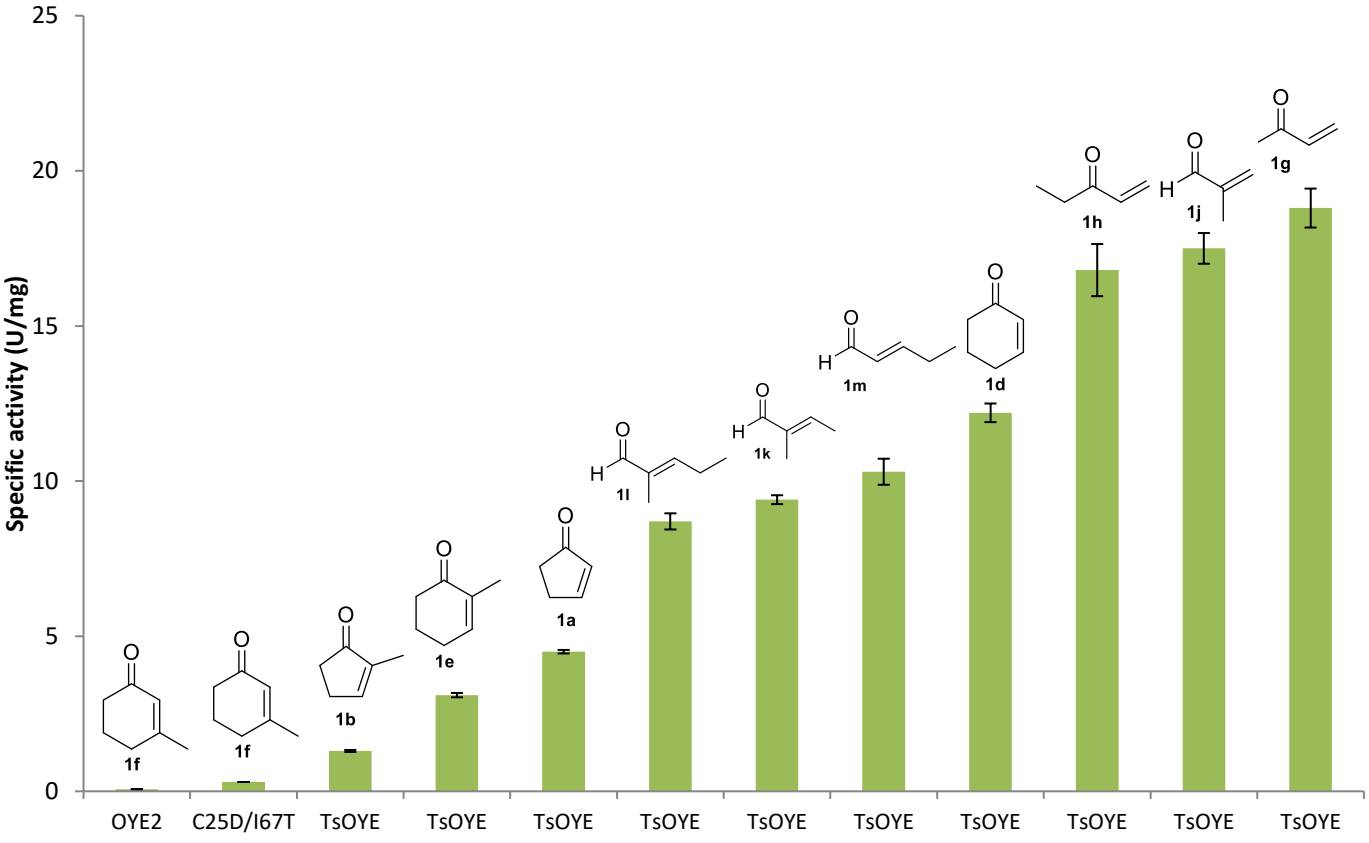

Figure 7. Specific activity of *Ts*OYE for different substrates. All substrates were tested in 50 mM Tris-HCl buffer pH 8.0 with 20 U/mL glucose oxidase (GOx), 20 mM glucose and 0.2 mM NADPH. Average of duplicates.

To determine what these activities would mean for the asymmetric reductions by *Ts*OYE, we performed 1-hour reactions in a Tris or ammonium formate buffer at pH 8.0 and 30 °C (Figure 8). We tried different preparations because of the suspected volatility of several substrates (see Materials and Methods). The synthetic cofactor benzyl nicotinamide (BNAH) was used for simplification of this first cascade step (see Appendix 7). BNAH is known to replace NADPH for OYEs and is an inexpensive alternative for screening.[36] We added a small excess of BNAH to the reaction when pre-dissolved in DMSO, because DMSO has a degrading impact on BNAH.

The 1-hour conversions of the cyclic unsaturated ketones showed that in different conditions, 10 mM of substrate was converted by *Ts*OYE. We screened some of the substrates where BNAH was directly added to the mixture instead of dissolving in DMSO first (Appendix 8). Nearly complete conversions were obtained for substrates **1a**, **1d**, **1e** and **1h**, moderate (<70%) ones in case of substrates **1l** and **1m** and no to very low conversions with 3-methyl-2-cyclopenten-1-one (**1c**) and 3-methyl-2-cyclohexen-1-one (**1f**) (Appendix 8). Regarding *trans*-2-methyl-2-pentenal (**1l**), we started the reaction with a mixture of both *cis* and *trans* isomers, preventing conversions above 50% as *Ts*OYE converts the *trans* isomer exclusively. 3-methyl-2-cyclohexen-1-one (**1f**) was reduced with the double mutant C25D/I67T, as described by Nett *et al.*, because this mutant accepts ß-methylated substrates better than wild-type *Ts*OYE.[35] OYE2 is also able to reduce these types of substrates, but gives the opposite enantiomer (*S* instead of *R*, Table 4).[35] 25 mM and 1 M ammonium formate buffer were not tested for **1f** because of the already low conversions with Tris buffer. The volatile, unsaturated aldehydes were inconsistent in product formation (Figure 8), which could be explained by the

evaporation of the compounds during the reactions. According to the conversions with Tris buffer, we observed that a 50 mM concentration of buffer salt was required in the reaction mixture. However, based on the reactions in ammonium formate, the high concentrations had limited effect on the reactions.

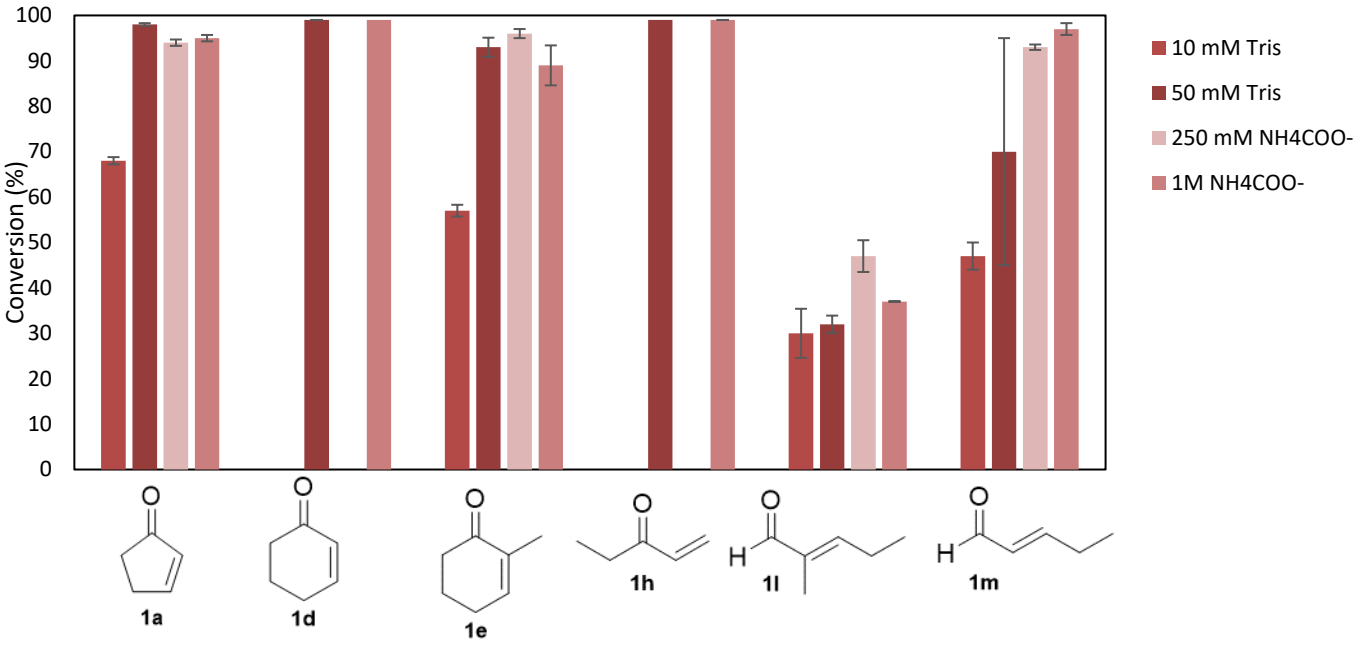

Figure 8. Conversions of different substrates by *Ts*OYE after 1 hour. The 15 mM BNAH was pre-dissolved in DMSO in the reaction mixture, so the mixture contained 10% v/v DMSO. **1d** and **1h** were only tested for 50 mM Tris and 1 M ammonium formate. Extraction was performed twice. Average of duplicates.

Table 4. Conversion of 10 mM 3-methylcyclohexenone by different OYE family members. [a]

Enzyme type	Conversion (%)	St. dev (%)	e.r. (*R*:*S*)
OYE2	20	0.5	1:99
***Ts*OYE C25D/I67T**	20	2.6	92:8

[a] Reaction conditions: 4 µM *Ts*OYE, 12 mM glucose and 10 mM NADH in a 50 mM Tris-HCl buffer at pH 8. e.r. = enantiomeric ratio.

Because of the low activity of *Ts*OYE for some substrates, we tested the reduction of **1b** and **1f** by different ERs from the Johnson Matthey enzyme kit (Table 5 and Table 6). Some of these ERs were already described in Bisagni *et al.*.[37] Table 5 showed that within 6 hours full conversion was obtained. However, we observed an enantiomeric excess of near 0%. From Table 6, we observe very low concentrations of enantiopure **2f**, not exceeding 2 mM. These ERs were unable to exceed the performance of the OYEs, so *Ts*OYE for **1b** and OYE2 for **1f** were considered the best options to proceed.

Table 5. Conversions from **1b** to **2b** by different ERs from the JM kit after 6 hours. Conversions were determined with peak areas on the GC.

Enzyme	Conversion (%)	e.e. (%)
ENE-107	>99	2.6
ENE-108	>99	2.9
ENE-109	82.9	3.3

Table 6. Conversions from **1f** to **2f** by different ERs from the JM kit after 24 hours. Concentrations were determined with calibration curves from Appendix 9.

Enzyme	Concentration (mM)	e.e. (%)
ENE-101	0.87	>99
ENE-102	0	>99
ENE-107	1.85	>99

4.3. Analysis of asymmetric reductions by TsOYE under different conditions

We screened the reduction of 2-methyl-2-cyclohexen-1-one (**1e**) under different conditions to determine its impact on the first step of the cascade (Figure 9). Two different types of cofactors were added to the reaction. The first option is to add NADPH, anhydrous glucose and GDH, forming the recycling system as described in the introduction. Another option is the addition of the synthetic cofactor BNAH, without any recycling system. The reactions were performed at a temperature of 30 °C for 1 hour. The conversions showed that the reaction was affected by the presence of high concentrations of ammonium formate buffer (Figure 10a). On the other hand, these effects are almost undetectable with BNAH as cofactor (Figure 10b). This showed that the recycling system was mostly affected by a high concentration of ammonium formate. Also, the conversions in pH 8.0 and pH 9.0 were similar, indicating that these changes would be unaffected by the *Ts*OYE.

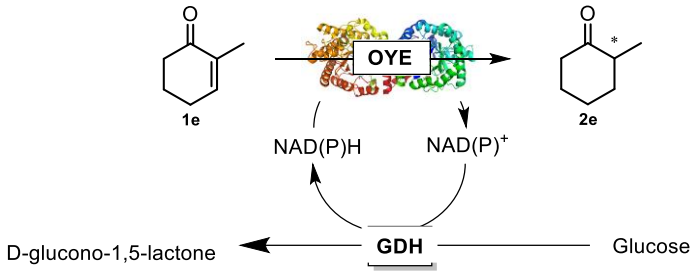

Figure 9. Scheme of the asymmetric reduction of 2-methyl-2-cyclohexen-1-one by *Ts*OYE.

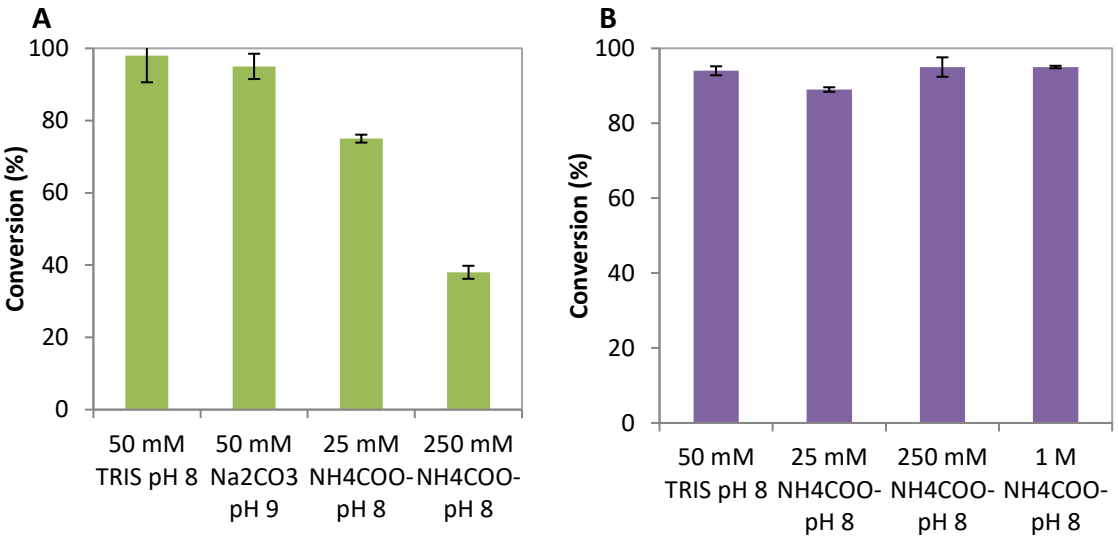

Figure 10. Conversions of 2-methyl-2-cyclohexen-1-one after 1 hour. Average of duplicates. Reaction conditions: 1% v/v DMSO, 2 µM *Ts*OYE and 10 mM 3-methyl-2-cyclohexen-1-one in different buffer types. A: with the GDH cofactor recycling system: 175 U/mL GDH-105 from Codexis, 0.1 mM NADPH, 12 mM glucose. B: with BNAH cofactor: 11 mM BNAH.

We investigated the impact of DMSO as well, because all substrates were prepared in a 1 M stock in DMSO. The DMSO amount in a reaction would be at least 1% v/v to ensure substrate solubilisation. This analysis was done at two different concentration of buffer, 25 and 250 mM of ammonium formate pH 8.0. We observed for both buffer concentrations a slight decrease in conversion when the percentage of DMSO was increased up to 20% v/v, but this slight decrease mostly occurred between 1 and 5 % v/v DMSO. Thus, using these amounts of DMSO would have nearly no impact on the conversions by *Ts*OYE. Compared with a buffer concentration of 250 mM, 1-hour reactions with 25 mM ammonium formate buffer resulted into slightly lower conversions (Figure 11).

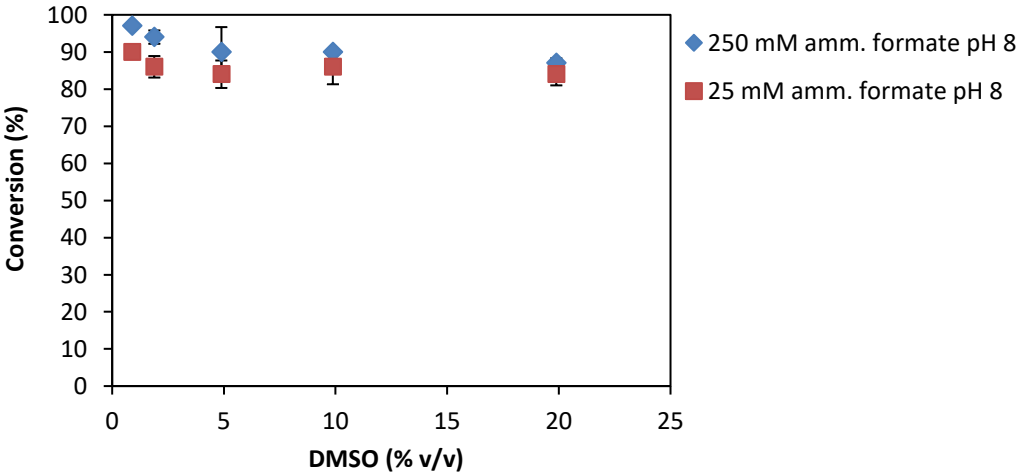

Figure 11. Conversions of 2-methylcyclohexenone to 2-methylcyclohexanone with different volume percentages of DMSO after 1 hour. Reaction conditions, 2 µM *Ts*OYE, 10 mM substrate, 0.1 mM NADPH cofactor and GDH recycling system. Average of duplicates.

To observe the effect on the reaction conditions on the *Ts*OYE from a kinetics perspective, we measured the specific activity of the *Ts*OYE to convert 2-cyclohexen-1-one under different conditions (Figure 12, see Appendix 6). The different *Ts*OYE batches had similar activities, showing that the same concentration of different batches provided an equal amount of enzyme activity in the reaction

mixture. High ammonium formate concentrations decreased the specific activity majorly (interestingly, this effect was not observed for the 1-hour conversion reactions above). Buffers at different pH showed that the reduction by *Ts*OYE decreased in pH 9.0 compared with pH 8.0. *Ts*OYE performed similarly in buffers with pH 7.0 and 8.0. The specific activity of *Ts*OYE, with and without 10 U/mg glucose oxidase (GOx) and 20 mM glucose, showed no difference. Nevertheless, this impact could be different for other substrates, hence we added GOx and glucose to determine the specific activity for each substrate (Figure 7).

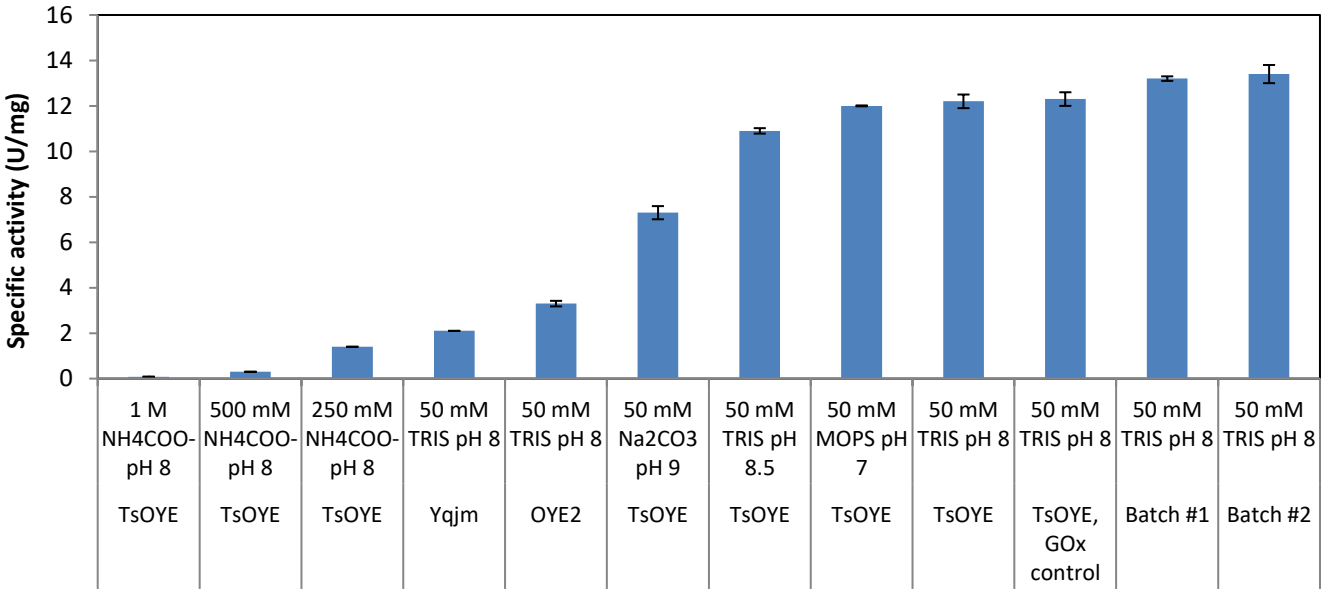

Figure 12. Specific activity of *Ts*OYE for substrate **1d** under different conditions with 0.2 mM NADPH. All experiments were performed with *Ts*OYE batch #3 unless noted otherwise. Average of duplicates.

Based on these results but also considering the optimum conditions of AmDHs, we still decided to proceed with a 1 M ammonium formate buffer. Because at pH 9.0 the *Ts*OYE activity would decrease even more, we decided to use a pH 8.0 in our cascades. Two enzymes would use the same recycling system, so the quantities of glucose and NAD(P)H were doubled compared to the 1-hour reactions.

4.4. Bi-enzymatic cascade reactions

We performed multiple cascade reactions to produce chiral amines (see Figure 13 and Figure 14). This was possible with the aid of the different AmDHs provided by the group at the Genoscope (see Materials and Methods). Based on their observations, we combined the OYEs with different AmDHs for different substrates (Table 7).

We tested multiple combinations to eventually finish as much different and pure amines as possible (Appendix 4). In the end, not all substrates were put into a cascade reaction. **1j** was too volatile to elute it on the GC column. **1c** and **1l** showed poor conversions for any of the AmDHs. If we had more time for experiments, cascades with **1h**, NADPH and *Cfus*AmDH or *Msme*AmDH would be tested.

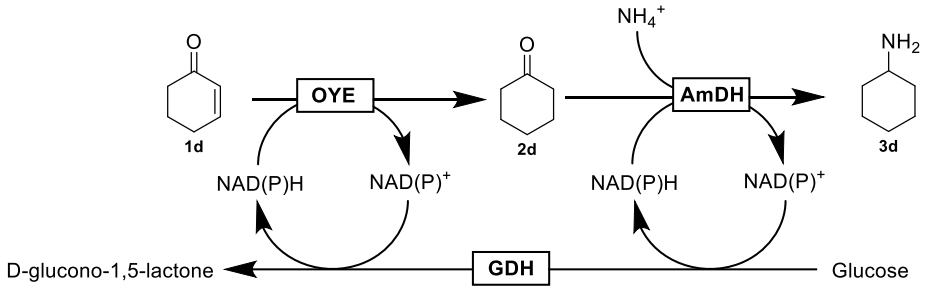

Figure 13. Example of a bi-enzymatic cascade reaction where 2-cyclohexen-1-one (**1d**) is first reduced (**2d**), before reductive amination with ammonia to form the targeted amine (**3d**).

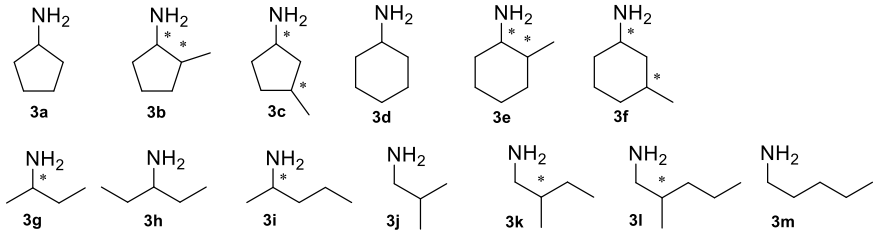

Figure 14. Overview of all desired amines produced by the enzymatic cascade.

Table 7. Overview of proposed bi-enzymatic cascade combinations. [a]

Substrate	ER	AmDH	Spec. Act.	Cofactor	Enantiomer
1a	*Ts*OYE	MATOU-568	+	NADPH	-
1b	*Ts*OYE	*Msme*AmDH	+/-	NADPH	(*R*)
1d	*Ts*OYE	MATOU-568	+	NADPH	-
1e	*Ts*OYE	MATOU-568	+	NADPH	(*R*,*S*)
1f	OYE2	*Msme*AmDH	+	NADPH	(*S*,*S*)
1g	*Ts*OYE	*Msme*AmDH	+	NADPH	(*S*)
1i	*Ts*OYE	*Msme*AmDH	+/-	NADPH	(*S*)
1k	*Ts*OYE	*Apau*AmDH	++	NADH	(*R*)
1m	*Ts*OYE	MATOU-568	+/-	NADPH	-

[a] Reaction conditions: 1 M ammonium formate buffer pH 8.0, 10 mM substrate, 24 mM glucose, 0.2 mM NAD(P)H, 3 U/mL GDH-105, 10 µM *Ts*OYE or 20 µM OYE2, 0.5 mg/mL AmDH.

With the aid of calibration curves (Appendix 9), we quantified the concentration for five amines (Figure 15). For other cascades where the standard amine was not available, conversions were calculated based on the GC peak area of the amine compared to the total area of substrate, intermediate and amine combined (Figure 16). Also, by derivatising with acetic anhydride (Appendix 10), we determined the enantiomeric and diastereomeric excess.

The cascades with the cyclic pentenones (**1a**, **1b**) showed poor to moderate amine concentrations. **1a** and **2a** were for both *Ts*OYE as AmDH moderate substrates. Also, **1b** and **2b** gave poor conversions for both substrates, and racemized in the reaction mixture. The cyclic hexenones (**1d**-**1f**) gave moderate to good conversions, both **3e** and **3f** were obtained in high e.e. and d.e.. However, **1f** resulted in low amounts of amine, which was not surprising based on previous results. Furthermore, **1m** was a poor substrate for *Ts*OYE, and **2m** was a bad substrate for the AmDHs.

The non-cyclic unsaturated ketones (**1g**, **1i**) were good to excellent substrates for *Ts*OYE, but poor for the AmDH. Nevertheless, **3g** was observed with high conversion, and high e.e. (92%). The pentylamine (**3i**) was quantified to 1.1 mM. Because of the low concentration of amine, it was hard to

determine on GC with a low signal what was the e.e.. Despite the difficulty, we observed an excellent enantiomeric excess of 99%.

1k was the best performing substrate with estimated corresponding amine concentration of 9.7 mM out of 10 mM of substrate. However, the derivatisation resulted into poor separation of the different enantiomer peaks, thus we estimated the e.e. to be approximately 60%.

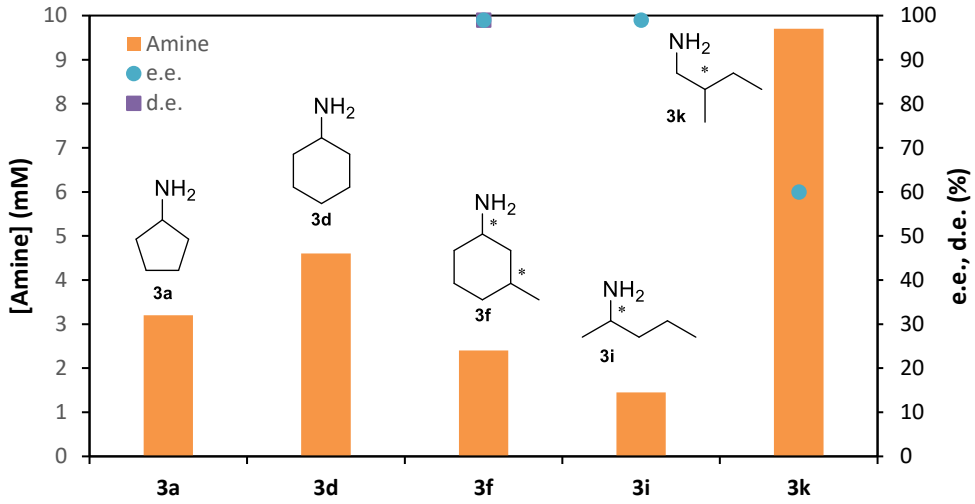

Figure 15. Amine quantifications after 24-hour cascade reactions with different substrates. Cascade contained 1 M ammonium formate, 3 U/mL GDH-105, 24 mM glucose, 0.2 mM NAD(P)$^+$, 0.5 mg/mL AmDH, 10 µM *Ts*OYE or 20 µM OYE2 (1f) and 10 mM substrate in DMSO.

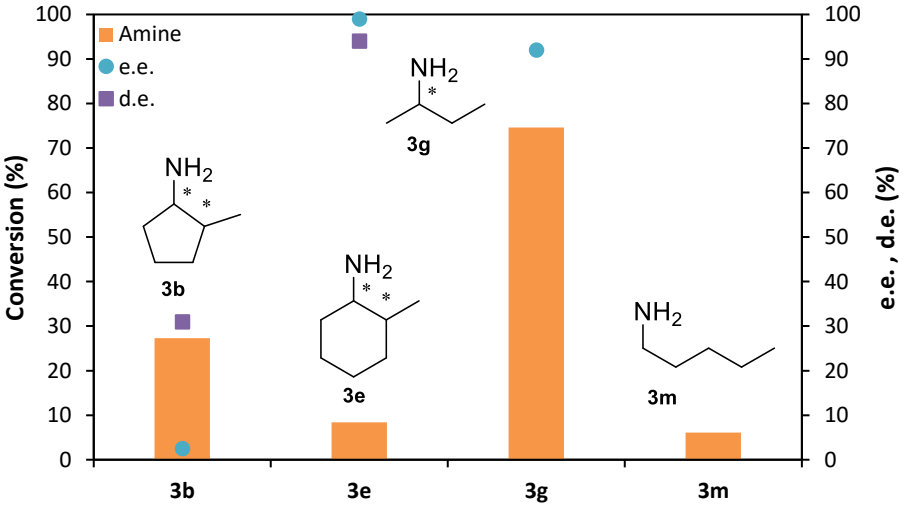

Figure 16. Conversions to amines after 24-hour cascade reactions with different substrates. Cascade contained 1 M ammonium formate, 3 U/mL GDH-105, 24 mM glucose, 0.2 mM NAD(P)$^+$, 0.5 mg/mL AmDH, 10 µM *Ts*OYE and 10 mM substrate in DMSO.

Interestingly, in the case of substrates **1d**, **1e**, **1i** and **1k**, we observed the formation of the corresponding alcohol product (Figure 17). These alcohols were identified with reference standards and quantified when possible with GC (Appendix 11). These products were unexpected, so several control reactions were performed in order to find the cause of this alcohol formation (Appendix 12). We observed no alcohol formation in the absence of AmDH. From the data obtained, we determined that this by-product formation is catalysed by the AmDHs, but further studies are required to confirm these results.

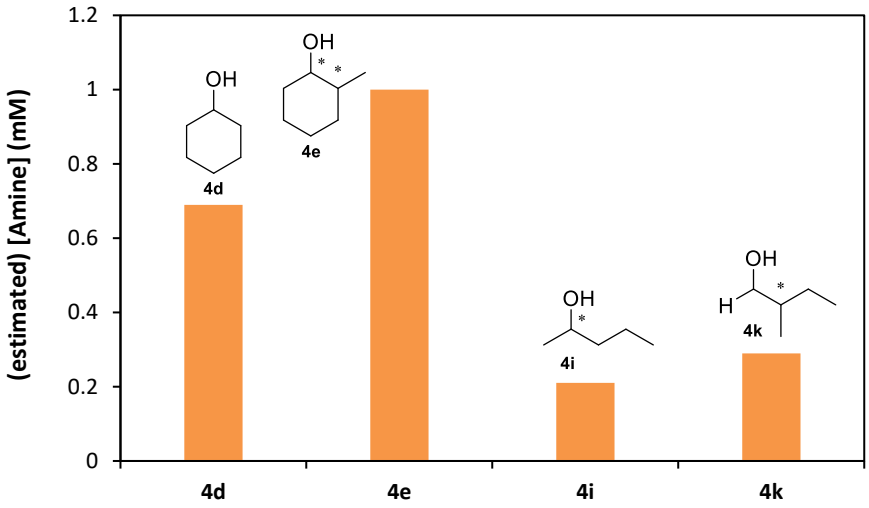

Figure 17. Estimations of alcohol concentrations for different substrates. Cascade contained 1 M ammonium formate, 3 U/mL GDH-105, 24 mM glucose, 0.2 mM NAD(P)$^+$, 0.5 mg/mL AmDH, 10 µM *Ts*OYE and 10 mM substrate in DMSO.

As AmDH-catalysed reactions are typically run at pH 9.0 to 10.0, we investigated the impact of the lower pH we used on the formation of amine and alcohol. At pH 8.0, 8.5 and 9.0, the same cascade for **1d** was performed (Figure 18, see Appendix 13). We obtained the highest amine concentration with pH 9.0. We observed slight alcohol formation when the pH was 8.0. This formation was as good as negligible at pH 9.0.

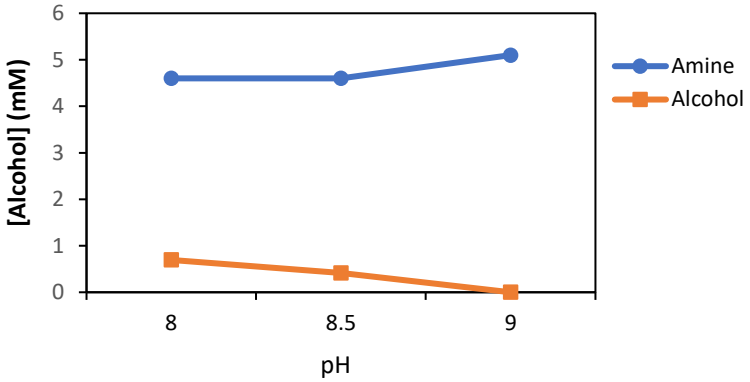

Figure 18. pH-impact on formation of the desired amine (cyclohexylamine) and the alcohol (cyclohexanol) as by-product.

We tested the AmDH-3 from the JM kit with the conditions as recommended by JM, and compared them with the conditions previously used with our AmDHs (Figure 19). The conditions as described in the JM kit, are a 2 M ammonium chloride buffer, pH 9.6, with substrate stocks in isoamyl acetate. We tested the 1 M ammonium formate buffer we used before and observed very poor concentrations of **3i** after 24 h. With 2 M ammonium chloride, pH 9.6, we obtained much higher amine concentrations than with a 1 M ammonium formate buffer pH 8.0. We also observed that 20% v/v of a co-solvent, isoamyl acetate, decreased the conversions.

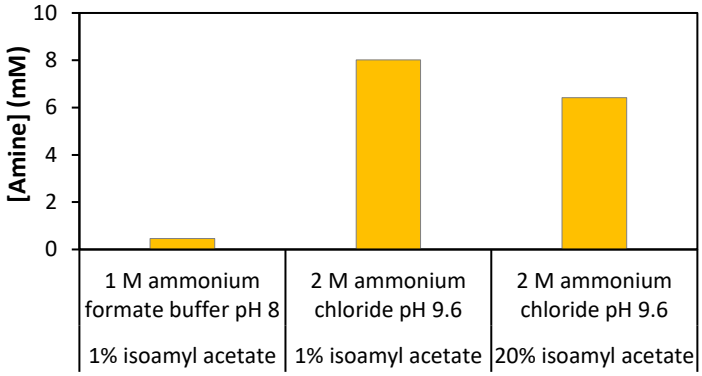

Figure 19. Amine concentrations obtained from 24-hour conversions from **2i** to **3i** by AmDH-3.

5. Discussion

5.1. Determining concentrations of purified enzyme

With the aid of UV-measurements, we successfully quantified the concentrations of different purified OYE stocks (Table 3). OYEs have a specific pattern over a wavelength from 300 nm to 600 nm.[23] However, the flavin incorporated into the enzyme has an influence on this effect. By adding a detergent, the flavin is released, and a spectrum of the real OYE concentration is shown.

5.2. Substrate screening

We established the substrate preferences of *Ts*OYE with the aid of measuring the specific activities for different substrates (Figure 7). For instance, α-methylation of the unsaturated ketone or aldehyde decreased the specific activity of *Ts*OYE. This pattern is clear for the cyclic substrates, because **1d** and **1a** give higher activities than **1e** and **1b**, respectively. ß-methylation of the substrate is unfavoured by *Ts*OYE. This could be explained by the substrate coordination in the active site. By adding a methyl group, the substrate does not longer fit into the active site. The double mutation improves the substrate positioning, despite that the specific activity is still low for **1f**.

We observe that smaller substrates result into higher specific activities of *Ts*OYE. **1g** and **1j** showed the highest activity of our substrate scope, followed by **1h**. This is probably because smaller substrates fit better into the *Ts*OYE active site. The activity towards different aldehydes indicate that also the length of the carbon chain has an impact, as **1k** has higher activity than **1l**. Also, based on the activities towards **1m**, **1k** and **1l**, we postulate that the α-methylation of the substrate has a larger impact on fitting into the active site than a longer carbon chain.

The reduction **1b** to **2b** with the ERs from Johnson Matthey (Table 5) shows this substrate is a great fit for ENE-107 and ENE-108. However, we observed complete racemization of **2b**, which is undesired for producing enantiopure compounds. If we applied this in a cascade, we would alter the reaction conditions to prevent high amounts of **2b** in the reaction mixture. In this way, **2b** would undergo reductive amination before it racemizes. Each enzyme tested for the reduction of **1f** into **2f** resulted into low intermediate concentrations. ß-methylated substrates are not suitable for these ERs, and it suggests that OYE2 is still the best performing ER to ß-methylated enones such as **1f**.

From the 1-hour conversions of several substrates in different buffer conditions, we observed that with BNAH as cofactor, *Ts*OYE was still capable to perform full conversion of **1d** to **2d** (Figure 10). The synthetic cofactor BNAH is more stable than NAD(P)H and improved the reaction rate. Also, the mechanism does not use a recycling system, so there is no rate limitation by such a system. The reactions with GDH are affected more significantly, indicating that the recycling system is the rate limiting step.

5.3. Impact of different conditions on *Ts*OYE performance

By screening multiple conditions of the reaction mixture, we determined the performance of *Ts*OYE under different, non-optimal conditions. We observed that high concentrations of buffer salts decrease the asymmetric reduction when a recycling system with GDH was present (Figure 10). This is probably because the ionic strength has a negative effect on enzyme activity, in this case GDH.[38] Nevertheless, high concentrations of ammonium are required for the AmDHs. The Genoscope performed experiments where higher concentrations of ammonium containing buffers ameliorated the amine production from saturated ketones and aldehydes. The optimal conditions for both enzymes cannot be accomplished in the same reaction mixture, so there should be a compromise to some extent. It is also known that OYEs have a higher activity than the AmDHs under the same conditions. So, regarding the type of buffer, the optimal conditions for the AmDHs are more important than for *Ts*OYE.

We also observed that the activity of *Ts*OYE decreased by 40% when the pH was increased from pH 8.0 to 9.0 (Figure 12). As is shown in Pesic *et al.*, the specific activity of YqjM, which is also a class III ER, the pH optimum is approximately 7.0.[39] Based on those experiments to obtain an optimal pH, we would expect for *Ts*OYE that the activity around pH 6-7 remains consistent, while the activity drops from pH 8.0. We observe a decrease similar of the drop-in activity of the YqjM, but we would expect an increase in activity when the pH is 7.0, which was not the case (Figure 12). This could be explained because the pH is too far from the optimum for an increased activity. Another reason would be that the measurements at different pH were also performed with different buffers, so at the same pH, an enzyme does has a different specific activity.[40]

Tyrosine plays an important role as proton donor in the *Ts*OYE reduction mechanism. The phenol of the tyrosine moiety has a pKa of 10.1, which means that 7.4% is deprotonated in pH 9.[38] It is already shown that the absence of this tyrosine has a major negative impact on the specific activity of *Ts*OYE.[24] Especially the tyrosine near the active site, Tyr177, is involved in substrate stabilization and protonation, which means that at higher pH the substrate in the enzyme is less stabilized and protonation becomes rate limiting. This would result in the decrease in enzyme activity.

5.4. Reaction mechanism AmDH

When we dived into the proposed mechanism by Mayol *et al.*, we noticed that the mechanism suggests it is dependent on the charge interactions between positively charged ammonium and the negatively charged glutamate residue (Figure 4).[5] However, ammonium has a pKa of 9.25, so at pH 8.0. 5% of the ammonium is deprotonated, and at pH 9.0, this is even 36%. When ammonium is protonated, it is not nucleophilic. So, the idea that ammonium attacks the carbonyl group of the substrate, while interacting with the glutamate side chain, is debatable.

It is more likely that the negative charge induces electrostatic interactions with the iminium intermediate instead of interacting with the amine donor. We would expect a mechanism as proposed by Tseliou *et al.*.[41] If we apply this mechanism to the AmDHs we used, we would expect that the amine donor directly attacks the substrate carbonyl group, positioned by hydrogen-bonding with the tyrosine (*Apau*AmDH) or tryptophan residue (*Cfus*AmDH and *Msme*AmDH). Then, an iminium intermediate, stabilized by the negatively charged glutamate residue, is formed by releasing water. This mechanism

shows that this hydrogen bonding is only predicted for one of the enantiomers (*R*), which probably explains how the enantioselectivity of the AmDHs is achieved.[41] Finally, NAD(P)H donates a hydride, and so the amine is released from the active site.

5.5. Reductive amination by AmDH-3 under different buffer conditions

In a 1 M ammonium formate buffer, AmDH-3 catalyses poor amounts of **2i** into **3i** after 24 hours (Figure 19). In the cascade, 1.5 mM of **3i** was obtained with *Msme*AmDH (Figure 15). So, replacing the AmDH will have a negligible or even negative impact on the cascade. However, with a 2 M ammonium chloride buffer pH 9.6, the AmDH-3 provides much higher concentrations of **3i**. This is probably because a higher buffer concentration also means higher concentrations of amine donor that are used by the AmDH. Also, according to JM, the optimal pH of AmDH-3 lies between 9.0 and 10.0. Furthermore, because of the high pH, most ammonium in the mixture is deprotonated (69%) and can therefore act as a nucleophile. As mentioned before, the high pH and buffer concentration decrease the activity of OYEs, so it is the question if this would improve the amine production when incorporated into a cascade.

Since product inhibition could occur at AmDHs, JM recommended to add an organic layer (20% v/v) because it will function as a product sink.[26] However, compared with 1% v/v organic solvent, in this case isoamyl acetate, 20% v/v decreased the amine concentration (Figure 19). We possibly observed no improvement because the 10 mM concentration we used in the reaction mixture is too low to inhibit more product formation.

5.6. Impact of pH on cascade reaction

We observed alcohol formation for different cascades with different AmDHs (MATOU-568, *Msme*AmDH and *Apau*AmDH) (Figure 17). Based on control reactions for these substrates, we determined that the alcohol formation occurs when the AmDH is present in the cascade mixture (Appendix 13). It is possible that the substrate is stabilized in the active site in absence of deprotonated ammonium, since the pH 8.0 is below the pKa of ammonium. This would enable the direct reduction of the saturated ketone into alcohols by NAD(P)H even if crystallographic data obtained to date positioned the hydride too far from the carbon of the ketone to be directly reduced.

The amount of amine observed at different pH (Figure 18) was slightly altered due to the formation of the alcohol product. At pH 9.0, the amine concentration is higher than at pH 8.5 and 8.0. As mentioned in the previous paragraph, more ammonium is deprotonated in higher pH, which allows the formation of the iminium intermediate. It also seemed that at higher pH less alcohol is formed. Because more deprotonated amine is in the reaction mixture, it is possible that the reductive amination outperforms the direct reduction of the carbonyl group. Also, as discussed before, we expect that the mechanism is dependent on the deprotonated ammonium concentrations, that are in excess in more basic conditions. Despite that pH 9.0 is less suitable for *Ts*OYE, the activity is still enough to convert most of **1d**. Surprisingly, we observed less unsaturated ketone at pH 9.0 than at pH 8.0. It is possible that the discrepancies in calibration curves cause this outcome.

5.7. General thoughts on proposed cascades

As described in the introduction, cascades increase the efficiency compared to running the reactions catalysed by OYEs and AmDHs separately. We observe that this cascade enables the production of moderate to good quantities of amines after 24 hours, with a high enantiomeric and diastereomeric excess. Also, this cascade connects the cofactor recycling system with both OYE as AmDH. This makes this cascade a more efficient system than for example cascades with combining ERs with TAs.[31] One main drawback of this cascade is the required high concentration of ammonia which drastically decreased the *Ts*OYE activity.

TAs are useful for forming an amine from a prochiral substrate, and in contrast with AmDHs, TAs are also applied to produce chiral amines from racemic mixtures by kinetic resolution.[11-12] Several examples show that with the aid of dynamic kinetic resolution conversions over 50% are possible.[12] In general, a cascade is simpler without dynamic kinetic resolution, because the performance is dependent of less parameters. For our cascade, some substrates occur in mixtures with both *cis* and *trans* isomers, from which a conversion of 50% is the maximum. *Cis* and *trans* isomers have many property differences, such as boiling point and polarity.[42] Because of these differences it is easier to purify an isomer than an enantiomer.

By combining two enzymes into producing amines, there is the challenge that both enzymes could catalyse the same substrate. However, the products of the unsaturated ketones and aldehydes reduced efficiently by OYEs, are not easily converted to the amine by the AmDHs, and *vice versa*. AmDHs have a limited substrate scope, which makes these enzymes less favourable than for example IREDs. Using different enzyme combinations could improve the amine productions. For instance, Pushpanath *et al*. showed AmDHs capable of the amination of multiple aromatic ketones.[26] Combining other enzymes with OYEs could give a new substrate scope that is produced in higher quantities. The current substrate scope contained several volatile compounds. We experienced issues in the total balance in some cascades, which could suggest evaporation of the substrate, intermediate or product.

We also observed that some substrates (**1b**, **1k** and **1l**) are prone to racemization of the intermediates (**2b**, **2k** and **2l**). It would be favourable that the *Ts*OYE is the rate limiting step in our cascade, so there is no chance of racemization of the intermediate. Possible solutions are for example increasing the AmDH concentration in the reaction mixture or decreasing the OYE concentration.

We are aware that in bi-enzymatic cascades the optimal reaction conditions for both enzymes are difficult to realise in one reaction mixture. OYEs lose lots of activity to satisfy the conditions of the AmDHs. Besides *Ts*OYE, GDH also clearly suffered from high ammonium formate concentrations. The only compromise in this cascade is the pH, as the optimal pH of *Ts*OYE (pH 6.3) is much lower than for the AmDHs (pH 9.0). The formation of alcohol in lower pH arises the question if this crooked compromise is too much of a compromise for the AmDH.

We observed that this cascade shows promising advantages but is not ready yet to produce chiral amines with the used OYEs and AmDHs on a larger scale. We still think that this combination of enzymes is a good solution for our goal. What could improve the outcome of these cascade is to fit OYEs with AmDHs that show more similar substrate preferences. For instance, this could be achieved by screening other ERs that match the substrate scope of the native AmDHs. Another alternative is to screen different AmDHs to obtain the most activity. For instance, under optimal conditions, MATOU-

568 has shown activities up to 11 U/mg towards aldehydes.[29] Finally, protein engineering is possibly a solution to obtain a wide variety of chiral amines. An example is the mutation of an AADH into an AmDH, which enabled the reductive amination of prochiral ketones with a specific activity of 0.69 U/mg.[27] Protein engineering provides many possibilities, and we will expect that this will improve the chiral amine production in the near future.

5.8. Conclusions

Our goal was to establish a bi-enzymatic cascade with the *Ts*OYE and AmDH enzymes to produce various chiral amines. We determined the capability of the cascades by determining the reaction conditions of each step, and the enantiopurity, the diastereomeric excess and conversion from substrate to amine. We designed an efficient bi-enzymatic cascade capable of producing chiral amines with high enantioselectivity and diastereomeric excess (both 99%). Before considering chiral amine production on a larger scale, there is still room for improvement, because most cascades resulted into amine concentrations of 5 mM when started with 10 mM substrate. Nevertheless, the combination of these types of enzymes shows potential to produce chiral amines efficiently.

6. Recommendations for further work

Because of COVID-19 pandemic outbreak in the Netherlands, we were not able to perform all experiments we had in mind to complete this thesis:

- Measure the specific activity of *Ts*OYE reducing **1i**. This is the only substrate where no activities were measured, so this should be done for completeness of the substrate scope analysis.
- New control reactions for substrate **4i** and extract the reaction mixtures with MTBE. This is necessary to confirm that in each control reaction no alcohol was formed without AmDHs.

The following experiments are recommended for further research:

- Perform other designed cascades at pH 9.0 besides substrate **1d** to confirm the absence of the alcohol by-product, and to determine the impact on amine production.
- Establish the cascade conditions in such a matter that the *Ts*OYE reduction is the rate limiting step, such as increasing the AmDH concentrations or decrease the *Ts*OYE concentrations. This would decrease the racemization for some of the substrates from our scope.
- Increase the substrate concentration in the reaction mixture and determine when an organic layer would function as a product reservoir.
- Try out reductive aminations with the native AmDHs in the ammonium chloride buffer. For the AmDH-3 from the JM kit this was a better buffer than the ammonium formate buffer we used, but we did not test this with the native AmDHs from Genoscope.
- Under the right conditions, AmDH-3 from Johnson Matthey is a good enzyme for reductive amination of non-aromatic ketones. Ketones from the substrate scope as **2g** and **2h** fit this profile, but testing AmDH-3 for these enzymes in a cascade should be performed in a higher pH, based on Figure 19, to observe any improvement of the whole cascade.
- Find AmDHs that match the substrate scope of ERs as much as possible. For instance, combine *Ts*OYE with AmDHs that can perform aromatic ketones and aldehydes.

7. Acknowledgements

I would like to thank Dr. C.E. Paul for the opportunity to perform my thesis in the research group BOC. I am also thankful for her great supervision and involvement in the progress of the thesis. I would also like to thank all technicians for making the laboratory work possible. Especially R.J.C. Oosten, L. Koekkoek-van der Weel and M.J.F. Strampraad were very helpful for showing different techniques I needed and guiding me through the laboratory. I would like to thank A. Fossey for intensive screening of AmDHs. Furthermore, , I would like to thank Dr.ir. C. Vergne-Vaxelaire, A. Fossey and Dr. O. Mayol from Genoscope and A. Caparco, A. Bommarius and J. Champion from Georgia Tech Institute for this collaboration and the opportunity to progress with my research by using AmDHs they produced and characterized. Finally, I would like to thank Johnson Matthey for sending an enzyme kit that we could use to try more enzyme combinations.

8. References

[1] N. J. Turner, *Nat. Chem. Biol.* **2009**, *5*, 568-574.
[2] K. Faber, *Biotransformations in Organic Chemistry*, 7th ed., Springer, Cham, Switzerland, **2018**.
[3] D. Ghislieri, N. J. Turner, *Top. Catal.* **2014**, *57*, 284-300.
[4] Z. H. Guan, K. Huang, S. Yu, X. Zhang, *Org. Lett.* **2009**, *11*, 481-483.
[5] O. Mayol, K. Bastard, L. Beloti, A. Frese, J. P. Turkenburg, J.-L. Petit, A. Mariage, A. Debard, V. Pellouin, A. Perret, V. de Berardinis, A. Zaparucha, G. Grogan, C. Vergne-Vaxelaire, *Nat. Catal.* **2019**, *2*, 324-333.
[6] A. Scholtissek, D. Tischler, A. Westphal, W. van Berkel, C. Paul, *Catal.* **2017**, *7*, 130.
[7] I. R. Shaikh, *Journ. Catal.* **2014**, 35.
[8] F. G. Mutti, J. Sattler, K. Tauber, W. Kroutil, *ChemCatChem* **2011**, *3*, 109-111.
[9] M. D. Patil, G. Grogan, A. Bommarius, H. Yun, *ACS Catal.* **2018**, *8*.
[10] O. Verho, J. E. Bäckvall, *J. Am. Chem. Soc.* **2015**, *137*, 14.
[11] S. A. Kelly, S. Pohle, S. Wharry, S. Mix, C. C. R. Allen, T. S. Moody, B. F. Gilmore, *Chem. Rev.* **2018**, *118*, 349-367.
[12] D. Koszelewski, K. Tauber, K. Faber, W. Kroutil, *Trends Biotechnol.* **2010**, *28*, 324-332.
[13] J. H. Schrittwieser, S. Velikogne, W. Kroutil, *Adv. Synth. Catal.* **2015**, *357*.
[14] P. N. Scheller, M. Lenz, S. C. Hammer, B. Hauer, B. M. Nestl, *ChemCatChem* **2015**, *7*, 3239-3242.
[15] G. A. Aleku, S. P. France, H. Man, J. Mangas-Sanchez, S. L. Montgomery, M. Sharma, F. Leipold, S. Hussain, G. Grogan, N. J. Turner, *Nat. Catal.* **2017**, *9*, 961-969.
[16] W. Kroutil, M. Rueping, *ACS Catal.* **2014**, *4*, 2086-2087.
[17] J. H. Schrittwieser, S. Velikogne, M. Hall, W. Kroutil, *Chem. Rev.* **2018**, *118*, 270-348.
[18] S. P. France, L. J. Hepworth, N. J. Turner, S. L. Flitsch, *ACS Catal.* **2017**, *7*.
[19] F. G. Mutti, T. Knaus, N. S. Scrutton, M. Breuer, N. J. Turner, *Science* **2015**, *349*, 1525-1529.
[20] E. Tassano, M. Hall, *Chem. Soc. Rev.* **2019**, *48*, 5596-5615.
[21] S. Kara, J. H. Schrittwieser, S. Gargiulo, Y. Ni, H. Yanase, D. J. Opperman, W. J. H. van Berkel, F. Hollmann, *Adv. Synth. Catal.* **2015**, *357*, 1687-1691.
[22] H. S. Toogood, N. S. Scrutton, *ACS Catal.* **2019**, *8*, 3532-3549.
[23] D. J. Opperman, L. A. Piater, E. van Heerden, *J. Bacteriol.* **2008**, *190*, 3076-3082.
[24] D. J. Opperman, B. T. Sewell, D. Litthauer, M. N. Isupov, J. A. Littlechild, E. van Heerden, *Biochem. Biophys. Res. Commun.* **2010**, *393*, 426-431.
[25] C.-I. Brändén, J. Tooze, *Introduction to protein structure*, 2nd ed., Garland Pub., New York, **1999**.
[26] A. Pushpanath, E. Siirola, A. Bornadel, D. Woodlock, U. Schell, *ACS Catal.* **2017**, *7*, 3204-3209.
[27] M. J. Abrahamson, E. Vazquez-Figueroa, N. B. Woodall, J. C. Moore, A. S. Bommarius, *Angew. Chem., Int. Ed. Engl.* **2012**, *51*, 3969-3972.
[28] O. Mayol, S. David, E. Darii, A. Debard, A. Mariage, V. Pellouin, J. L. Petit, M. Salanoubat, V. de Berardinis, A. Zaparucha, C. Vergne-Vaxelaire, *Catal. Sci. Technol.* **2016**, *6*, 7421-7428.
[29] A. Caparco, E. Pelletier, J. L. Petit, A. Fossey, B. Bommarius, V. Berardinis, A. Zaparucha, J. Champion, A. Bommarius, C. Vergne-Vaxelaire, *Adv. Synth. Catal.* **2020**.
[30] D. Monti, M. C. Forchin, M. Crotti, F. Parmeggiani, F. G. Gatti, E. Brenna, S. Riva, *ChemCatChem* **2015**, *7*, 3106-3109.
[31] L. Skalden, C. Peters, L. Ratz, U. T. Bornscheuer, *Tetrahedron* **2016**, *72*, 7207-7211.
[32] E. Millipore, *User Guide: Amicon® Ultra-15 Centrifugal Filter Devices*, **2012**.
[33] G. Healthcare, *Instructions 52-1308-00 BB: PD-10 Desalting Columns*, **2007**.
[34] Uptima, *BC Assay: Protein Assay Kit*, **n.y.**
[35] N. Nett, S. Duewel, A. A. Richter, S. Hoebenreich, *ChemBioChem* **2017**, *18*, 685-691.
[36] T. Knaus, C. E. Paul, C. W. Levy, S. de Vries, F. G. Mutti, F. Hollmann, N. S. Scrutton, *J. Am. Chem. Soc.* **2016**, *138*, 1033-1039.

[37] B. Domínguez, U. Schell, S. Bisagni, T. Kalthoff, *Johnson Matthey Technol. Rev* **2016**, *60*, 243-249.
[38] H. Bisswanger, *Practical enzymology*, 2nd, completely rev. ed., Wiley-Blackwell, Weinheim, **2011**.
[39] M. Pesic, E. Fernándeez-Fueyo, F. Hollmann, *Front. Microbiol.* **2017**, *2*, 3866-3871.
[40] A. Cornish-Bowden, *Fundamentals of enzyme kinetics*, 4th, completely revised and greatly enlarged edition. ed., Wiley-Blackwell, Weinheim, Germany, **2012**.
[41] V. Tseliou, M. F. Masman, W. Bohmer, T. Knaus, F. G. Mutti, *ChemBioChem* **2019**, *20*, 800-812.
[42] J. Clayden, N. Greeves, S. G. Warren, *Organic chemistry*, 2nd ed., Oxford University Press, Oxford ; New YorK, **2012**.

9. Appendices

Appendix 1: SDS-PAGEs of purified OYEs

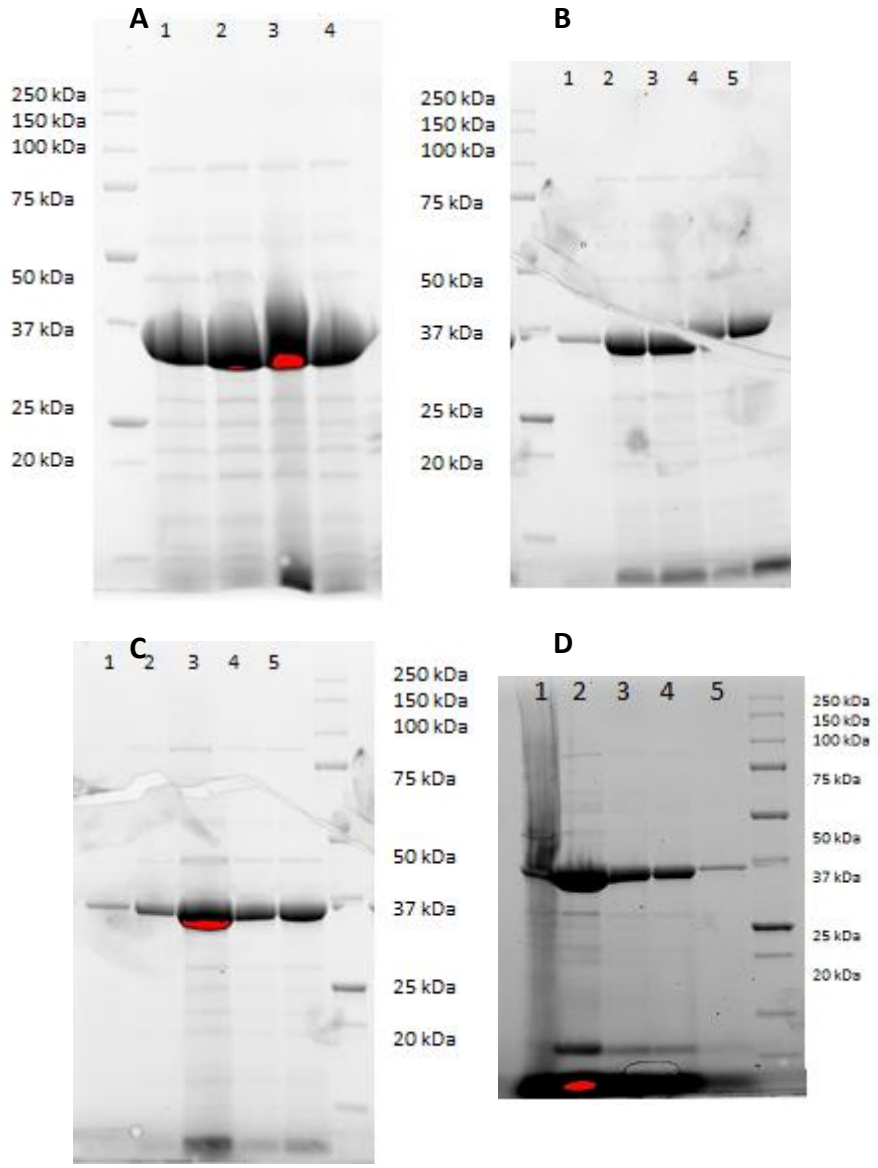

Figure A1.1. Sodium dodecyl sulphate polyacrylamide gel electrophoresis (SDS-PAGE) of OYEs. Each sample was prepared by adding an equivalent volume of Laemmli buffer. From this mixture, 15 µL was loaded onto the gel. A: Lane 1: First batch of *Ts*OYE after desalting. 2: Second batch of TsOYE after desalting. 3: First batch of *Ts*OYE C25D/I67T after desalting. 4: Second batch of *Ts*OYE C25D/I67T after desalting. B: Enzyme purification of *Ts*OYE WT. Lane 1: 10 µL sample after heat incubation/centrifugation. 2: 1 µL first batch of purified enzyme after desalting. 3: 10 µL of first batch flow through after desalting. 4: 1 µL second batch of purified enzyme after desalting. 5: 10 µL of second batch flow through after desalting. C: Enzyme purification of *Ts*OYE C25D/I67T. Lane 1: 10 µL sample after heat incubation and centrifugation. 2: 1 µL first batch of purified enzyme after desalting. 3: 10 µL of first batch flow through after desalting. 4: 1 µL second batch of purified enzyme after desalting. 5: 10 µL of second batch flow through after desalting. D: Purification steps of *Ts*OYE from 25 October. Lane 1: 11 µL dissolved cell pellet (from suspending with 25 µL Milli-Q and 25 µL Laemmli buffer). 2: 10 µL broth after heat purification. 3: 2 µL of enzyme before adding FMN excess. 4: 2 µL desalted and final *Ts*OYE. 5: 10 µL flow through after desalting.

Appendix 2: Determination of enzyme concentrations by UV spectroscopy

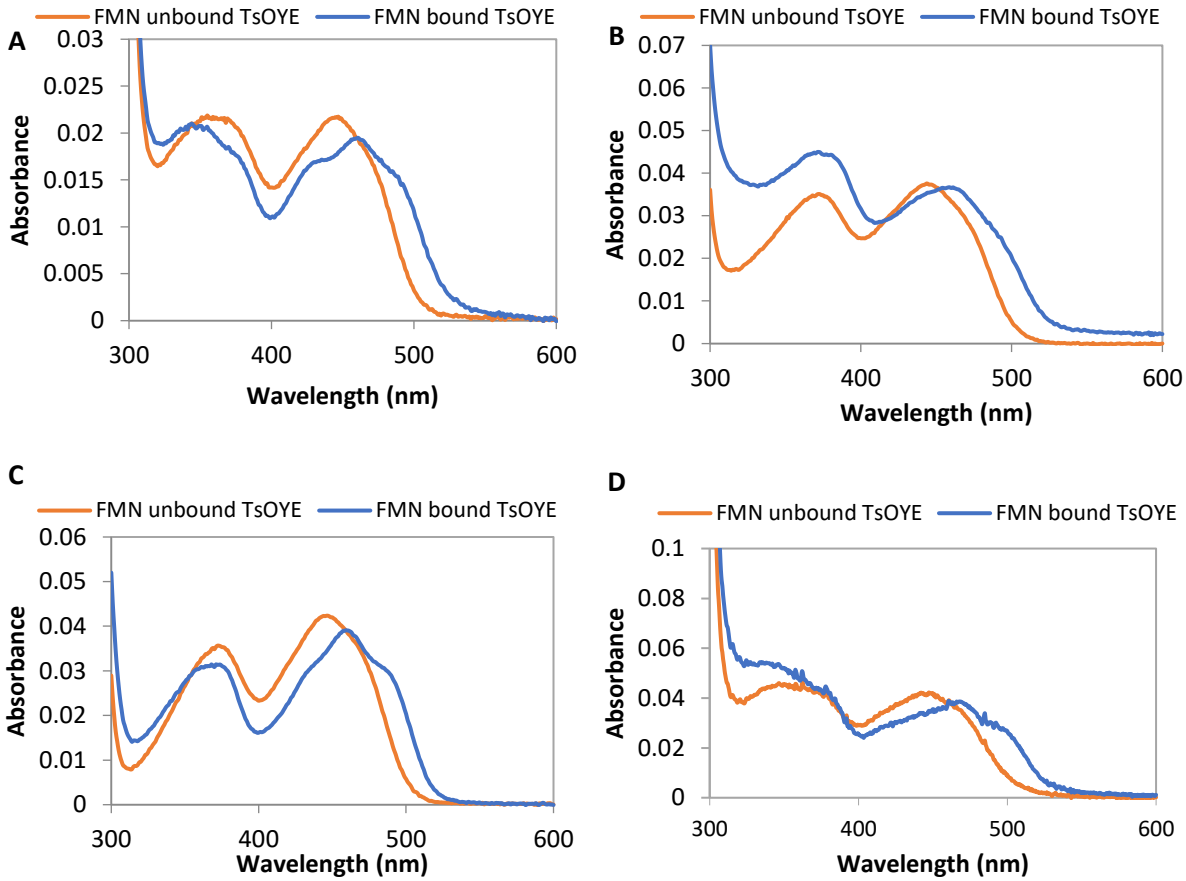

Figure A2.1. Ultraviolet (UV) spectra obtained by diluting purified enzyme in Milli-Q, before (blue) and after adding 2% v/v SDS detergent (orange). A: UV-spectrum of 1.80 µM of WT *Ts*OYE. B: UV-spectrum of 3.45 µM of *Ts*OYE C25D/I67T. C: UV-spectrum of 3.12 µM OYE2. D: UV-spectrum of 3.41 µM YqjM.

To convert these obtained spectra into concentration, the Beer-Lambert law was applied:

$$A = \varepsilon * c * d$$

The used cuvettes had a diameter of 1 cm, and the extinction coefficient of *Ts*OYE is equal to ε = 12,200 $M^{-1}cm^{-1}$. The absorbance of the enzyme can be found at a wavelength of 446 nm. With this information, the concentrations are calculated as follows:

$$c = \frac{A_{446}}{\varepsilon * d}$$

This concentration corresponds to the concentration inside the cuvette, so to know the concentration of the stock, these should be multiplied with the dilution factor. This includes the addition of 20 µL detergent as well.

To gain the concentrations in mg/ml, the following calculation was performed:

$$c\left(\frac{mg}{ml}\right) = \frac{c(\mu M)}{1{,}000{,}000\ \mu M/M} * 36{,}000\ g/mol$$

The concentrations of the first mutant stock were determined by calculating the concentrations as shown above and take the average of the two different measurements. Note that the second batch of the *Ts*OYE C25D/I67T had different concentrations when measured over time, so these values are

assumed to be unreliable. This concentration should be determined once the mutant will be used in a reaction.

The third batch of WT *Ts*OYE was determined with the previously described method. Before adding an excess of FMN, it was determined based on the UV that the concentration of the FMN containing enzyme was equal to 85 µM. By assuming that 60% of all enzymes contained FMN, it was determined that the total enzyme concentration (85/0.6) equalled to 142 µM. So based on these calculations, an excess of 57 µM FMN should be added to the solution. After the PD10 desalting, it was determined by UV that the final concentration of TsOYE was around 60 µM. This number contradicted the assumption that not all enzymes contained the FMN cofactor. When considered that the dilution factor of the desalting is 1.6, it could be assumed that all enzymes in the 85 µM stock contained FMN, as 85/1.6 = 61 µM. This means that all the enzyme had FMN incorporated already.

Appendix 3: Determination of enzyme concentration by protein staining

Calibration curve

To determine the protein concentrations based on the BCA assay, a calibration curve is made with 0, 0.5, 1 and 2 mg/mL BSA. The calibration curve is shown in Figure A3.1.

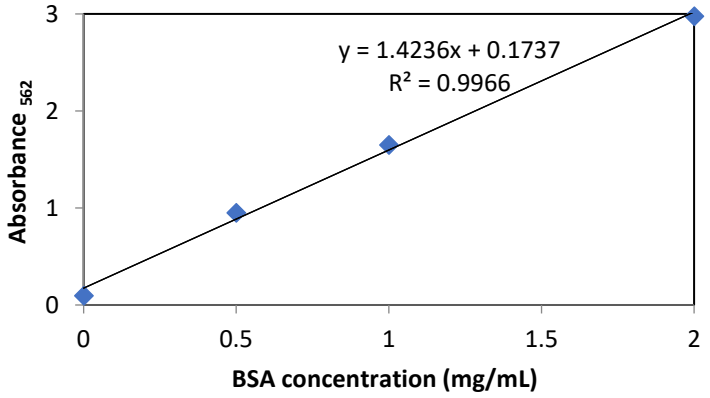

Figure A3.1. Calibration curve with known BSA concentrations. The samples are measured at a wavelength of 562 nm.

Calculation from optical densities to enzyme concentration

Table A3.1. Dilutions of purified protein solutions measured at an adsorption of 562 nm. Different numbers correspond to different batches with different concentrations. The measurements were performed in duplicate.

Sample type	Dilution factor	#1	#2	Average
***Ts*OYE #1**	10	0.68	0.72	0.7
***Ts*OYE #1**	20	0.48	0.46	0.47
***Ts*OYE #2**	10	1.1	1.1	1.1
***Ts*OYE #2**	20	0.62	0.61	0.61
C25D/I67T #1	10	0.95	0.94	0.94
C25D/I67T #1	20	0.76	0.6	0.68
C25D/I67T #2	10	0.74	0.76	0.75
C25D/I67T #2	20	0.4	0.48	0.44
***Ts*OYE #3**	2	1.3	1.2	1.3
***Ts*OYE #3**	4	0.78	0.78	0.78

The equation of the calibration curve is:

$$y = 1.42x + 0.17$$

By filling in the adsorptions for y, the concentrations can be calculated in mg/mL. The dilution factors are also incorporated, for example with a 10-fold dilution:

$$x = \frac{y - 0.17}{1.42} * 10$$

These values were converted in µM, assumed that both *Ts*OYE variants are around 36 kDa:

$$concentration\ (\mu M) = \frac{concentration\ \left(\frac{g}{L}\right)}{36{,}000\ g/mol} * 1{,}000{,}000\ \frac{\mu mol}{mol}$$

Appendix 4: Substrates, intermediates and product names

Table A4.1. List of alkene substrates, carbonyl intermediates, amine products and alcohol by-products, with assigned numbers.

	Alkene substrates		**Carbonyl intermediates**		**Amine products**		**Alcohol products**
1a	2-cyclopenten-1-one	**2a**	cyclopentanone	**3a**	cyclopentylamine	**4a**	cyclopentanol
1b	2-methyl-cyclopenten-1-one	**2b**	2-methylcyclopentanone	**3b**	2-methylcyclopentylamine	**4b**	2-methylcyclopentanol
1c	3-methyl-2-cyclopentenone	**2c**	3-methylcyclopentanone	**3c**	3-methylcyclopentylamine	**4c**	3-methylcyclopentanol
1d	2-cyclohexen-1-one	**2d**	cyclohexanone	**3d**	cyclopentylamine	**4d**	cyclohexanol
1e	2-methyl-2-cyclohexen-1-one	**2e**	2-methylcyclohexanone	**3e**	2-methylcyclopentylamine	**4e**	2-methylcyclohexanol
1f	3-methyl-2-cyclohexen-1-one	**2f**	3-methylcyclohexanone	**3f**	3-methylcyclopenylamine	**4f**	3-methylcyclohexanol
1g	3-buten-2-one	**2g**	2-butanone	**3g**	2-aminobutane	**4g**	2-butanol
1h	penten-3-one	**2h**	diethylketone	**3h**	3-aminopentane	**4h**	3-pentanol
1i	penten-2-one	**2i**	2-pentanone	**3i**	2-aminopentane	**4i**	2-pentanol
1j	methacrolein	**2j**	isobutyraldehyde	**3j**	isobutylamine	**4j**	isobutanol
1k	*trans*-2-methyl-2-butenal	**2k**	2-methylbutanal	**3k**	2-methylbutylamine	**4k**	2-methylbutanol
1l	*trans*-2-methyl-2-pentenal	**2l**	2-methylvaleraldehyde	**3l**	2-methylpentylamine	**4l**	2-methylpentanol
1m	*trans*-2-pentenal	**2m**	valeraldehyde	**3m**	amylamine	**4m**	pentanol

Appendix 5: GC analyses of bioconversions

GC columns and methods

Compound analyses for 1-hour reduction reactions were carried out on Shimadzu GC-2010 gas chromatographs (Shimadzu, Japan) with an AOC-20i Auto injector equipped with a flame ionization detector (FID), using nitrogen or helium as the carrier gas. Compounds were dissolved in ethyl acetate or diethyl ether depending on the boiling point. The final concentration was after this equal to 10 mM.

The following labels are given for different column types used:

A. Hydrodex ß-TBDAc (50 m × 0.25 mm × 0.25 µm) injection at 250 °C, flow 3 mL/min, split ratio 50, linear velocity 37 cm/sec, column flow 4 mL/min, nitrogen as carrier gas.
B. CP-Sil 8 CB (25 m × 0.25 mm × 1.20 µm), injection at 340 °C, split ratio 100, linear velocity 30 cm/sec, column flor 4 mL/min, nitrogen as carrier gas.
C. CP-Sil 8 CB (50 m × 0.53 mm × 1 µm), splitless, injection at 340 °C, flow 20 mL/min, nitrogen as carrier gas.
D. CP-Wax 52 CB (50 m × 0.53 mm × 2.0 µm), splitless, injection at 250 °C, flow 20 mL/min, nitrogen as carrier gas.
E. Hydrodex β-TBDM (50 m × 0.25 mm × 0.15 µm), injection at 250 °C split ratio 50, linear velocity 38 cm/s, column flow 2.23 mL/min, helium as carrier gas.
F. CP-Wax 52 CB (25 m × 0.53 mm × 2.0 µm), split ratio 100, injection at 250 °C, flow 4 mL/min, nitrogen as carrier gas.

Different GC columns were used to separate each series of compounds (Table A5.1).

Table A5.1. List of all compounds and applied internal standards (IS) with their corresponding GC columns and methods.

Compound	GC column	GC oven program	Retention time (min)
a	C	80 °C hold 6.83 min 30 °C/min to 325 °C hold 1 min	**1a 2-cyclopenten-1-one 4.0** **2a cyclopentanone 3.2**
a	B	80 °C hold 3 min 5 °C/min to 90 °C hold 5 min 20 °C/min to 325 °C hold 1 min	**1a 2-cyclopenten-1-one 7.8** **2a cyclopentanone 6.7** **3a cyclopentylamine 5.8** **dodecane (IS) 16.6**
b	E	80 °C hold 5 min 5 °C/min to 100 °C hold 10 min 5 °C/min to 120 °C hold 5 min 20 °C/min to 240 °C hold 1 min	**1b 2-methyl-2-cyclopenten-1-one 13.4** **2b 2-methylcyclopentanone 10.7, 11.0** **3b 2-methylcyclopentylamine 9.8, 9.9, 11.0** **dodecane (IS) 25.6**
c	A	100 °C hold 5 min 10 °C/min to 135 °C hold 4.25 min 20 °C/min to 220 °C hold 1 min	**1c 3-methyl-2-cyclopenten-1-one 17.2** **2c 3-methylcyclopentanone 11.5, 11.6**
d	B	80 °C hold 3 min 345 °C/min to 345 °C hold 1 min	**1d 2-cyclohexen-1-one 7.3** **2d cyclohexanone 6.9** **dodecane (IS) 9.7**
d	B	80 °C hold 3 min 5 °C/min to 100 °C hold 4 min 25 °C/min to 345 °C hold 1 min	**1d 2-cyclohexen-1-one 11.6** **2d cyclohexanone 9.8** **3d cyclohexylamine 8.4** **dodecane (IS) 16.1**
e	C	100 °C hold 3 min 25 °C/min to 140 °C hold 1 min 10 °C/min to 150 °C hold 1 min 25 °C/min to 345 °C hold 1 min	**1e 2-methyl-2-cyclohexen-1-one 7.8** **2e 2-methylcyclohexanone 6.9** **dodecane (IS) 10.4**
e	C	100 °C hold 3 min 25 °C/min to 145 °C hold 6 min 25 °C/min to 345 °C hold 1	**1e 2-methyl-2-cyclohexen-1-one 7.8** **2e 2-methylcyclohexanone 6.9** **3e 2-methylcyclohexylamine 6.0, 6.3** **dodecane (IS) 10.4**
f	E	80 °C hold 5 min 5 °C/min to 100 °C hold 10 min 5 °C/min to 120 °C hold 5 min 20 °C/min to 240 °C hold 1 min	**1f 3-methyl-2-cyclohexen-1-one 28.8** **2f 3-methylcyclohexanone 19.5, 20.0** **3f 3-methylcyclohexylamine 14.4, 14.7, 16.5, 16.7** **dodecane (IS) 25.6**
g	D	50 °C hold 6 min 25 °C/min to 230 °C hold 1 min	**1g 3-buten-2-one 1.9** **2g 2-butanone 2.4**
g	B	65 °C hold 6 min 230 °C/min to 345 °C hold 1 min	**1g 3-buten-2-one 4.1** **2g 2-butanone 4.3** **3g 2-aminobutane 4.0** **dodecane (IS) 14.9**
h	F	65 °C hold 6 min 20 °C/min to 345 °C hold 1 min	**1h penten-3-one 5.1** **2h diethylketone 4.3** **dodecane (IS) 11.0**

i	C	65 °C hold 6 min 5 °C/min to 70 °C hold 3 min 20 °C/min to 340 °C hold 1 min	**1i penten-2-one 7.3** **2i 2-pentanone 5.4** **3i 2-aminopentane 5.2** **dodecane (IS) 17.8**
j	n.a.		
k	C	60 °C hold 3 min 10 °C/min to 70 °C hold 5 min 10 °C/min to 140 °C hold 3 min 20 °C/min to 340 °C hold 1 min	**1k *trans*-2-methyl-2-butenal 7.5** **2k 2-methylbutanal 4.9** **3k 2-methylbutylamine 6.2** **dodecane (IS) 21.9**
l	A	100 °C hold 7.5 min 5 °C/min to 140 °C hold 2.5 min 25 °C/min to 240 °C hold 1 min	**1l *trans*-2-methyl-2-pentenal 10.7** **2l 2-methylvaleraldehyde 6.0, 6.2** **tridecane (IS) 13.2**
m	D	60 °C hold 3 min 5 °C/min to 70 °C hold 2 min 25 °C/min to 245 °C hold 1 min	**1m *trans*-2-pentenal 6.3** **2m valeraldehyde 3.1** **dodecane (IS) 12.6**
m	C	50 °C hold 4 min 5 °C/min to 60 °C hold 2 min 5 °C/min to 65 °C hold 4 min 20 °C/min to 345 °C hold 1 min	**1m *trans*-2-pentenal 10.4** **2m valeraldehyde 7.5** **3m amylamine 9.5** **dodecane (IS) 18.0**

In case of **a**, **d**, **e**, **g** and **m**, two methods were designed: one for the separation of compound **1** and **2**, and another method to separate **1**, **2** and **3**. In this case, this new method and the corresponding GC column are shown for each substrate.

GC chromatograms

Compound series a

Table A5.2. Method applied for the reference consisting of 2-cyclopenten-1-one and cyclopentanone.

Rate (°C/min)	Temp. °C	Hold (min)
0	80	6.83
30	325	1

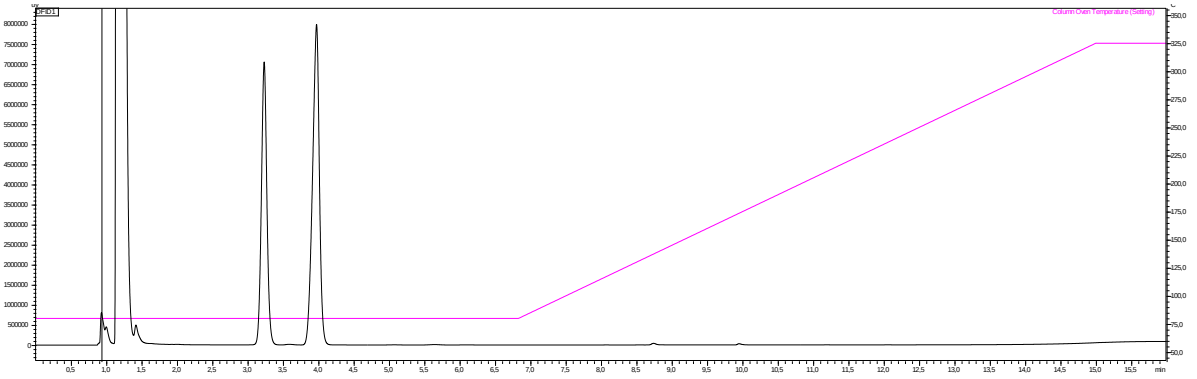

Figure A5.1. Gas chromatogram of 2-cyclopenten-1-one (4.0 min) and cyclopentanone (3.2 min).

Table A5.3. Method applied on the GC column labelled C for the reference consisting of 2-cyclopenten-1-one, cyclopentanone and cyclopentylamine.

Rate (°C/min)	Temp. (°C)	Hold (min)
0	80	3
5	90	5
20	320	1

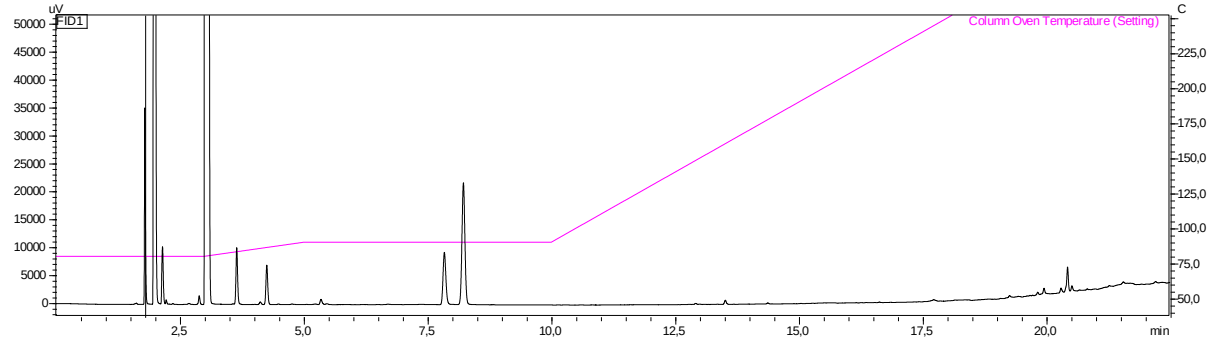

Figure A5.2. Gas chromatogram of 2-cyclopenten-1-one (8.2 min).

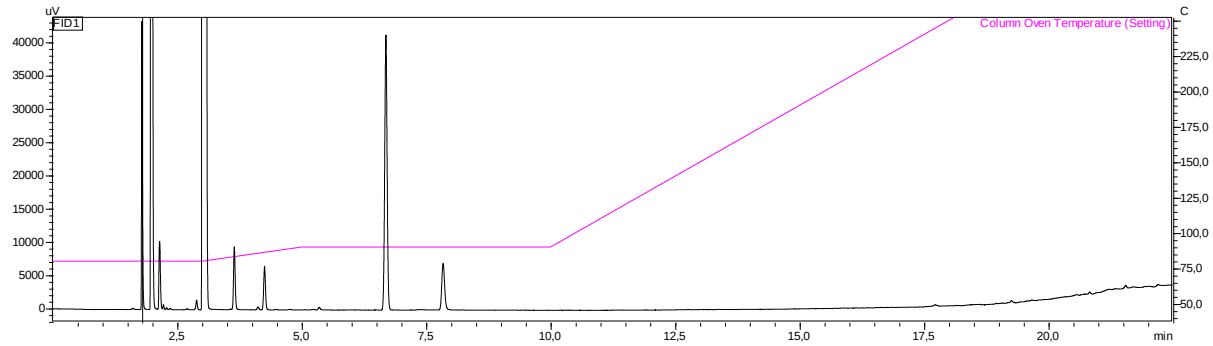

Figure A5.3. Gas chromatogram of cyclopentanone (6.7 min).

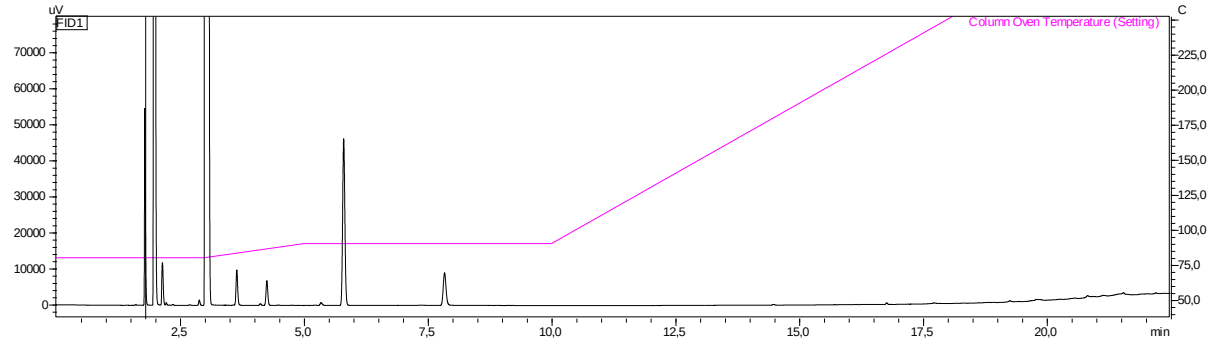

Figure A5.4. Gas chromatogram of cyclopentylamine (5.8 min).

Compound series b

Table A5.4. Method applied for the reference consisting of 2-methyl-2-cyclopenten-1-one and 2-methylcyclopentanone.

Rate (°C/min)	Temp. (°C)	Hold (min)
0	80	5
5	100	10
5	120	5
20	240	1

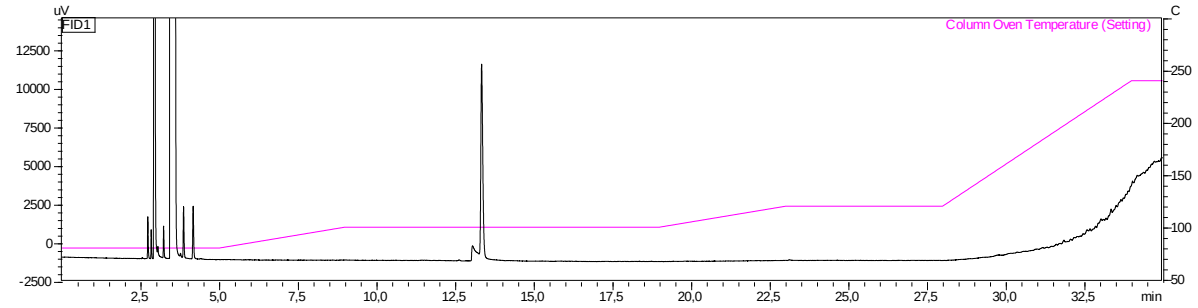

Figure A5.5. Gas chromatogram of 2-methyl-2-cyclopenten-1-one (13.4 min).

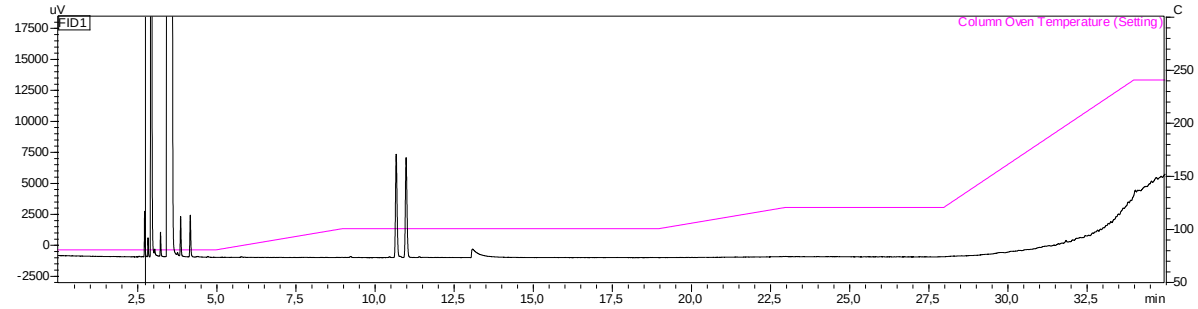

Figure A5.6. Gas chromatogram of 2-methyl-cyclopentanone (10.7 and 11.0 min).

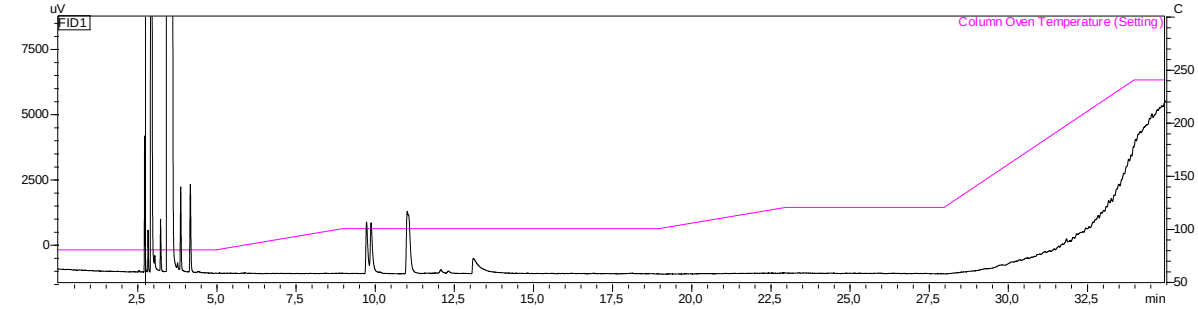

Figure A5.7. *Gas* chromatogram of 2-methyl-cyclopentylamine (9.8, 9.9 and 11.0 min).

Compound series c

Table A5.5. Method applied for the reference consisting of 3-methyl-2-cyclopenten-1-one and 3-methylcyclopentanone.

Rate (°C/min)	Temp. (°C)	Hold (min)
0	100	5
10	135	4.25
20	220	1
25	245	1

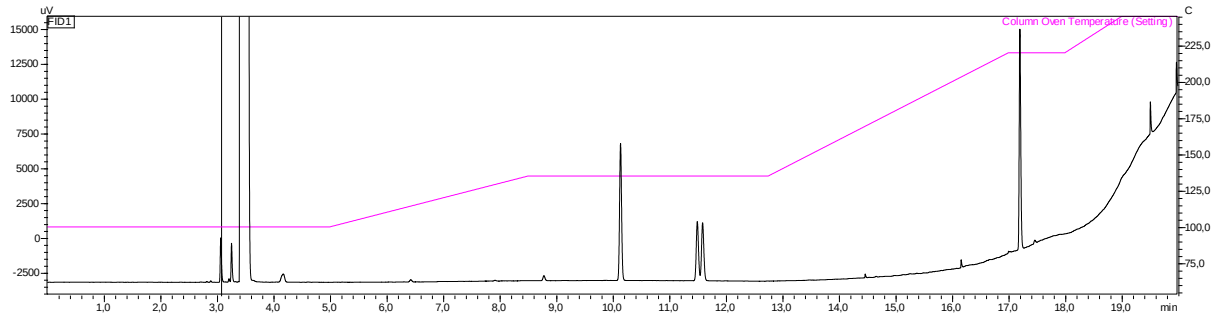

Figure A5.8. Gas chromatogram of 3-methylcyclopenten-1-one (10.2) and 3-methylcyclopentanone (11.5, 11.6).

Compound series d

Table A5.6. Method applied for the reference consisting of 2-cyclohexen-1-one and cyclohexanone.

Rate (°C/min)	Temp. (°C)	Hold (min)
0	80	3
25	345	1

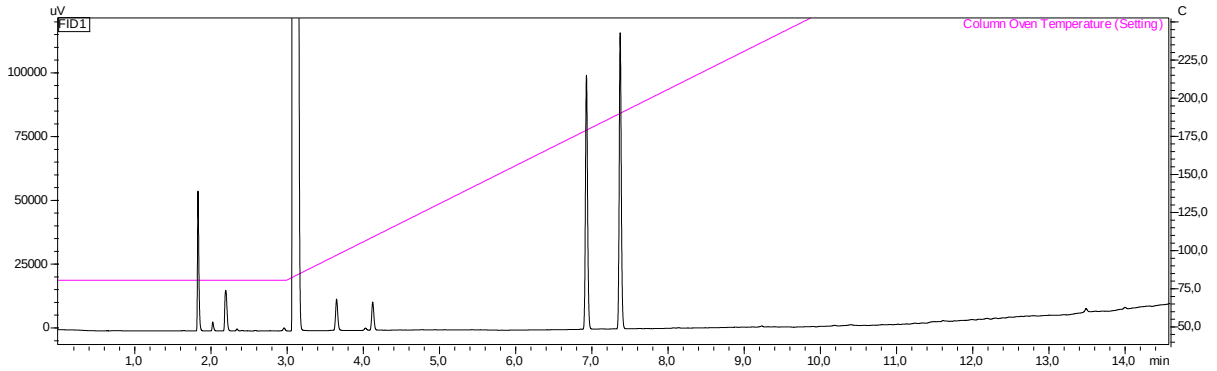

Figure A5.9. Gas chromatogram of 2-cyclohexen-1-one (7.3 min) and cyclohexanone (6.9 min).

Table A5.7. Method applied for the reference consisting of 2-cyclohexen-1-one, cyclohexanone and cyclohexylamine.

Rate (°C/min)	Temp. (°C)	Hold (min)
0	80	3
5	100	4
25	345	1

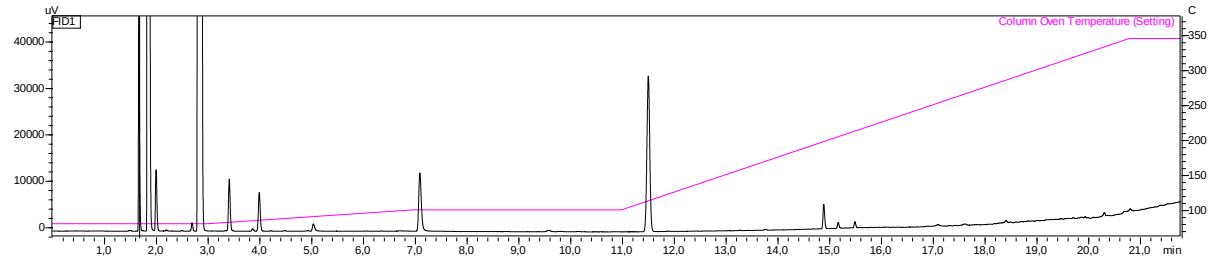

Figure A5.10. Gas chromatogram of 2-cyclohexen-1-one (11.6 min).

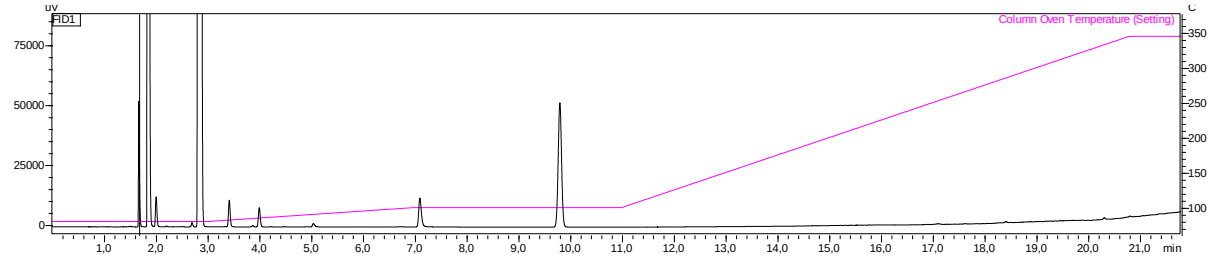

Figure A5.11. Gas chromatogram of cyclohexanone (9.8 min).

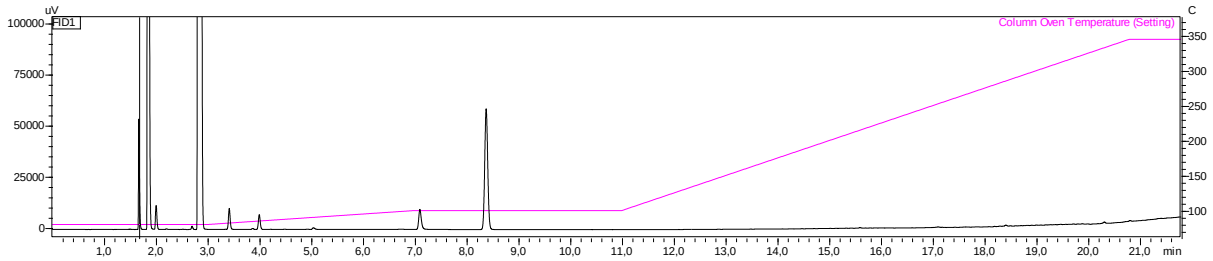

Figure A5.12. Gas chromatogram of cyclohexylamine (8.4 min).

Compound series e

Table A5.8. Method applied for the reference consisting of 2-methyl-2-cyclohexen-1-one and 2-methylcyclohexanone

Rate (°C/min)	Temp. (°C)	Hold (min)
0	100	3
25	140	1
10	150	1
25	345	1

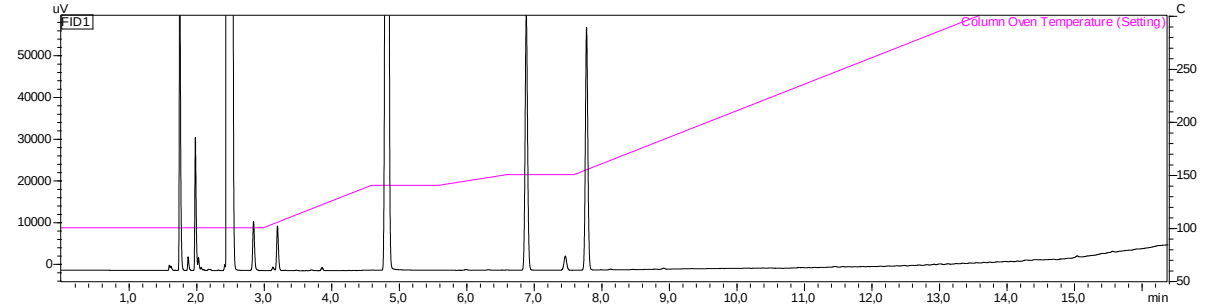

Figure A5.13. Gas chromatogram of 2-methyl-2-cyclohexen-1-one (7.8 min) and 2-methylcyclohexanone (6.9 min).

Table A5.9. Method applied on the GC column labelled C for the reference consisting of 2-methyl-2-cyclohexen-1-one, 2-methylcyclohexanone and 2-methylcyclohexylamine.

Rate (°C/min)	Temp. (°C)	Hold (min)
-	100	3
25	145	6
25	345	1

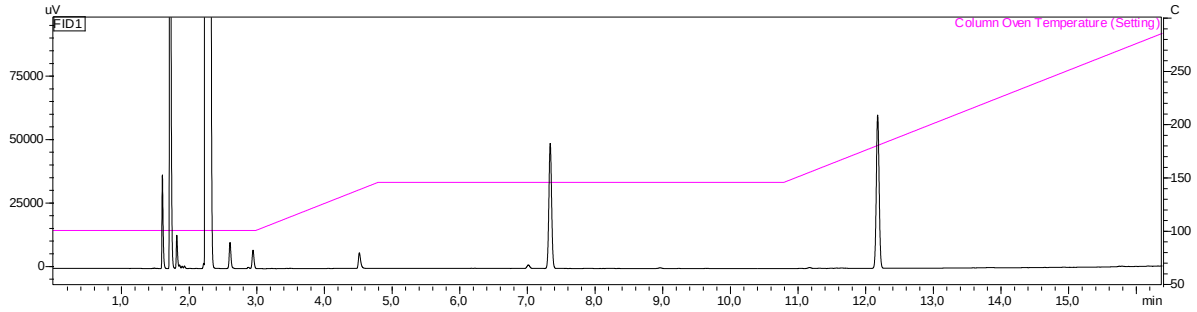

Figure A5.14. Gas chromatogram of 2-methyl-2-cyclohexen-1-one (7.4 min).

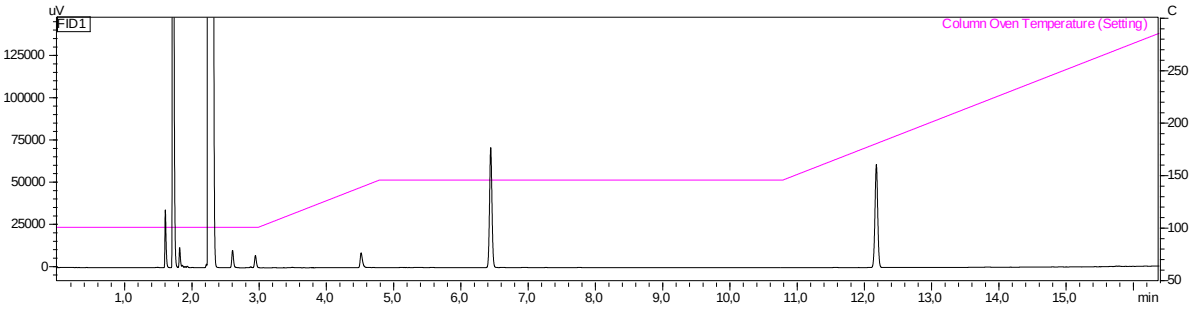

Figure A5.15. Gas chromatogram of 2-methylcyclohexanone (6.5 min).

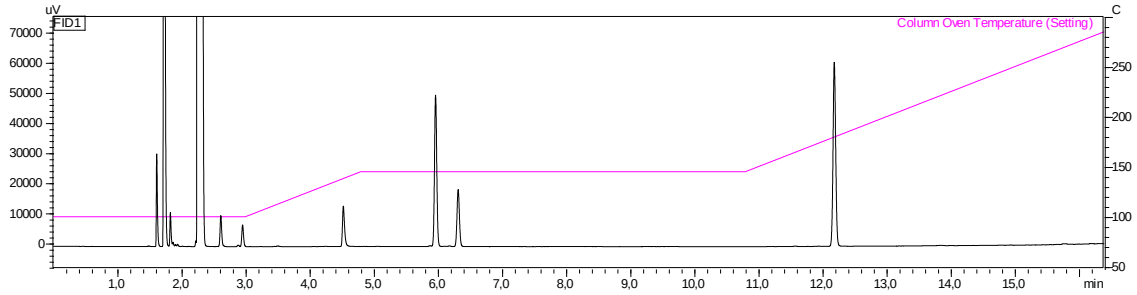

Figure A5.16. Gas chromatogram of 2-methylcyclohexylamine (6.0 and 6.3 min).

Compound series f

Table A5.10. Method applied for the reference consisting of 3-methyl-2-cyclohexen-1-one and 3-methylcyclohexanone.

Rate (°C/min)	Temp. (°C)	Hold (min)
0	80	5
5	100	10
5	120	5
20	240	1

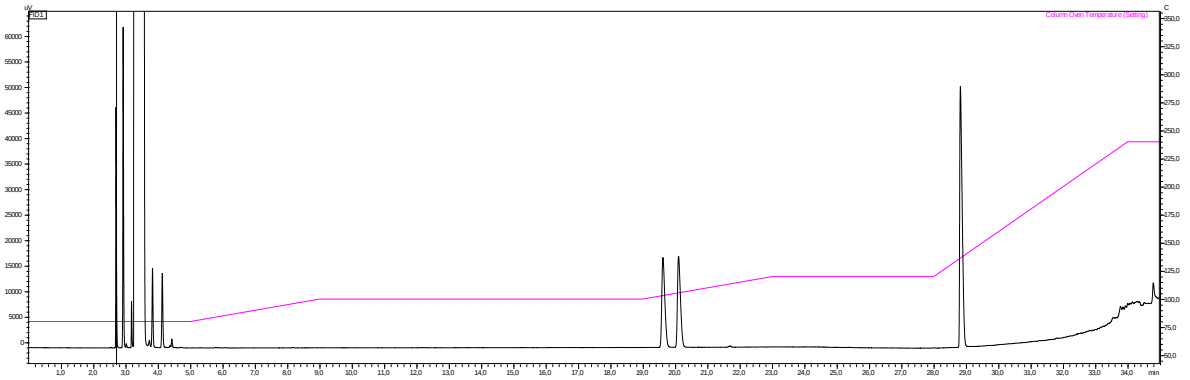

Figure A5.17. Gas chromatogram of 3-methyl-2-cyclohexen-1-one (28.8 min) and 3-methylcyclohexanone (19.5 and 20.0 min).

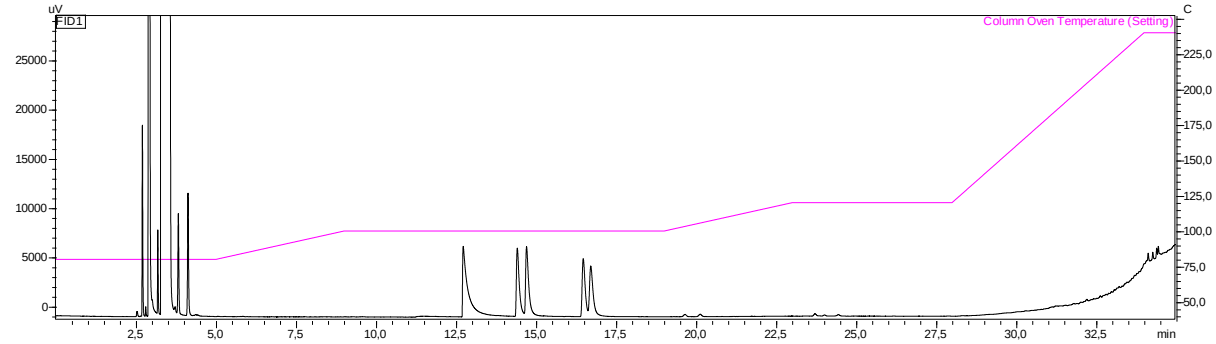

Figure A5.18. Gas chromatogram of 3-methylcyclohexylamine (14.4, 14.7, 16.5 and 16.7 min).

Compound series g

Table A5.11. Method applied for the reference consisting of 3-buten-2-one and 2-butanone.

Rate (°C/min)	Temp. (°C)	Hold (min)
0	65	6
25	230	1

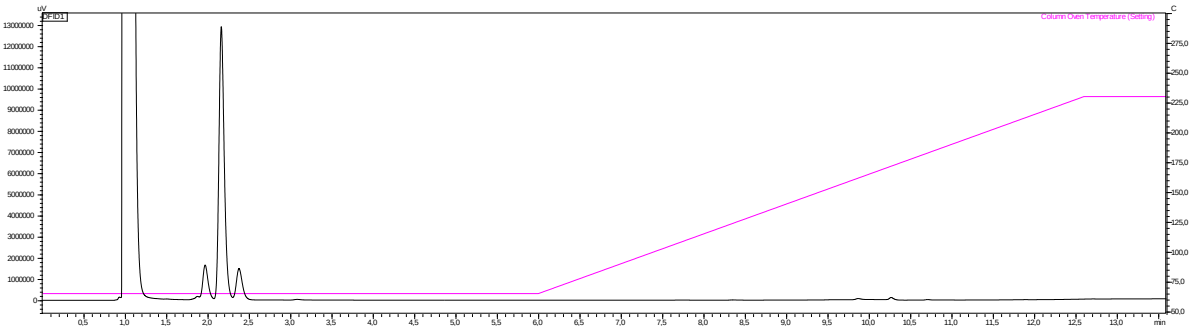

Figure A5.19. Gas chromatogram of 3-buten-2-one (2.7 min) and 2-butanone (2.2 min).

Table A5.12. Method applied on the GC column labelled C for the reference consisting of 3-buten-2-one, 2-butanone and isobutylamine.

Rate (°C/min)	Temp. (°C)	Hold (min)
0	50	6
20	345	1

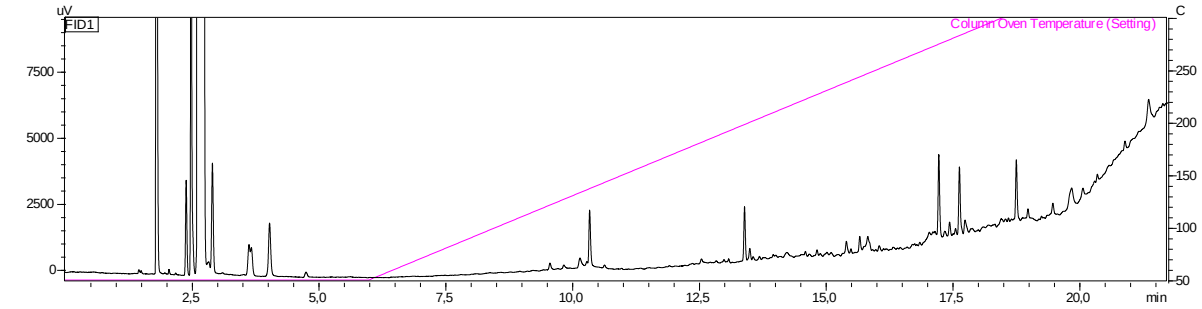

Figure A5.20. Gas chromatogram of 3-buten-2-one (4.1min).

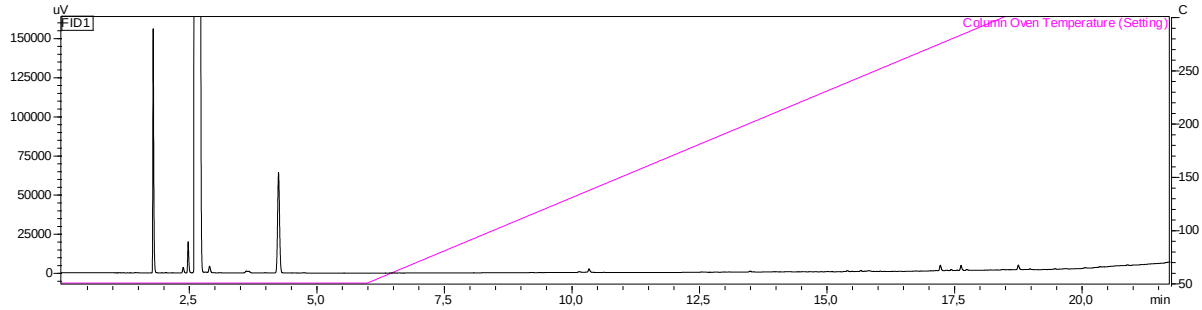

Figure A5.21. Gas chromatogram of 3-buten-2-one (4.3 min).

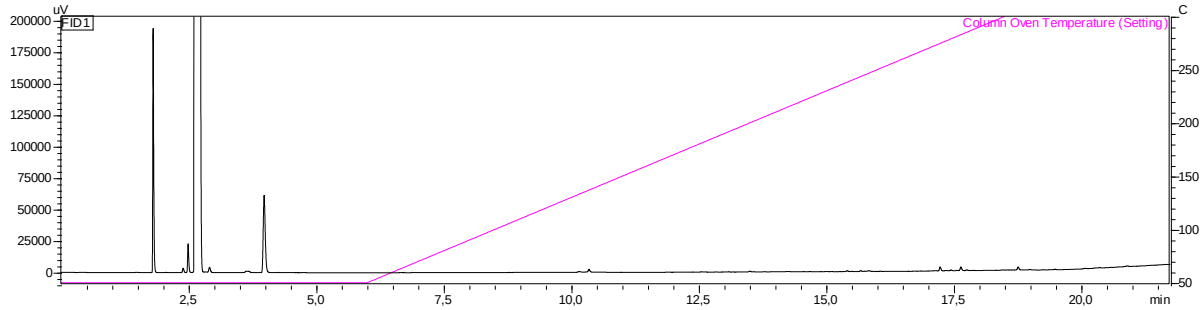

Figure A5.22. Gas chromatogram of isobutylamine (4.0 min).

Compound series h

Table A5.13. Method applied for the reference consisting of penten-3-one and diethylketone.

Rate (°C/min)	Temp. (°C)	Hold (min)
0	75	7
10	250	1

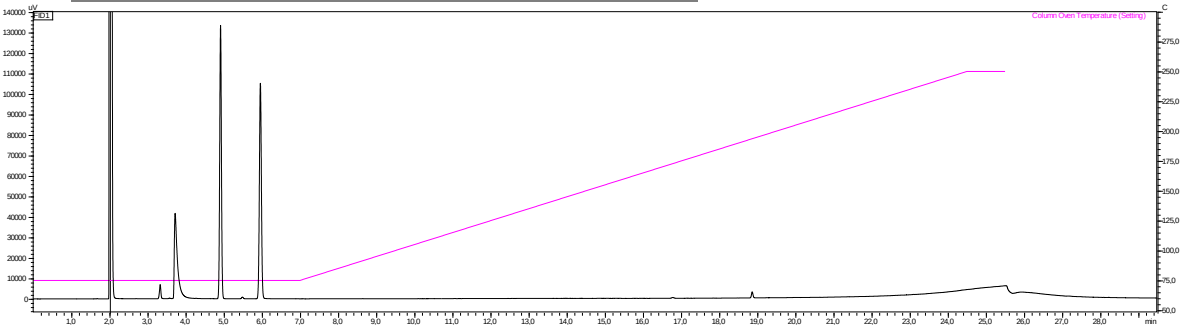

Figure A5.23. Gas chromatogram of penten-3-one (6.0 min) and diethylketone (4.9 min).

Compound series i

Table A5.14. Method applied for the reference consisting of penten-2-one and 2-pentanone.

Rate (°C/min)	Temp. (°C)	Hold (min)
-	65	6
5	70	3
20	340	1

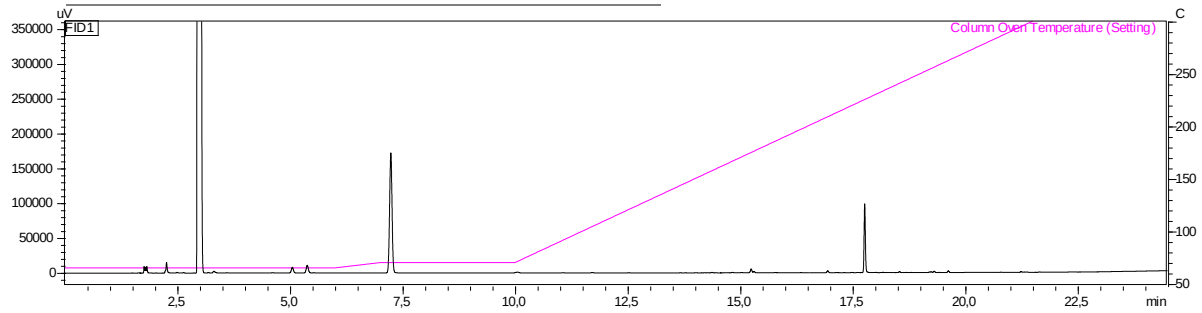

Figure A5.24. Gas chromatogram of penten-2-one (7.3 min).

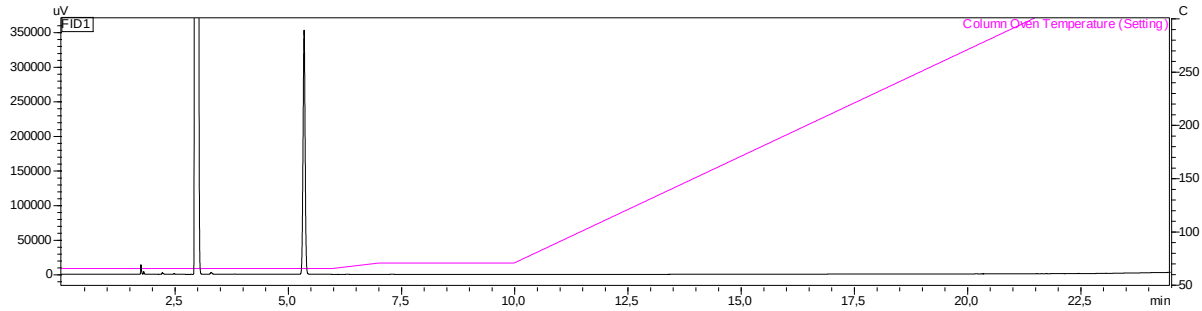

Figure A5.25. Gas chromatogram of penten-2-one (5.4 min).

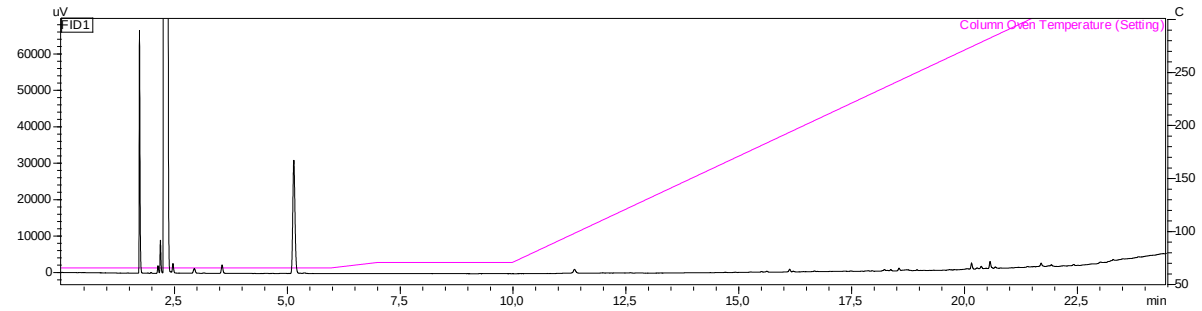

Figure A5.26. Gas chromatogram of 2-pentylamine (5.2 min).

Compound series k

Table A5.15. Method applied for the reference consisting of *trans*-2-methylbutenal and 2-methylbutyraldehyde.

Rate (°C/min)	Temp. (°C)	Hold (min)
-	60	3
10	70	3
10	140	5
20	340	1

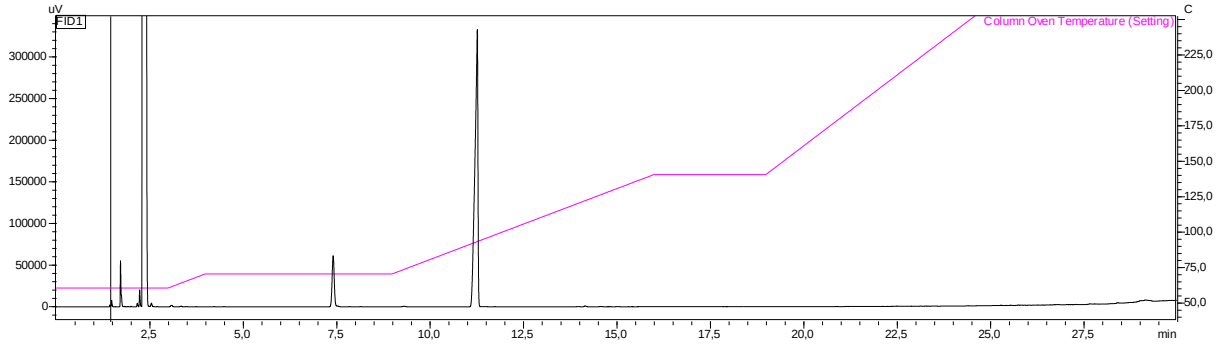

Figure A5.27. Gas chromatogram of *trans*-2-methylbutenal (7.5 min).

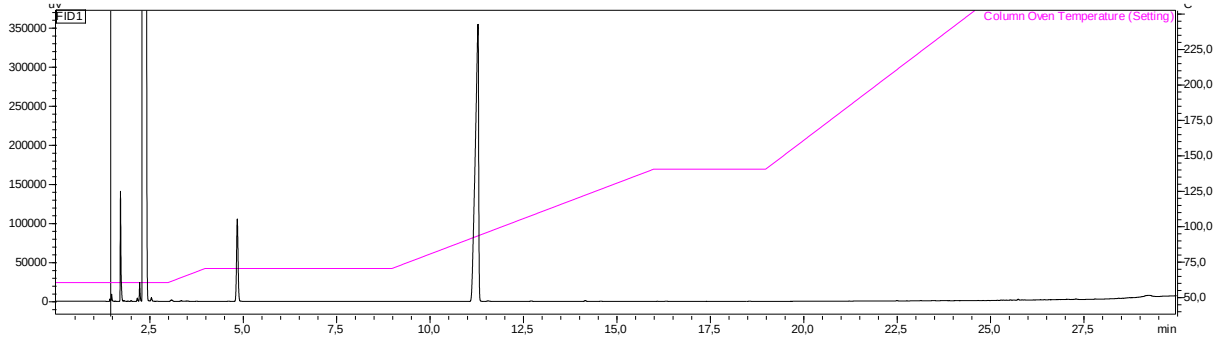

Figure A5.28. Gas chromatogram of *trans*-2-methylbutyraldehyde (4.9 min).

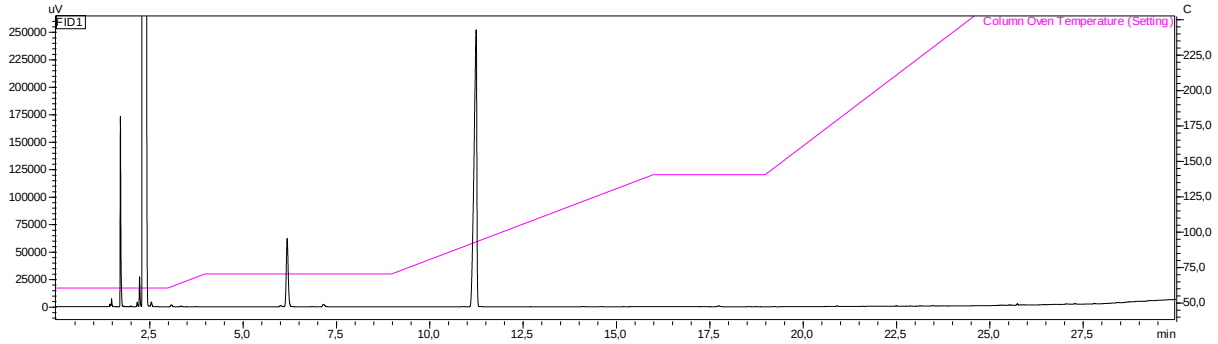

Figure A5.29. Gas chromatogram of 2-pentylamine (6.2 min).

Compound series l

Table A5.16. Method applied for the reference consisting of 2-methyl-2-pentenal and 2-methylvaleraldehyde.

Rate (°C/min)	Temp. (°C)	Hold (min)
0	100	7.5
5	140	2.5
25	240	1.03

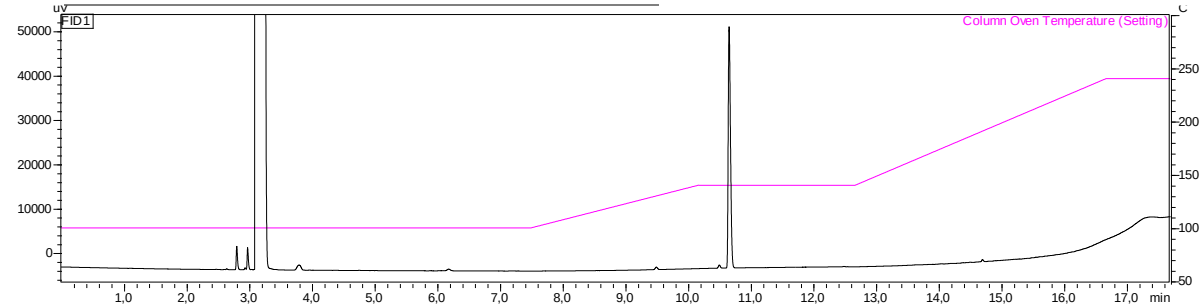

Figure A5.30. Gas chromatogram of t*rans*-2-methylpentenal (10.7 min).

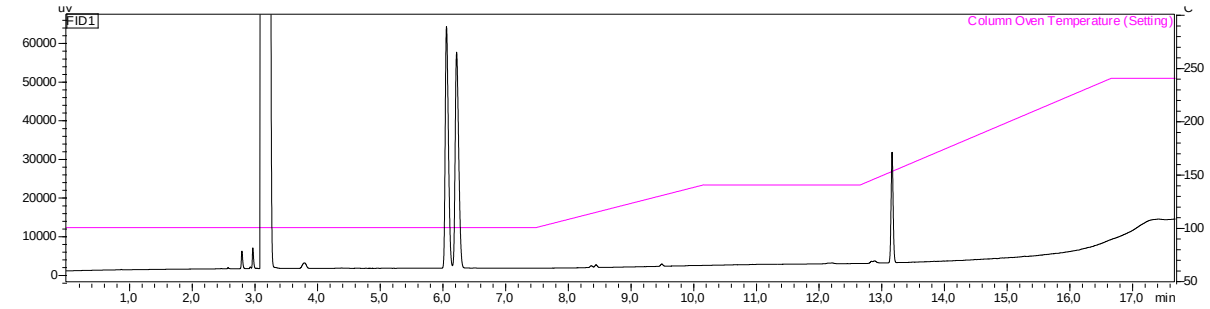

Figure A5.33. Gas chromatogram of 2-methylvaleraldehyde (6.0 and 6.2 min).

Compound series m

Table A5.17. Method applied for the reference consisting of t*rans*-2-pentenal and valeraldehyde.

Rate (°C/min)	Temp. (°C)	Hold (min)
0	60	3
5	70	3
25	245	1

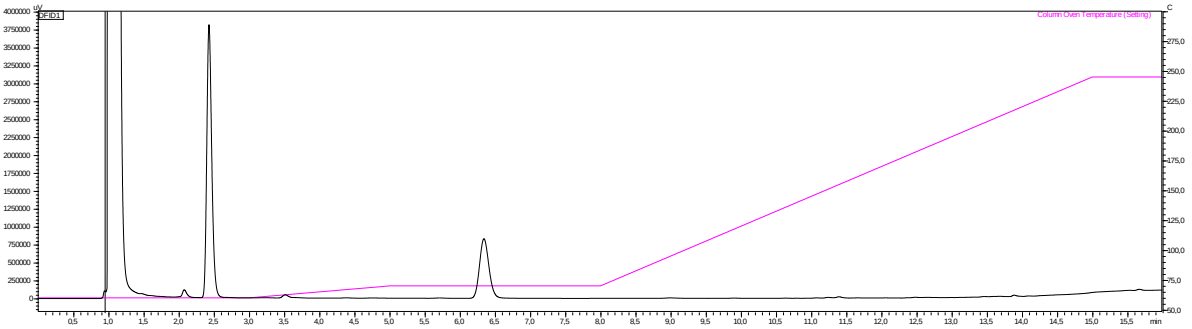

Figure A5.31. Gas chromatogram of trans-2-pentenal (6.3 min).

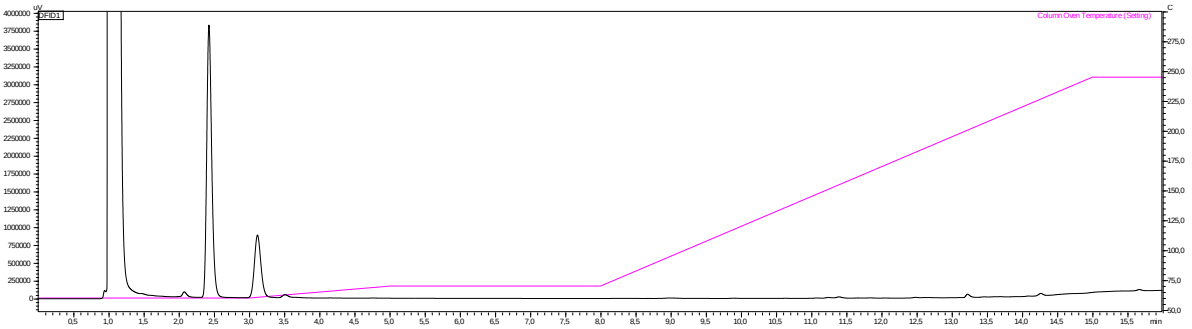

Figure A5.32. Gas chromatogram of valeraldehyde (3.1 min).

Table A5.18. Method applied on the GC column labelled C for the reference consisting of 3-buten-2-one, 2-butanone and isobutylamine.

Rate (°C/min)	Temp. (°C)	Hold (min)
0	50	4
5	60	2
5	65	4
20	345	1

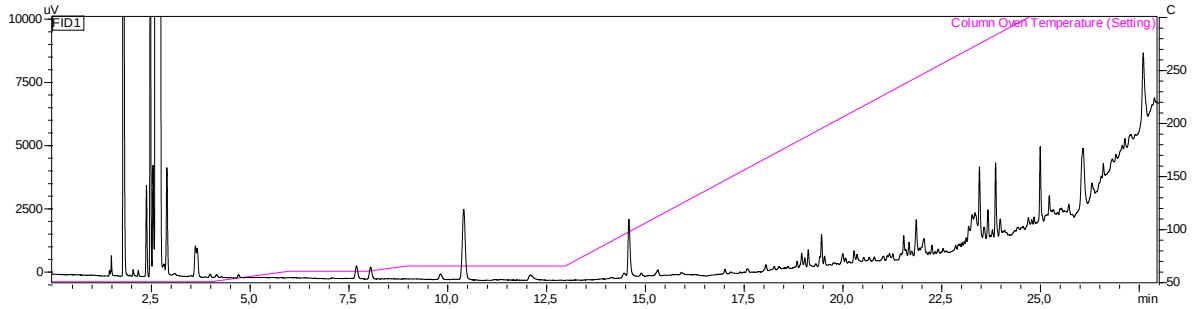

Figure A5.33. Gas chromatogram of t*rans*-2-pentenal (10.4 min).

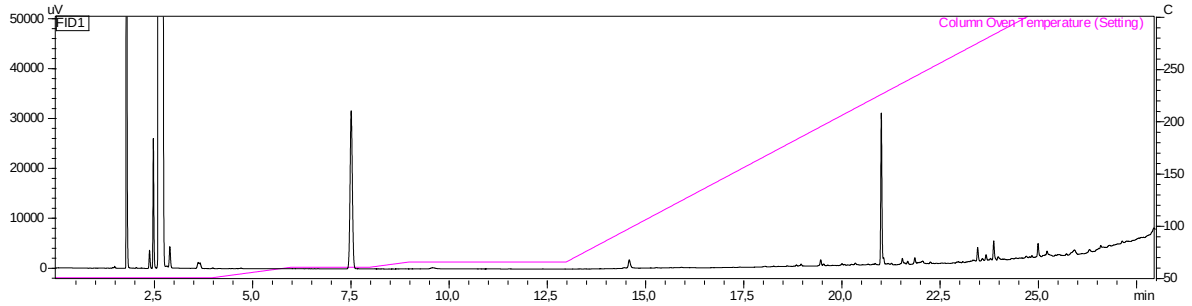

Figure A5.34. Gas chromatogram of valeraldehyde (7.5 min).

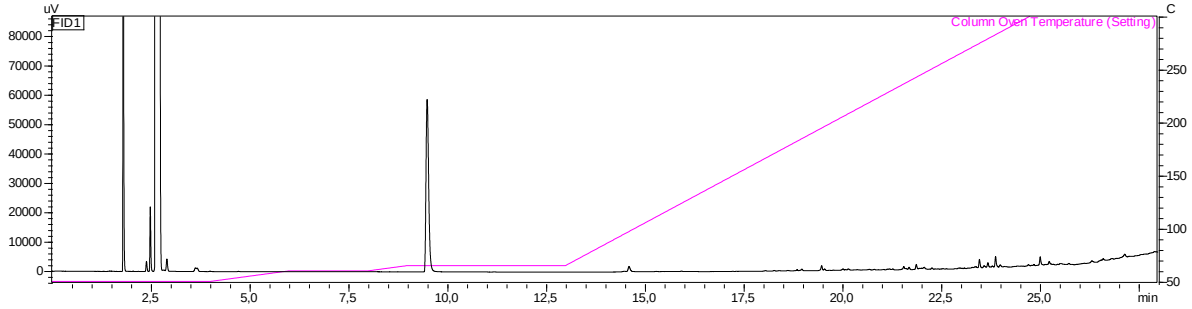

Figure A5.35. Gas chromatogram of amylamine (9.5 min).

Appendix 6: Specific activity calculations

It is given that the extinction coefficient of NAD(P)H is equal to 6220 $M^{-1}cm^{-1}$. 2 mL of Tris buffer was used for every reaction. Also, 10 mM substrate, such as 2-cyclohexen-1-one, 0.1 mM NADPH and 0.05 µM *Ts*OYE of the 25 October batch were added during the UV measurements. For this substrate, the observed slope was equal to 0.134 A/min.

With Beer-Lamberts law, the concentration decrease per minute can be determined:

$$c = \frac{A}{\varepsilon * d}$$

$$\frac{0.134}{6220 * 1} = 2.16 * 10^{-5} \frac{M}{minute} = 21.6 \frac{\mu mol}{L * minute}$$

By multiplying with the total reaction volume, U is calculated:

$$21.6 \frac{\mu mol}{L * minute} * 2.7 * 10^{-3} L = 0.045 \frac{\mu mol}{minute} = 0.045\ U$$

For the kinetic measurements, a 10.2 mM dilution of *Ts*OYE with Milli-Q was made to make a total of 1mL stock. If 10 µL from that stock was added to the reaction, then

$$10.2 \frac{\mu mol}{L} = 10.2 * 10^{-11} \frac{\mu mol}{\mu L}$$

$$10.2 * 10^{-11} \frac{\mu mol}{\mu L} * 10 \mu L = 10.2 * 10^{-11}\ \mu mol$$

$$10.2 * 10^{-11}\ \mu mol * 36{,}000 \frac{g}{mol} = 3.67 * 10^{-3}\ mg$$

This means that the specific activity is equal to

$$\frac{0.045 \frac{\mu mol}{minute}}{3.67 * 10^{-3}\ mg} = 12.2\ U/mg$$

Appendix 7: Structure and reaction scheme with 1-benzyl-1,4-dihydronicotinamide

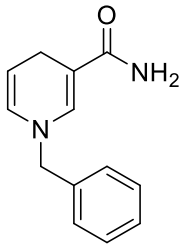

Figure A7.1 Molecular structure of synthetic cofactor BNAH.

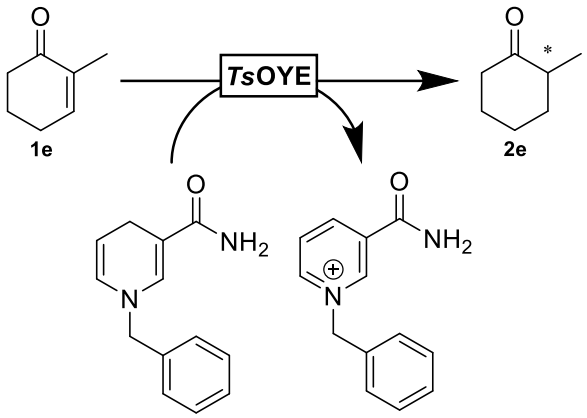

Figure A7.2. Reaction mechanism of asymmetric reduction by *Ts*OYE with synthetic cofactor BNAH.

Appendix 8: ß-methylated enone reduction by OYE2 and *Ts*OYE C25D/I67T

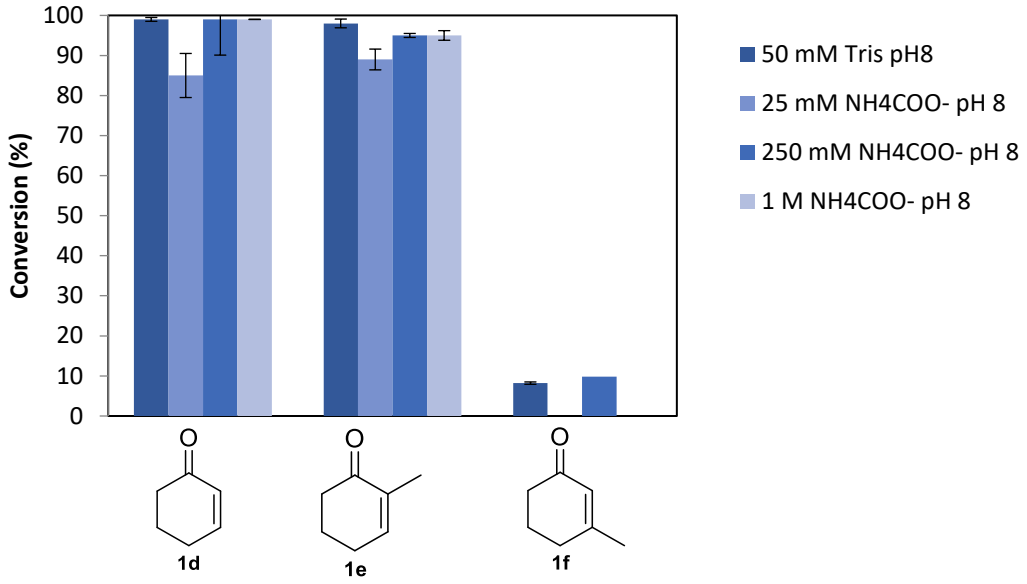

Figure A8.1. Conversions of different substrates by *Ts*OYE after 1 hour. In case of **1f**, *Ts*OYE C25D/I67T was used for 50 mM Tris and 250 mM ammonium formate buffer. 11 mm BNAH is added as powder to the reaction mixture. Average of duplicates.

Table A8.1. Asymmetric reduction of ß-methylated cyclic enones by OYE2 and the *Ts*OYE C25D/I67T double mutant for 1 h.

Substrate	**Enzyme**	**[Enzyme] (µM)**	**Conv. (%)**	**St. dev (%)[a]**	**e.r. (*R*:*S*)[b]**
1c	OYE2	2	1.1	0.1	1:99
1c	OYE2	4	3.2	0.2	1:99
1c	C25D/I67T	2	0	0	n.a.
1c	C25D/I67T	4	0	0	n.a.
1f	OYE2	2	10	0.2	1:99
1f	OYE2	4	20	0.5	1:99
1f	C25D/I67T	2	20	0.1	92:8
1f	C25D/I67T	4	20	2.6	92:8

[a] Reactions were performed in duplicate. [b] e.r. = enantiomeric ration.

Appendix 9: GC calibration curves

Compound series a

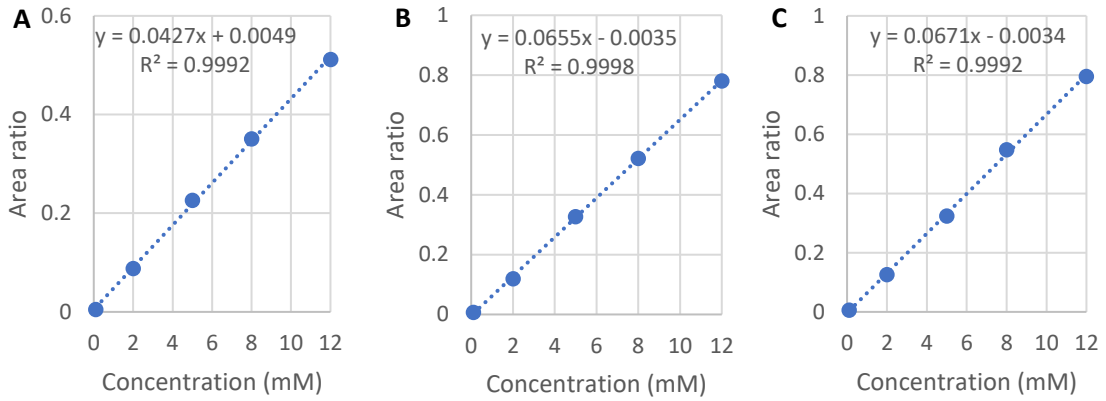

Figure A9.1. Calibration curves to quantify compounds of the substrate series a. Peak area ratios were compared with 5 mM dodecane as internal standard. Average of duplicates. A: 1a. B: 2a. C: 3a.

Compound series d

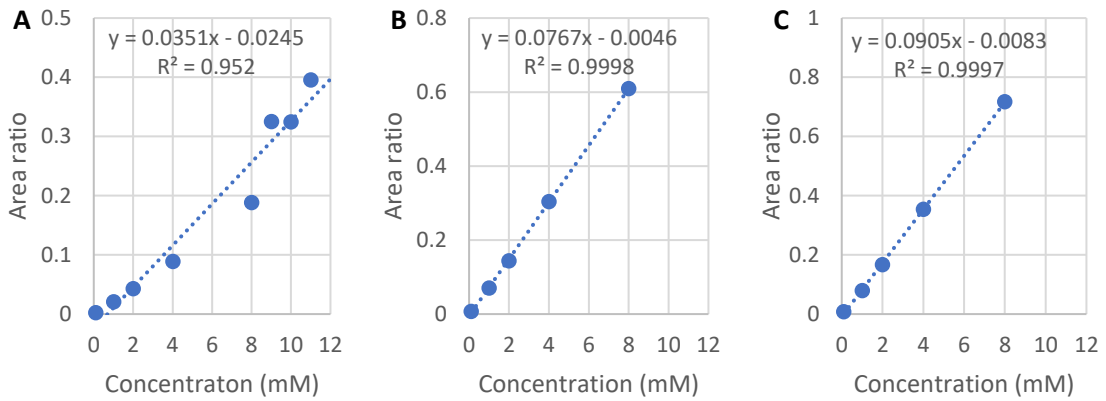

Figure A9.2. Calibration curves to quantify compounds of the substrate series d. Peak area ratios were compared with 5 mM dodecane as internal standard. Average of duplicates. A: 1d. B: 2d. C: 3d.

Compound series f

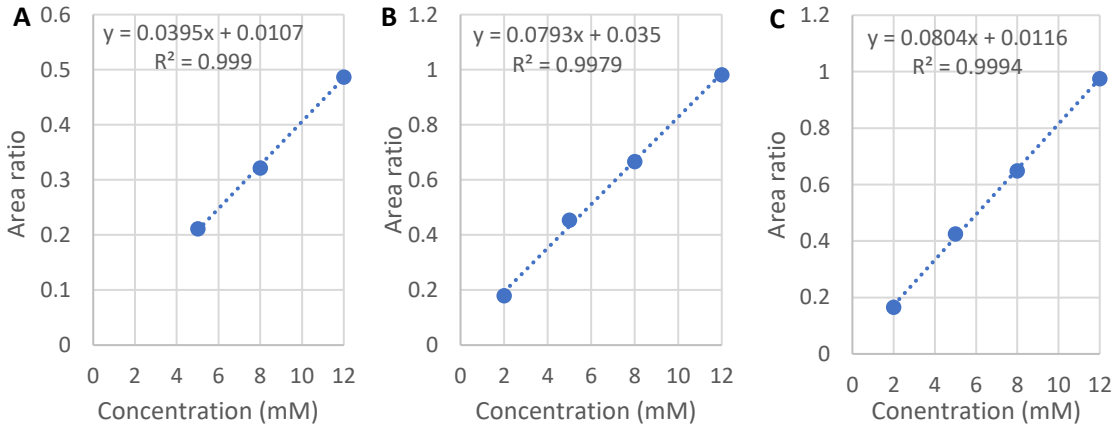

Figure A9.3. Calibration curves to quantify compounds of the substrate series f. Peak area ratios were compared with 5 mM dodecane as internal standard. Average of duplicates. A: 1f. B: 2f. C: 3f.

Compound series i

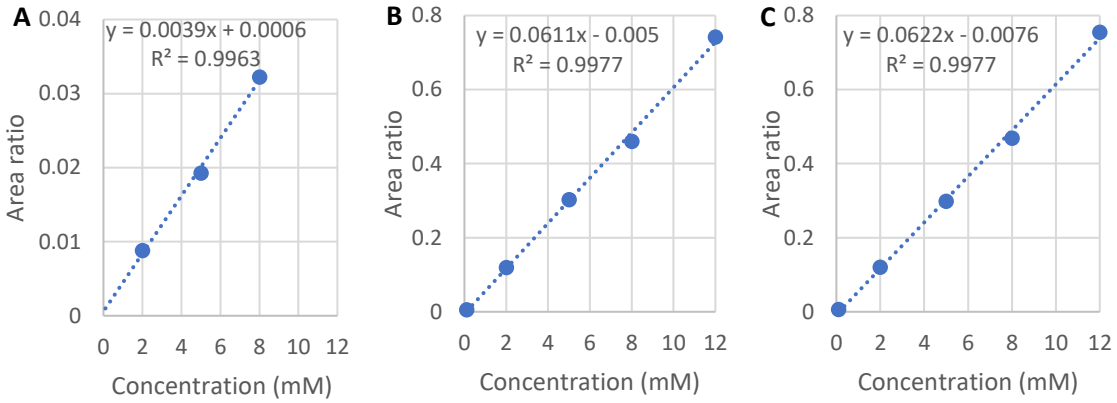

Figure A9.4. Calibration curves to quantify compounds of the substrate series i. Peak area ratios were compared with 5 mM dodecane as internal standard. Average of duplicates. A: 1i. B: 2i. C: 3i.

Compound series k

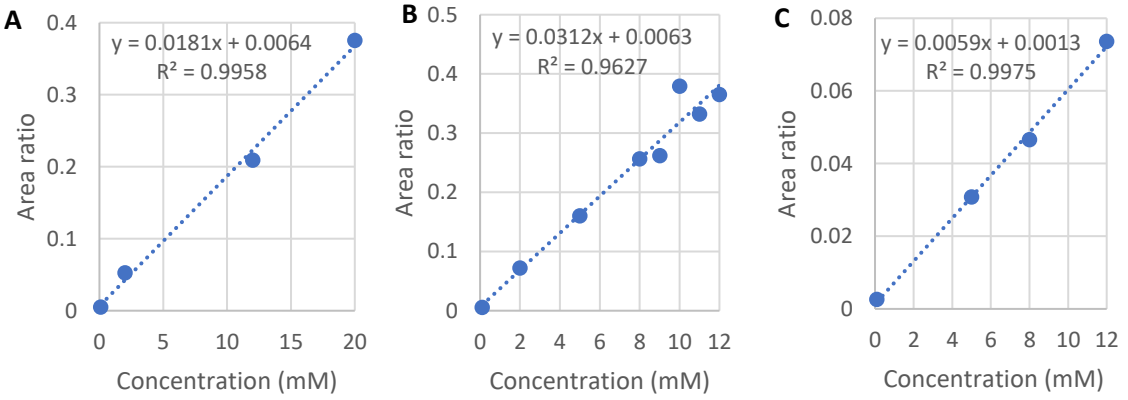

Figure A9.5. Calibration curves to quantify compounds of the substrate series k. Peak area ratios were compared with 5 mM dodecane as internal standard. Average of duplicates. A: 1k. B: 2k. C: 3k.

Appendix 10: Derivatisation of obtained chiral amines

For the chiral amines labelled with **3e**, **3g**, **3i**, and **3k**, the chiral amine was derivatised with the aid of acetic anhydride. The method for **3e** was made on the column labelled B. The methods for **3g**, **3i** and **3k** were made on the column labelled H.

G. LIPODEX E (50 m × 0.25 mm × 0.25 µm), split ratio 100,. injection at 200 °C, linear velocity 38 cm/s, column flow 2.16 mL/min, helium as carrier gas.
H. CP-Chirasil Dex CB (25 m × 0.32 mm × 0.25 µm) injection at 250 °C, split ratio 150, linear velocity 30 cm/s, column flow 1.55 mL/min, helium as carrier gas.

Compound series e

Table A10.1. Method applied for the reference consisting of acetylated 2-methylcyclohexylamine

Rate (°C/min)	Temp. (°C)	Hold (min)
-	100	2
5	130	15
25	225	1

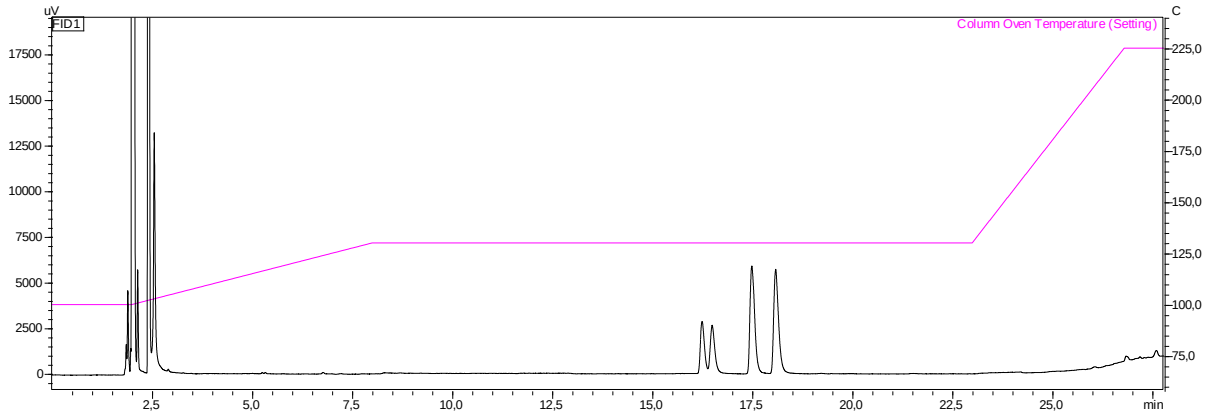

Figure A10.1. Gas chromatogram of acetylated 2-methylcyclohexylamine (16,2, 16.5, 17.5 and 18.0 min).

Compound series g

Table A10.2. Method applied for the reference consisting of acetylated 2-aminobutane.

Rate (°C/min)	Temp. (°C)	Hold (min)
-	100	2
5	140	10
25	220	1

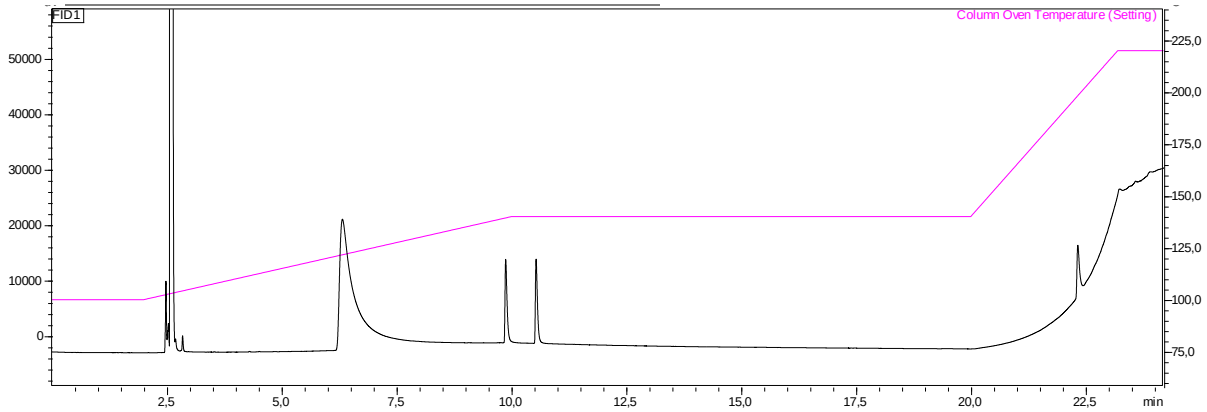

Figure A10.2. Gas chromatogram of acetylated 2-aminobutane (9.8 and 10.5 min).

Compound series i

Table A10.3. Method applied for the reference consisting of acetylated 2-pentylamine.

Rate (°C/min)	Temp. (°C)	Hold (min)
-	100	2
5	140	10
25	220	1

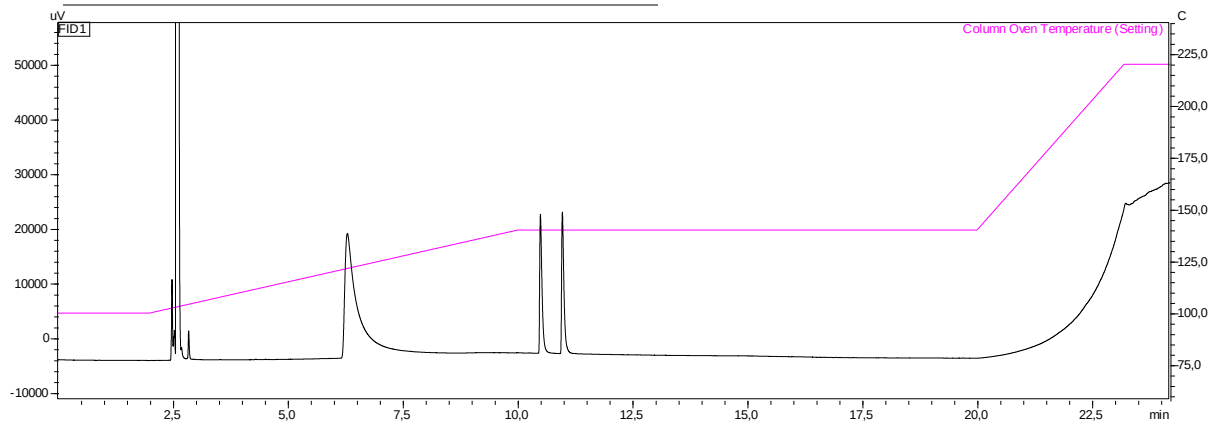

Figure A10.3. Gas chromatogram of acetylated 2-pentylamine (10.5 and 11.0 min).

Compound series k

Table A10.4. Method applied for the reference consisting of acetylated 2-methylpentylamine.

Rate (°C/min)	Temp. (°C)	Hold (min)
-	100	2
5	125	10
25	220	1

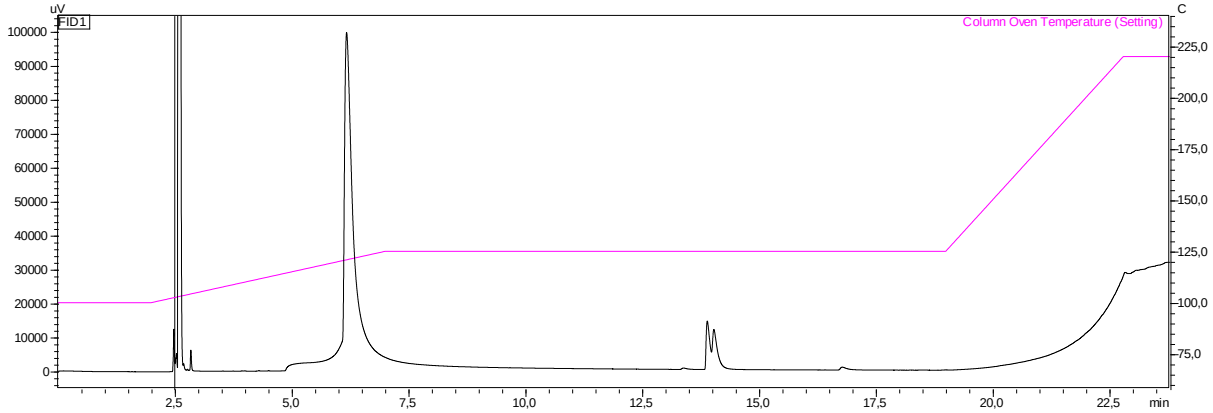

Figure A10.4. Gas chromatogram of acetylated 2-methylbutylamine (13.9 and 14.0 min).

Appendix 11: Alcohol compound labels and quantifications

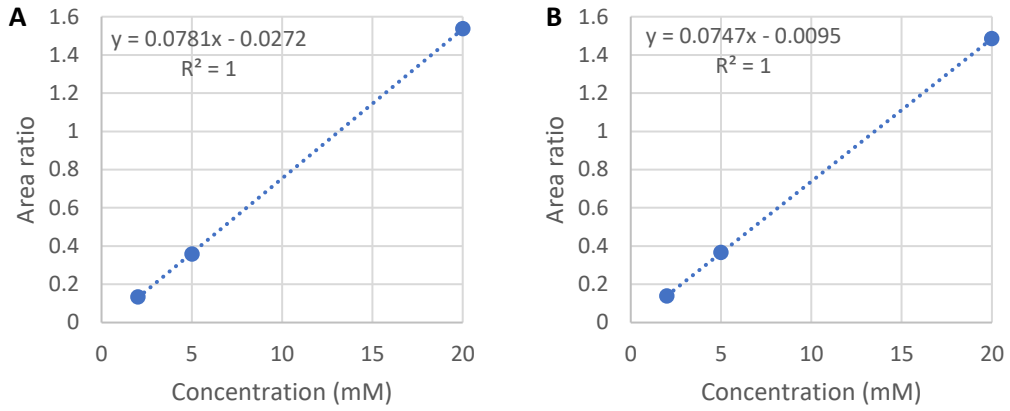

Figure A11.1. Calibration curve of the alcohol by-product for the different substrate series. Peak area ratios were compared with 5 mM dodecane as internal standard. Average of duplicates. A: 4d. B: 4i.

2-methylcyclohexanol (**4e**) had the same retention time on the GC method as 2-methylcyclohexylamine (**3e**). To estimate the amount of alcohol in the mixture, it was calculated how much derivatized alcohol was present compared to peak area of the derivatized amine. By calculating these ratios, it was calculated what percentage of the amine peak corresponded to the alcohol. Because the alcohol was also derivatised, it was possible to determine the e.e. and d.e. from the chromatogram (Figure A11.2). With this reference, it was determined that these were both higher than 99 %.

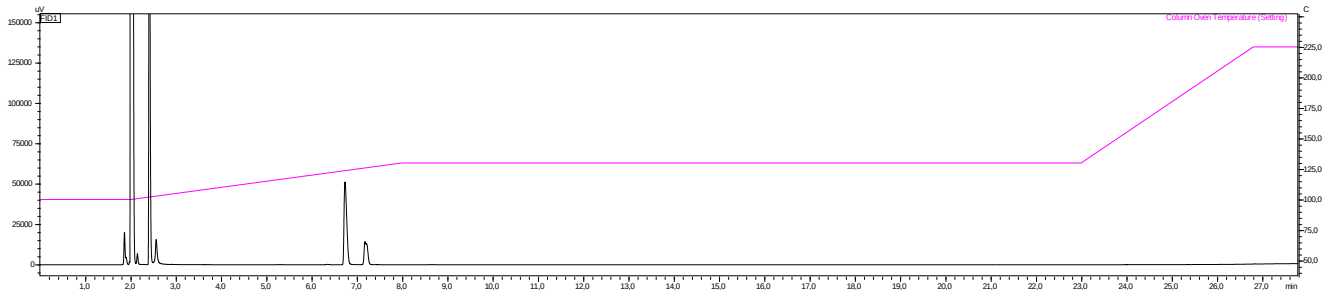

Figure A11.2. Gas chromatogram of derivatized **4e** (6.8 & 7.2 min).

The amount of 2-aminopentane was a rough estimation. The calibration curve was made with EtOAc, where we saw peak overlap with the alcohol. The cascades were made with MTBE, where this as not the case. Based on the internal standard from the cascade mixture, it was estimated what would be the peak area if it was extracted with ethyl acetate. This number was added to the observed GC peak area, and with this number, calculations were made based on the calibration curve.

Appendix 12: Control reactions of alcohol-forming cascades

Because the quantities of AmDHs to work with were limited, we left out AmDHs in our control reactions (Table A12.1). None of these reactions showed any alcohol formation, suggesting that the cause of the alcohol side-product is the presence of AmDHs.

Table A12.1. Overview of components present (x) and absent (-) in all numbered control reactions.

Control reaction	AmDH	*Ts*OYE	GDH	Glucose	$NADP^+$	Substrate
1	-	x	x	x	x	x
2	-	-	x	x	x	x
3	-	x	-	x	x	x
4	-	x	x	-	x	x
5	-	x	x	x	-	x
6	-	x	x	x	x	-

For the compound series **d**, **e**, **i** and **k**, chromatograms of the alcohol references, alcohol forming cascades and control reactions without AmDH (labelled 1) are shown, to clarify how we determined the alcohol formation.

Compound series d

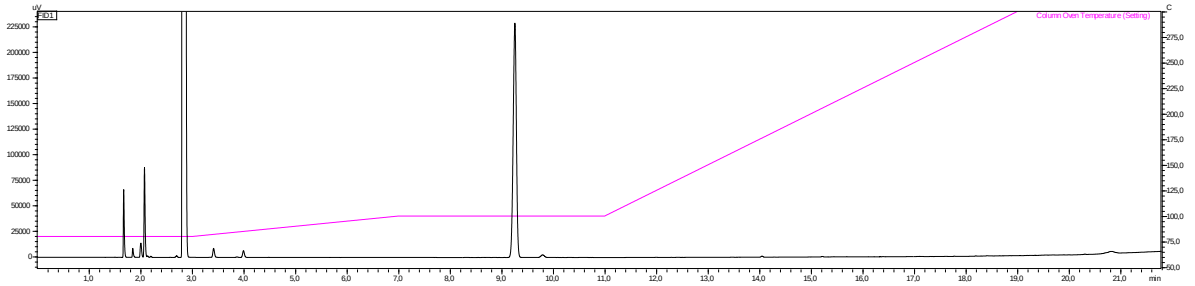

Figure A12.1. Gas chromatogram of 4d (9.3 min).

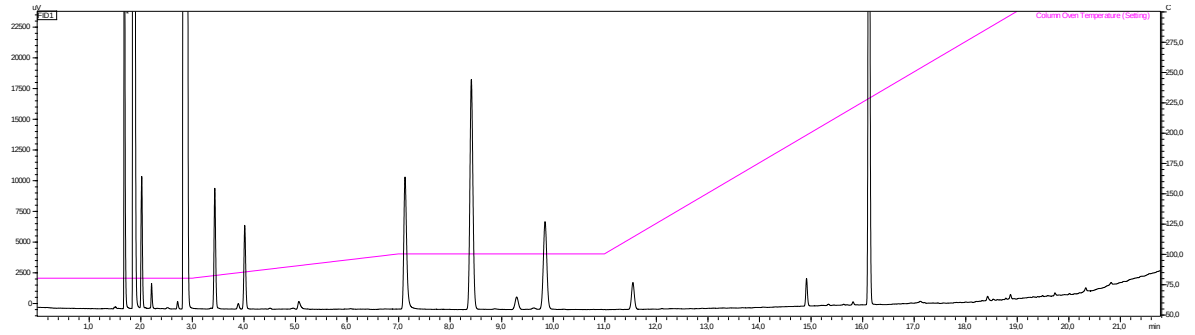

Figure A12.2. Gas chromatogram of a cascade reaction mixture with substrate **1d** at pH 8 .

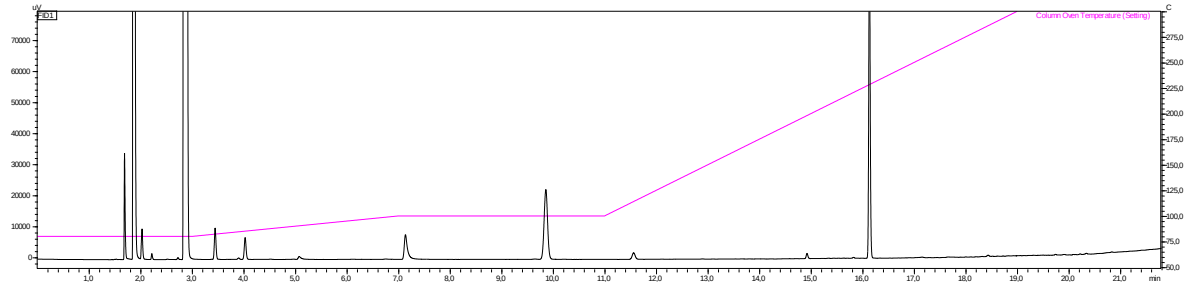

Figure A12.3. Gas chromatogram of the control reaction 1 with substrate **1d**.

Compound series e

We analysed the following cascades with an achiral GC colum. We also observed that the retention times of **3e** and **4e** overlap. With a chiral GC column, we were able to separate **3e** and **4e**. This is why cascade samples were loaded onto the chiral column B as well. On these chromatograms we observed both **3e** and **4e**, meaning that alcohol was formed in the cascades.

Controls were performed on the achiral column C. In the control reactions, no peak was observed at the retention time where we would expect **3e** or **4e**, showing that no alcohol was formed without AmDH.

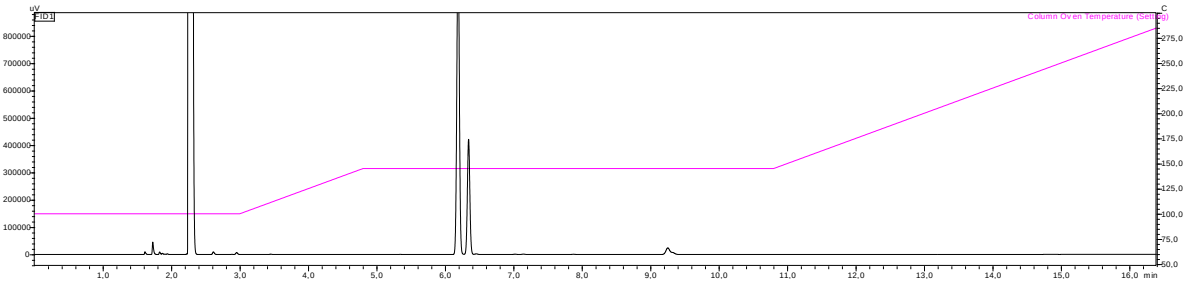

Figure A12.4. Gas chromatogram of **4e** (6.2, 6.4 min).

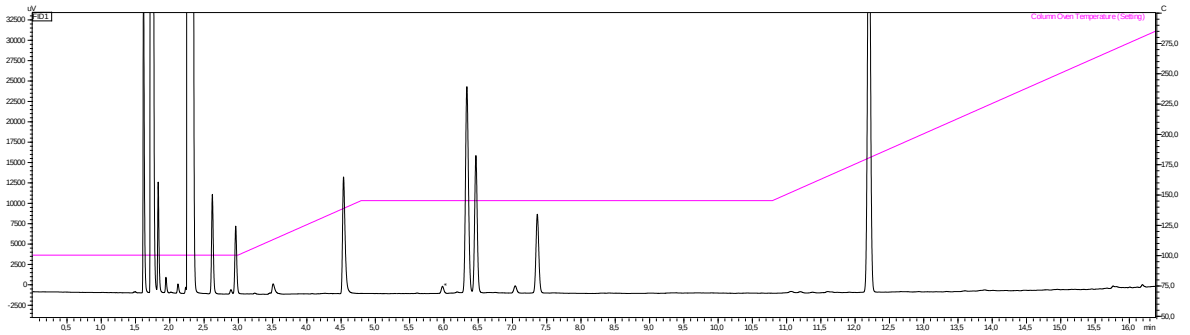

Figure A12.5. Gas chromatogram of a cascade reaction mixture with substrate **1e** on the GC column labelled C.

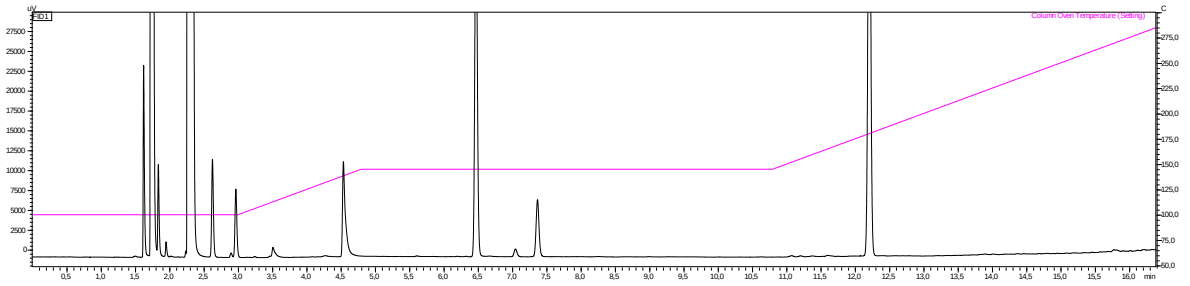

Figure A12.6. Gas chromatogram of control reaction 1 with substrate **1e** on the GC column labelled C.

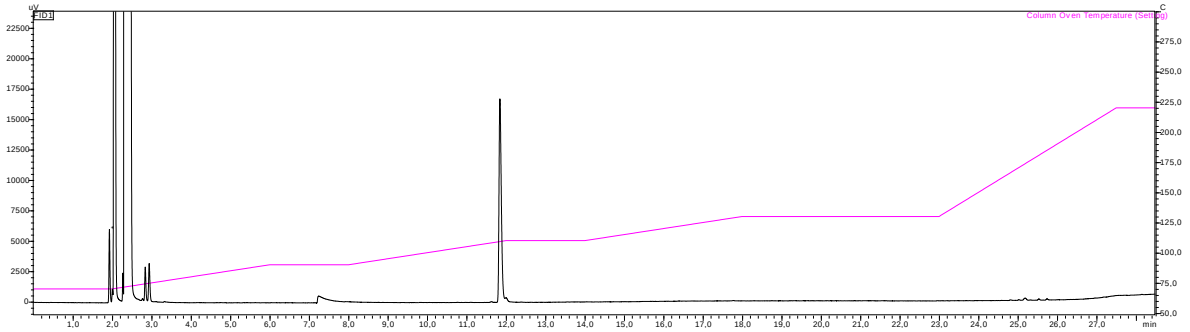

Figure A12.7. Gas chromatogram of **1e** on the chiral column labelled B (11.9).

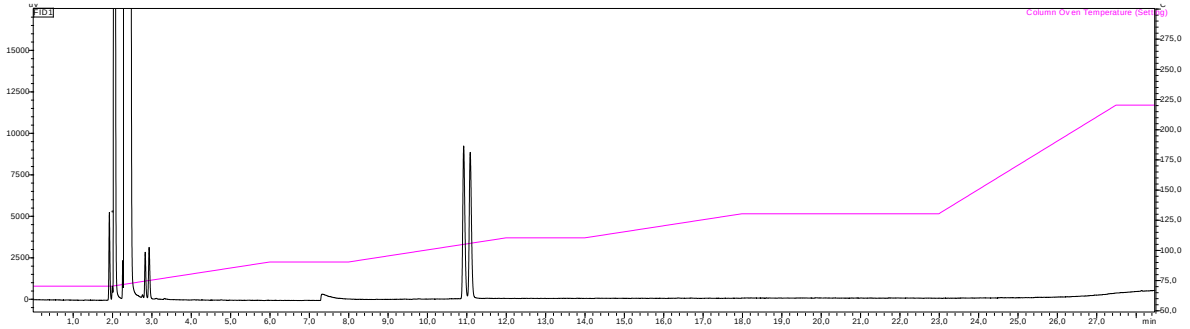

Figure A12.8. Gas chromatogram of **3e** on the chiral column labelled B (10.9, 11.1).

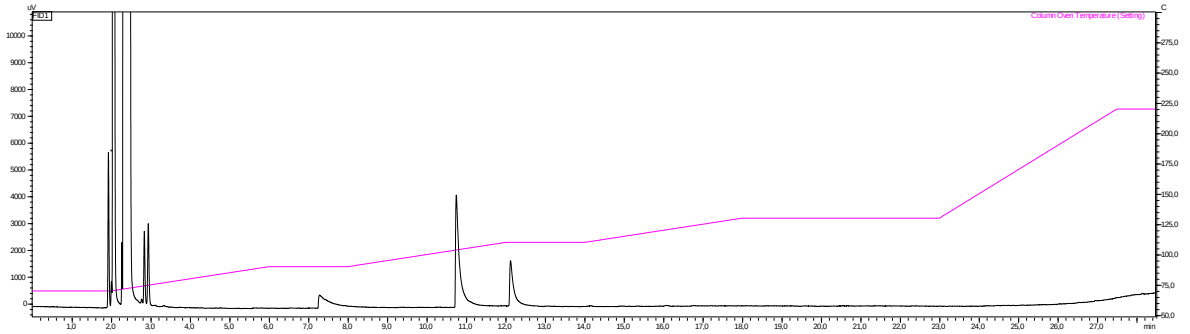

Figure A12.9. Gas chromatogram of **3e** on the chiral column labelled B (10.8, 12.2).

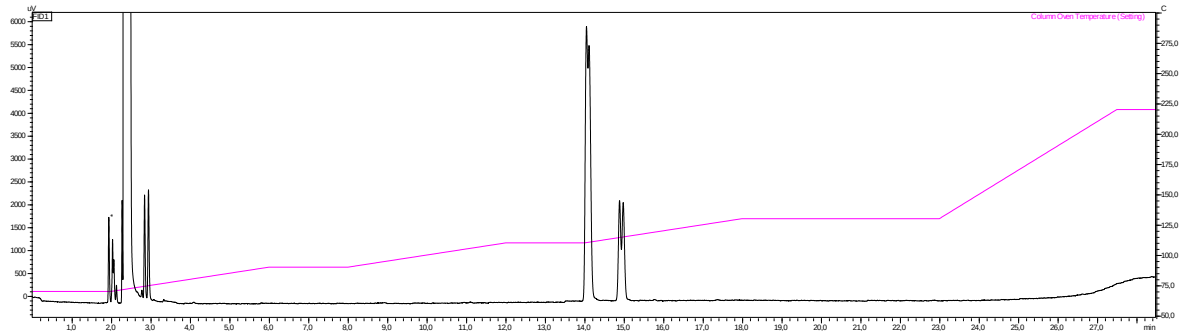

Figure A12.10. Gas chromatogram of **4e** on the chiral column labelled B (14.1, 14.2, 14.9, 15.0).

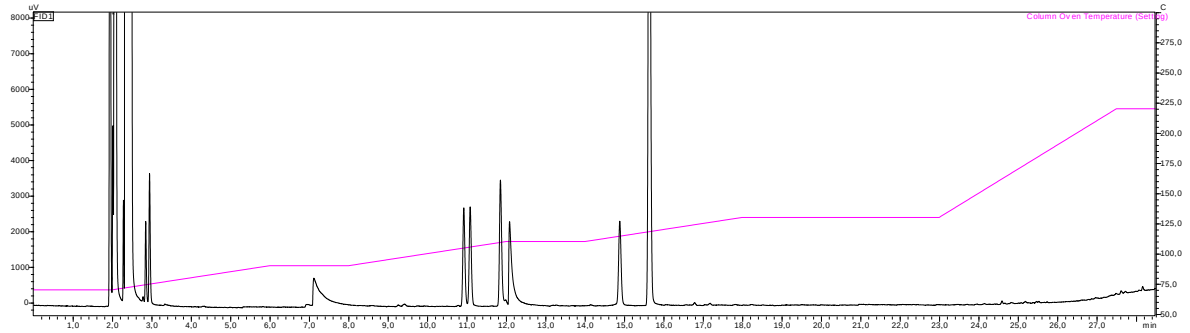

Figure A12.11. Gas chromatogram of a cascade reaction mixture with substrate 1e on the chiral column labelled B. This chromatogram shows the same sample as shown in Figure A12.4.

Compound series i

What should be noted is that we observed on the chromatogram the peak for **4i** overlaps with one of the solvent peaks (ethyl acetate). This means that the control reactions should be redone with a solvent without any overlap, such as methyl *tert*-butyl ether (MTBE). Nevertheless, one control reaction and a cascade were extracted with MTBE. From these chromatograms, we show that alcohol was obtained from the cascade reaction.

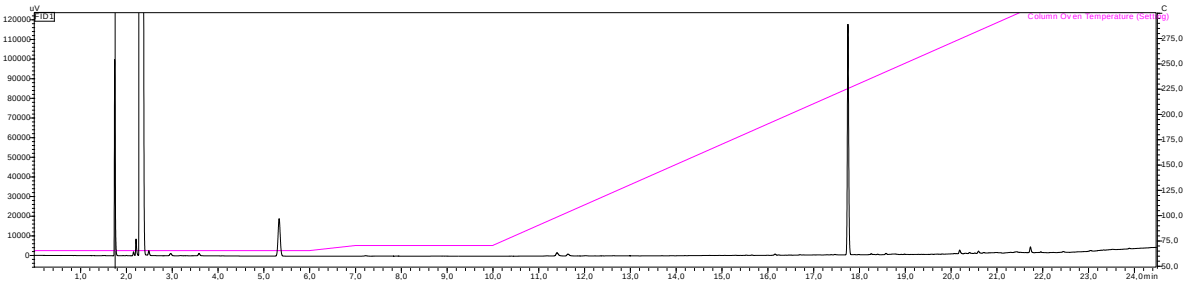

Figure A12.12 . Gas chromatogram of **4i** (5.6 min).

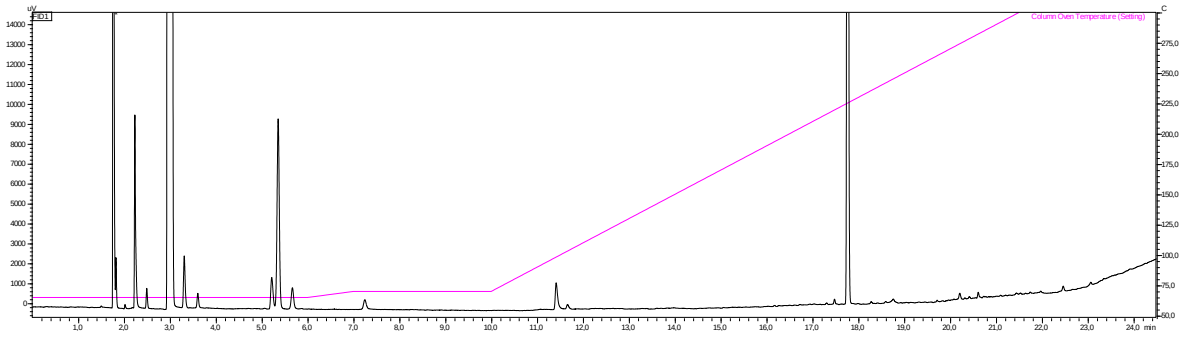

Figure A12.13. Gas chromatogram of a cascade reaction mixture with substrate **1i** extracted with MTBE.

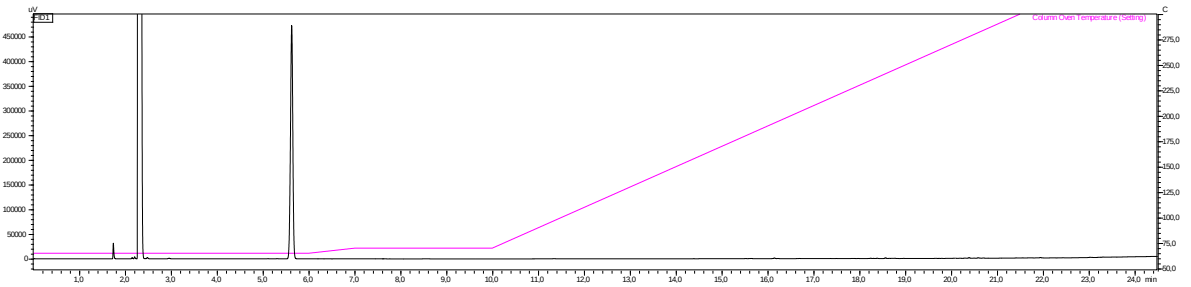

Figure A12.14. Gas chromatogram of control reaction 1 with substrate **1i**.

Compound series k

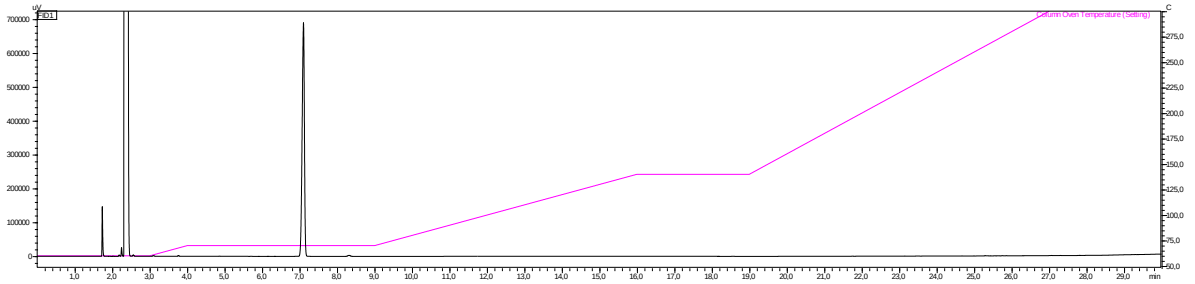

Figure A12.15 . Gas chromatogram of **4k** (7.1 min).

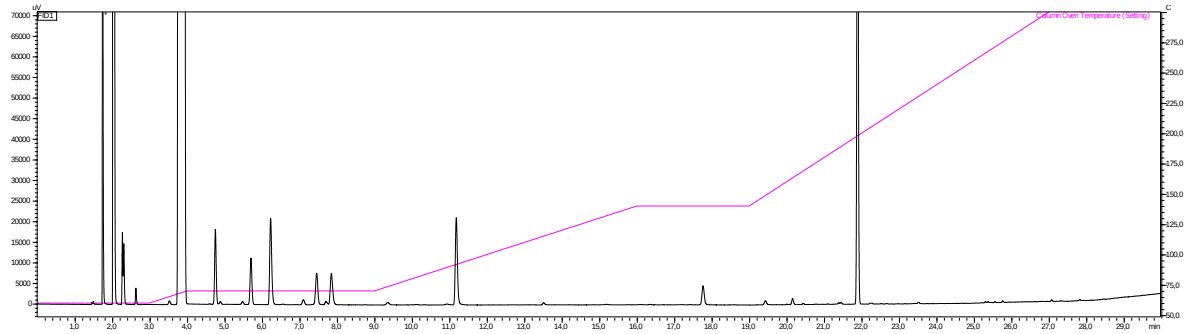

Figure A12.16. Gas chromatogram of a cascade reaction mixture with substrate **1k**.

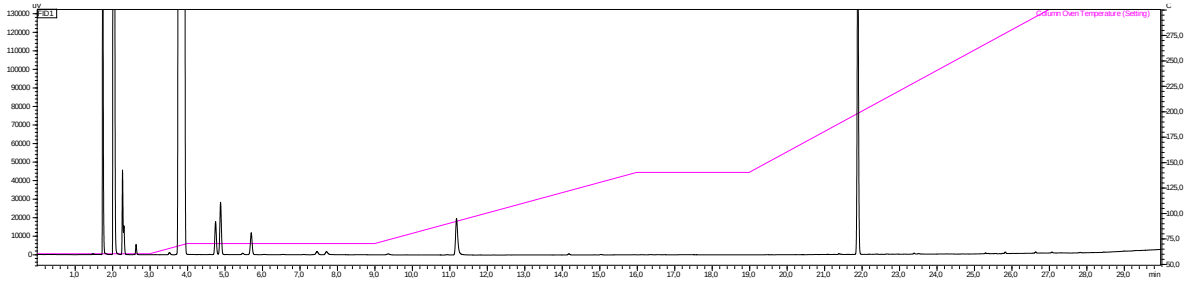

Figure A12.17. Gas chromatogram of control reaction 1 with substrate **1k**.

Appendix 13: GC chromatograms of cascades at different pH

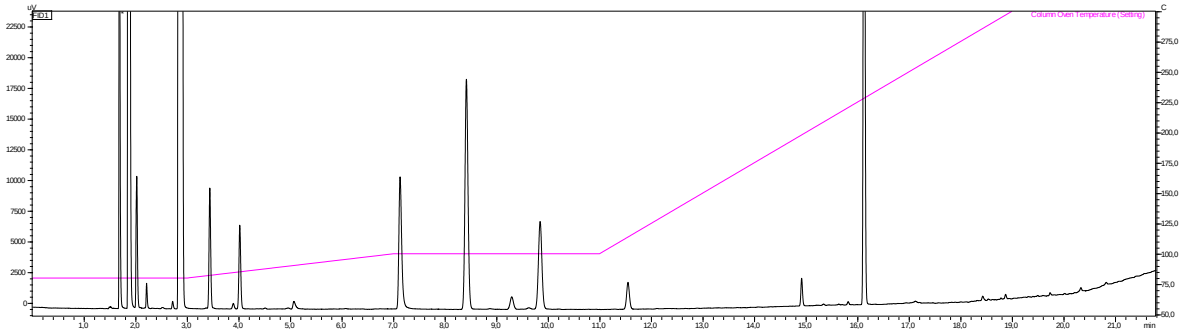

Figure A13.1. Gas chromatogram of a cascade reaction mixture with substrate 1d at pH 8 (see Figure A11.2).

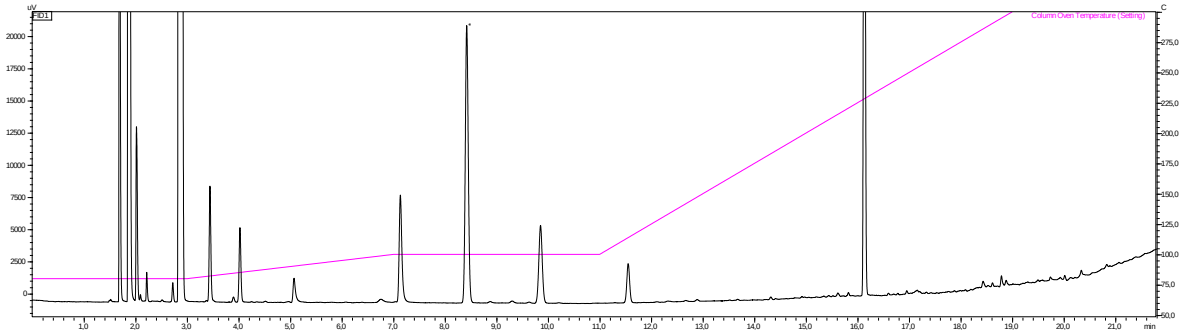

Figure A13.2. Gas chromatogram of a cascade reaction mixture with substrate **1d** at pH 8.5.

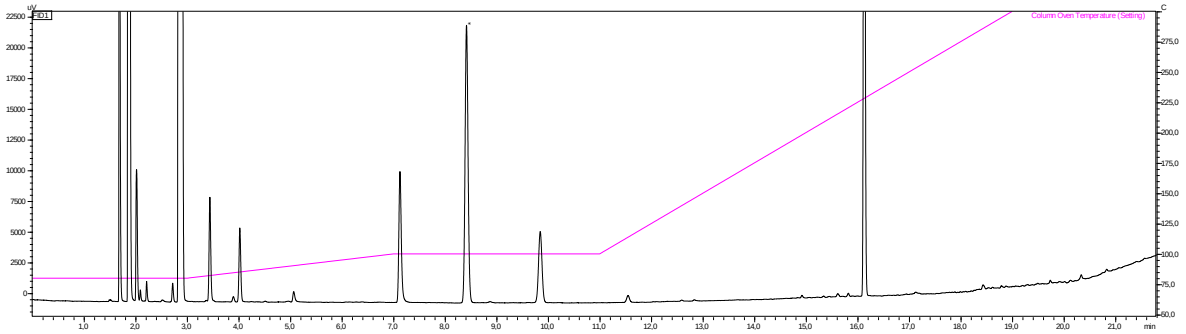

Figure A13.3. Gas chromatogram of a cascade reaction mixture with substrate **1d** at pH 9.